AD 46323

UNCLASSIFIED

Final Technical Report
on the Development of the
Multi-Jet Engine

Report 2003-1-R5

AEROPHYSICS DEVELOPMENT CORPORATION
PACIFIC PALISADES, CALIFORNIA

2003-1-R5
Oct. 1, 1954

Copy No. 9

FINAL TECHNICAL REPORT
on the
DEVELOPMENT OF THE MULTI-JET ENGINE
covering period from
June 1, 1953 to October 1, 1954

D. Bitondo — Project Engineer
E. L. Knuth — Propulsion Engineer
C. P. Hedges — Electronics Engineer

Sponsored by
United States Air Force
Wright Air Development Center
Wright Patterson Air Force Base

Contract No. AF 33(616)-2129
Expenditure Order: X506-230
ADC Project Number: 2003-1

Approved by W. Bollay
Technical Director

FINAL TECHNICAL REPORT

on the

DEVELOPMENT OF THE MULTI-JET ENGINE

October 1, 1954

FOREWORD

This report was prepared by the Aerophysics Development Corporation under U. S. Air Force Contract AF 33(616)-2129. This is the final technical report of the experimental performance analysis carried out from June 1, 1953 to October 1, 1954 under the research and development contract identified by Expenditure Order No. X506-230.

SUMMARY AND RECOMMENDATIONS

An engine which has less weight than a piston engine and which has still a relatively low specific fuel consumption is desired as a propulsion system for helicopters. Results of a previous study (Cf. Reference 1) indicate that a new type of engine termed "Multi-Jet" engine promises to be an engine of this type and that a helicopter powered with a Multi-Jet engine will carry a greater payload than helicopters powered with any other propulsion device. A Multi-Jet engine (see Figure 1) producing a thrust of 150 pounds at a peak gas temperature of 3000°F was estimated to have a diameter of 8 inches, a length of 20 inches, a weight of 43 pounds, and a specific fuel consumption of 1.86 lbs/hour/lb thrust. (Calculated variations of thrust and specific fuel consumption with flight velocity are given in Figure 2.) On the basis of these promising calculations, the experimental verification of the theoretical performance characteristics of a Multi-Jet engine was considered to be a useful undertaking.

The Multi-Jet engine is a wave (or pulse-jet) engine similar somewhat to the Swiss Compex. It differs, however, in that the combustion is carried out within the same chamber in which the shock compression is carried out. The Multi-Jet engine, described in more detail in Reference 1, is shown schematically in Figure 1. It promises to be useful particularly for application to subsonic vehicles such as helicopters, subsonic missiles, target aircraft or jet trainer aircraft, in fact, wherever a low cost jet power plant would have application. The critical phase in the development of the Multi-Jet engine is the development of an intermittent flow cycle which yields optimum thrust

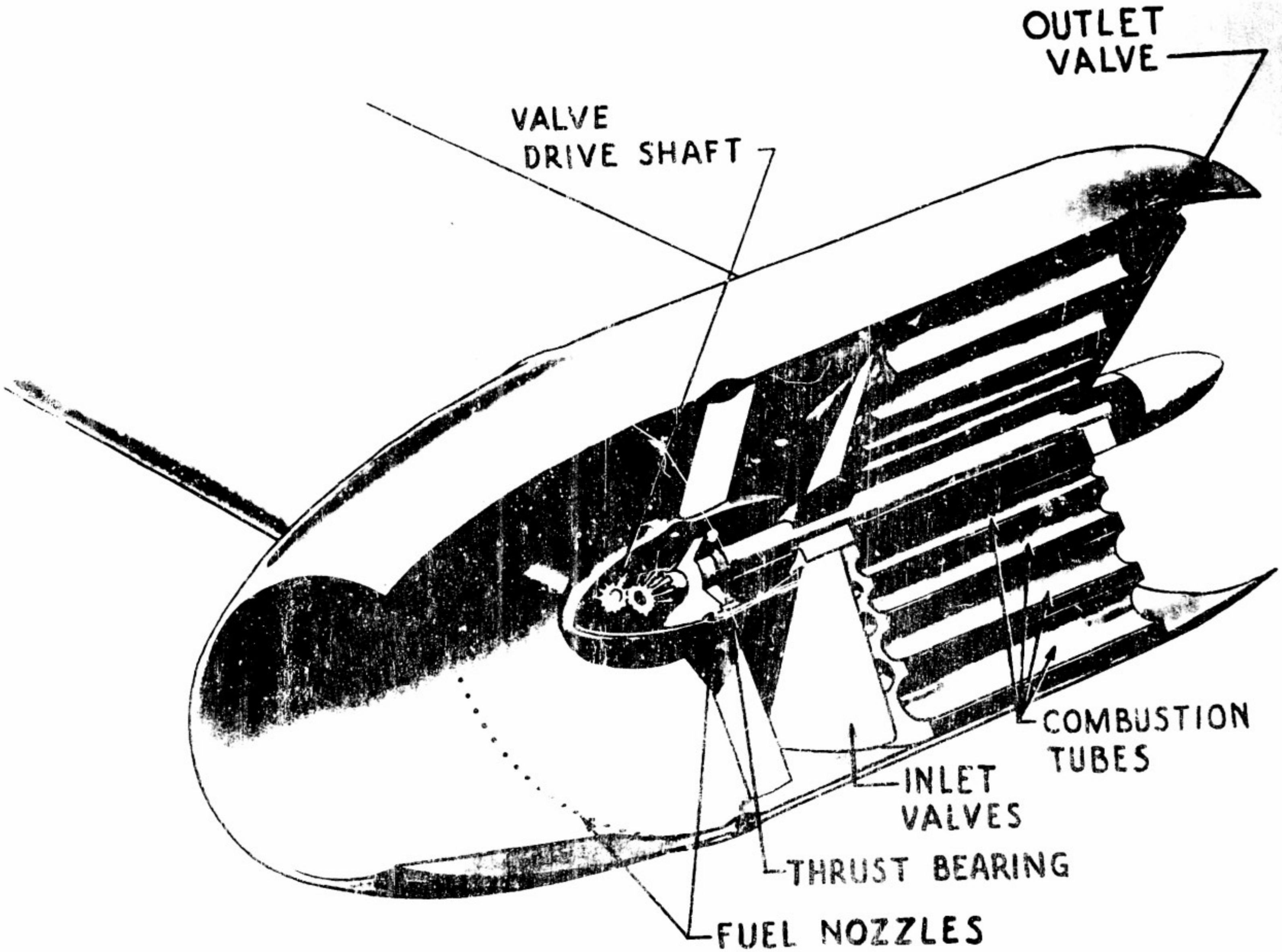

FIGURE I

PERSPECTIVE VIEW OF THE MULTI - JET

PREPARED BY

CHECKED BY

AEROPHYSICS DEVELOPMENT CORPORATION

PACIFIC PALISADES, CALIFORNIA

2003-1-R5

Oct. 1, 1954

FIGURE 2

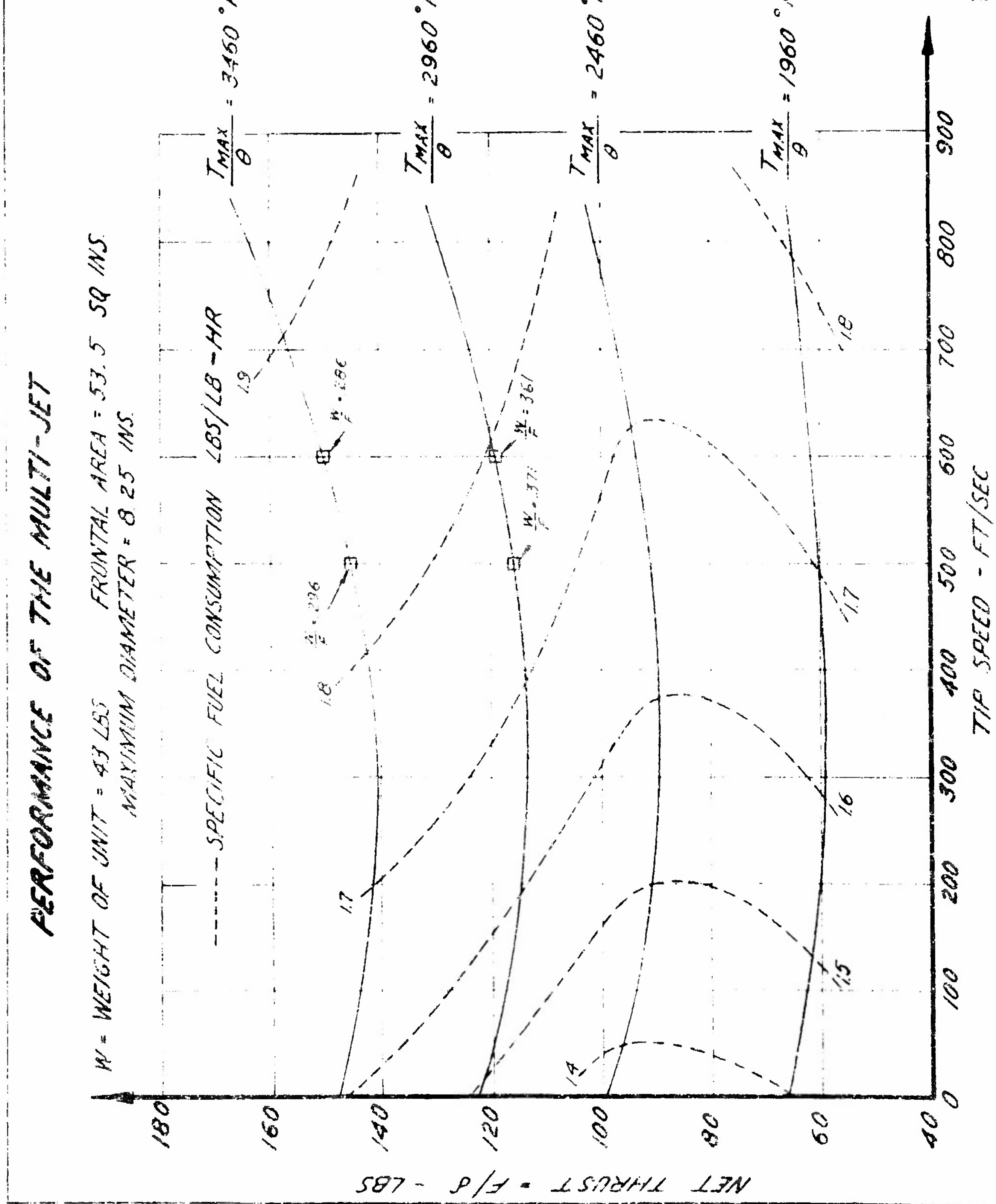

and specific fuel consumption.

The evolution of the predicted performance was expected to occur in the following steps:

1. Develop an engine which will operate on the Multi-Jet cycle and which will produce high peak combustion-chamber pressures. The higher the peak combustion-chamber pressure of the pulsating-type engine, the greater the ability of this engine to produce a high net thrust. (This contractor has developed already an experimental engine which has achieved combustion-chamber pressures of approximately 6.5 atmospheres. Compare this pressure with 2.5 atmospheres, a typical peak combustion-chamber pressure for usual pulse-jet engines.)
2. Time properly the several phases of the cycle in order to utilize efficiently the high peak combustion-chamber pressures to produce a large average thrust. The high-pressure gases should be exhausted in a rearward direction and parallel to the engine center line; the lengths of the several phases should be short in order to produce a large number of impulses per unit time.
3. Phase properly the scavenge cycle to avoid loss of combustible fuel-air mixture. Passing unburned fuel through the combustion tube would lead obviously to a high specific fuel consumption.
4. Inject fuel and mix it with the supply air in a manner such that a high combustion efficiency is realized. Once again, exhausting unburned fuel would lead to a high specific fuel consumption.

During the present contract period, a test engine (Multi-Jet Test Engine No. 2) suitable for quantitative testing was designed, built and instrumented for use in this engine-development program. Since setting up the instrumentation took longer than expected (the last instruments were not put into operation until June, 1954) and since it was not possible to obtain a clear understanding of the phenomena within the engine until this instrumentation was completed, quantitative testing was not initiated in time to complete all of the above-mentioned four steps. During the last four months of the program, however, peak combustion-chamber pressures were increased rapidly and the equipment was found suitable for precise measurements of cycle pressures, wall temperatures, and engine thrust.

After the test engine was put into operation, the original configuration of the engine was varied on the basis of test results until operation on the Multi-Jet cycle (including cyclic ignition of the fresh charge by means of non-stationary surface combustion with no decrease in combustion-tube wall temperature) was realized. Further modifications of this engine permitted operation at higher air-flow rates (scavenge-phase flow velocities of approximately 500 feet per second), also with cyclic ignition of the fresh charge by means of non-stationary surface combustion with no decrease in combustion-tube wall temperature. Emphasis was placed then on the improving of the engine configuration in order to obtain high peak combustion-chamber pressures. (Combustion-chamber pressure ratios had not exceeded 4 up to this point in the program.) On the basis of conclusions drawn from pressure-time diagrams, engine changes were made until a combustion-chamber pressure ratio of [illegible].5 was realized. (See Figure 3 for a summary of work performed and progress achieved.) Theoretical calculations (Cf. Reference 1) indicate that pressure ratios greater than 8 can be achieved if scavenging is complete, mixing of fuel and air is thorough, burning is complete, and sealing of the combustion-tube ends with the valve blades is adequate.

Figure 4 shows a photograph of the pressure-time diagram obtained during one of the most recent test runs. An investigation of the photograph shows: (1) a rapid rise of pressure as soon as the tube is closed (the double valve-timing mark indicates the time when the tube is only half closed) and (2) a high pressure plateau indicating that combustion is completed and that the stay time of the mixture within the tube is too long. It can be seen that the combustion time can be reduced appreciably. Such a reduction should result in a configuration that will produce a greater value of net thrust and a lower value of specific fuel consumption.

Results of the theoretical study (Cf. Figure 5, also Reference 1) indicate that (for the combustion-chamber pressures which were realized) the engine is capable of producing a net thrust of 6.4 pounds per square inch of the combustion-tube flow area and a specific fuel consumption of 1.6 pounds of fuel per hour per pound thrust. Consequently, emphasis should be placed now on the following steps: (a) the development of an engine which will use these high peak combustion-chamber pressures in a manner such that a high net thrust is realized, and (b) the development of an engine which will produce this high net thrust with relatively low fuel-flow rates.

PREPARED BY H. H. S.	AEROPHYSICS DEVELOPMENT CORPORATION	REPORT NO. 2003-1-R5
CHECKED BY	P. O. BOX 657, PACIFIC PALISADES, CALIFORNIA	DATE OCT. 1, 1954

TIME	JUNE	JULY	AUGUST	SEPT	OCT	NOV	DEC	JAN	FEB	MAR	APRIL	MAY	JUNE	JULY	AUG	SEPT
PROGRESS OF TEST ENGINE #2 AND ITS EQUIPMENT	PRELIMINARY DESIGNING		DESIGNING AND DRAWING			CONSTRUCTING AND ASSEMBLING OF ENGINE			CHECKING AND CALIBRATING OF ENGINE AND EQUIPMENT		TESTS STARTED TO DETERMINE OPERATING CONFIGURATION OF VALVES & COMBUSTION TUBE					
			PROCURING OF EQUIPMENT							OPERATING OF TEST ENGINE NO. 2						
INSTRUMENTATION	PRELIMINARY DESIGNING OF INSTRUMENTS				DESIGNING OF CIRCUITS PROCURING OF RECORDERS ON G.F.E. LIST			BUILDING & TESTING OF PRIME INSTRUMENTS & CIRCUITS WHICH FEED RECORDER			BUILDING & TESTING OF CIRCUITS ASSOCIATED WITH TAPE RECORDER				TAPE RECORDER PUT INTO OPERATION	

FIGURE 3

WORK AND PROGRESS SCHEDULE

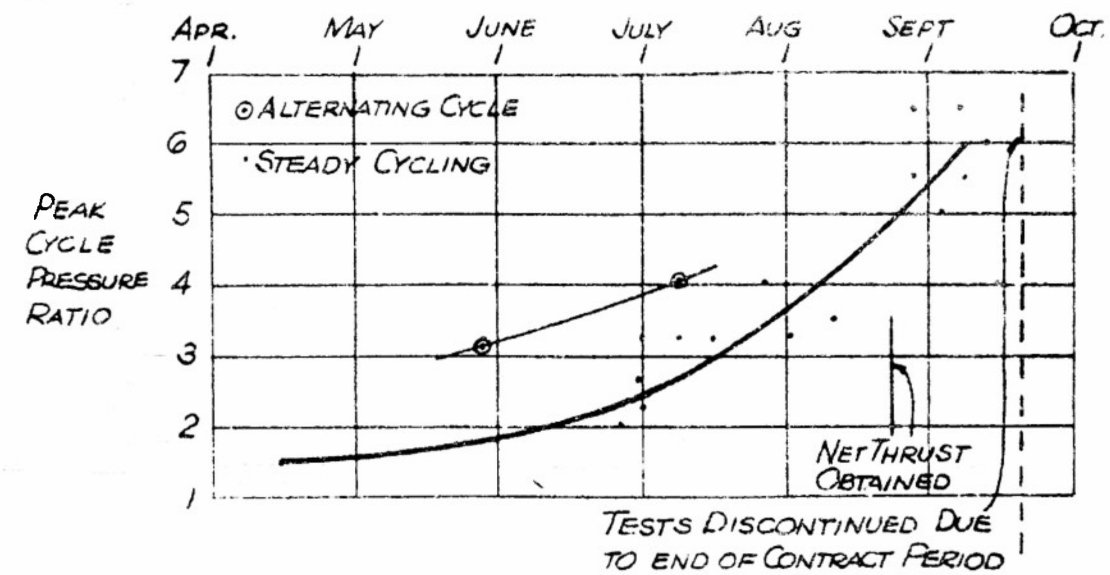

Figure 4.

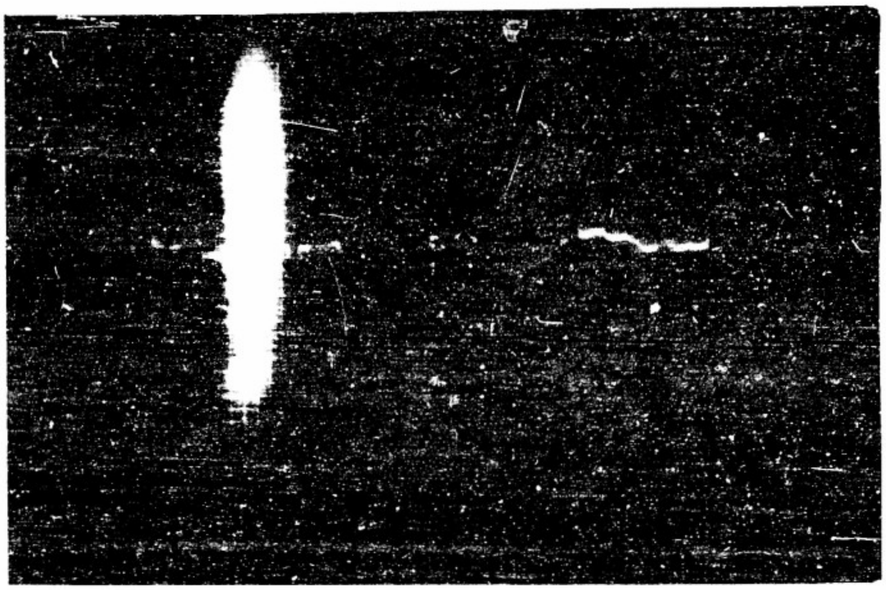

Photograph of Pressure-Time Diagram

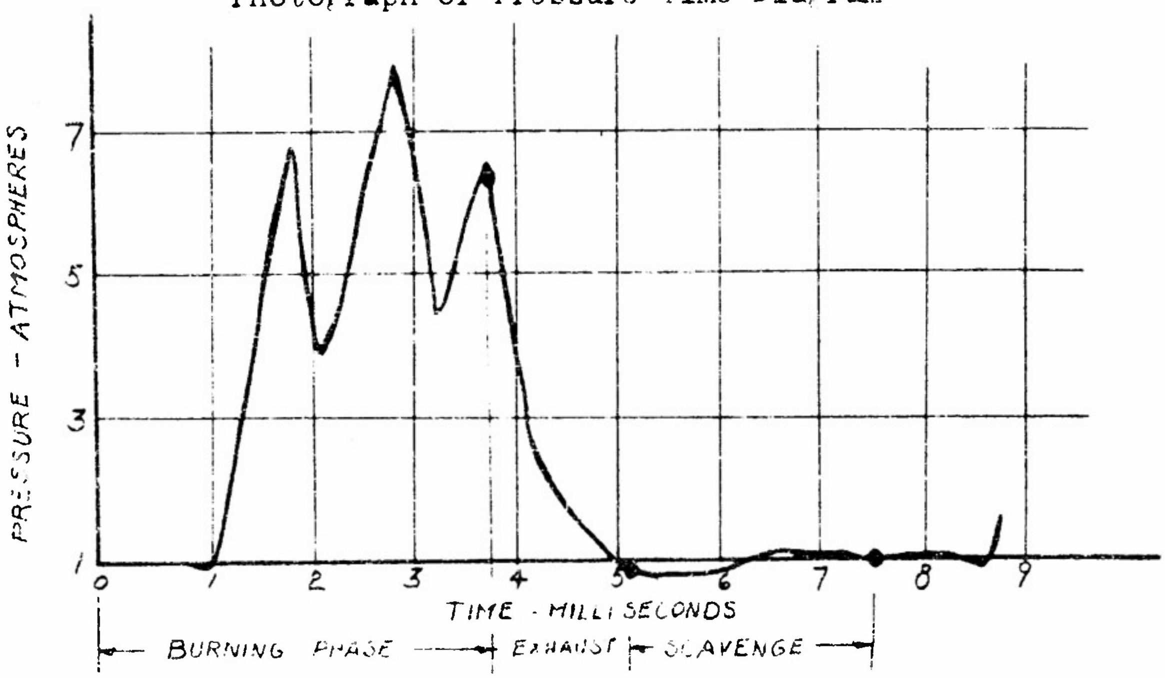

FIGURE 5

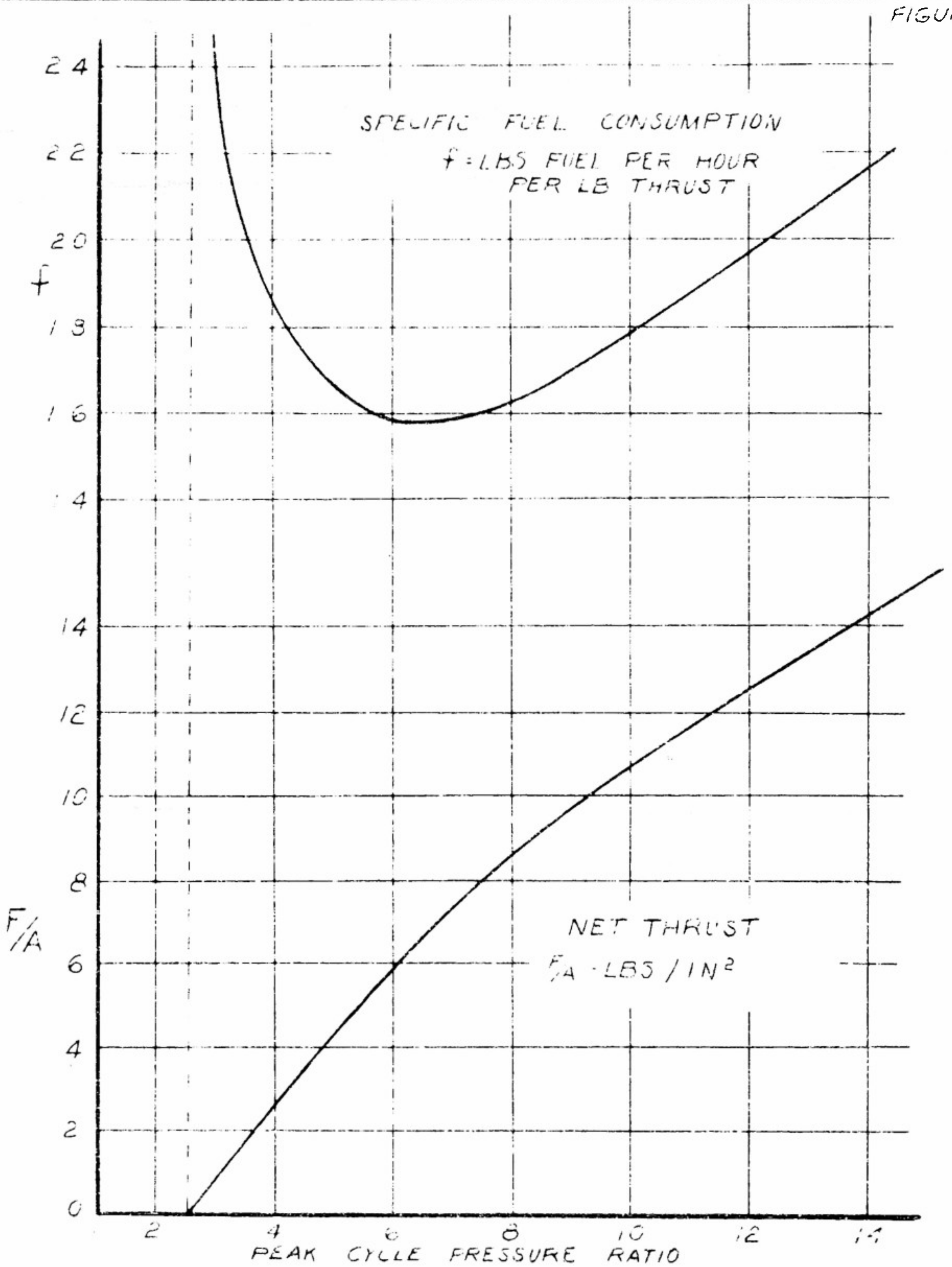

THEORETICAL PERFORMANCE FOR SCAVENGE $M_s = 0.4$

It will be noted that Figure 5 indicates zero thrust at a pressure ratio of about 2.5 and a rapidly increasing net thrust with increasing pressure ratio. In this respect, the Multi-Jet engine is similar somewhat to a gas turbine, for which engine the compressor efficiency and turbine efficiency must exceed set minimum values before net power can be obtained.

It is recommended that testing be continued using the existing test facilities for a period of one year in order to continue the development of a Multi-Jet engine which produces a large net thrust with a low specific fuel consumption. Since no additional expensive equipment is needed, the bulk of the expenditures would be for labor and operating supplies. It is believed that a development program of this type would produce a new type of engine suitable particularly for use in medium-range helicopters and would yield new data concerning non-stationary fluid flows and surface combustion of combustible fluids.

ABSTRACT

Work performed and results obtained under contract No. 33 (616)-2129 are discussed. The test engine constructed and used during this period is described, along with the instrumentation provided for the tests performed. Test results are discussed. Analyses of problems pertaining to Multi-Jet Engine operation are presented. Also discussed are tests performed on the engine first constructed and used under the previous contract (No. 33 (616)-37). It is concluded that data sufficient for determining a Multi-Jet engine configuration suitable for quantitative testing has been obtained, but that further information is needed before an efficient configuration can be established. It is recommended that testing of the present test engine be continued for a period of one year.

CONTENTS

LIST OF ILLUSTRATIONS

SECTION I

INTRODUCTION

Prior to the beginning of the present contract period on June 1, 1953, a one-year preliminary-design study and performance analysis of the Multi-Jet Engine (Reference 1) was completed under Air Force Contract AF 33(616)-37. Under this contract a preliminary-design study and performance analysis of a Multi-Jet Engine suitable for application to a helicopter rotor system was made. During this same period, exploratory experimental tests were made with single combustion tubes which tests demonstrated satisfactorily (1) that surface combustion can be initiated periodically by the hot walls of the combustion tubes and (2) that some of the tested materials will withstand for extended periods of time the effects of a peak gas temperature of 2500°F in conjunction with the effects of pulsating pressures.

On the basis of the analytical work carried out during the previous contract period (Reference 1) a test program aimed at verifying experimentally the theoretical performance characteristics of a Multi-Jet Engine was started. The first step in such a research program would be to obtain experimental data upon which a prediction of the attainable performance of the Multi-Jet Engine described above could be based. This step includes the development of an engine configuration (determined, e.g., by size of valve ports, tube lengths, and tube diameters) which operates on the Multi-Jet cycle, produces net thrust, and lends itself to quantitative testing. The second step would be to investigate in detail the configuration changes that affect the performance. These configuration changes include changes in the valve-clearance dimensions, the rapidity with which the valves open and close, and the combustion tube dimensions (length and diameter).

The following information was obtained from tests conducted during this contract period: (1) measurement of combustion-chamber pressure as a function of time; (2) measurement of mean fuel and air flows; and (3) measurement of net thrust. From the above measurements, peak cycle pressure ratios, specific fuel consumption, and thrust per unit flow area of the single tube were calculated.

Figure 3 presents a summary of the work performed and the progress achieved during the past 15 months. The design of Multi-Jet Test Engine No. 2 (which is the engine used to obtain the experimental performance data) and it's associated equipment is described in Section II. The instrumentation is described in Section III. Section IV includes (1) the description of tests carried out on Multi-Jet Test Engine No. 1 (which is the engine constructed during the previous contract period); (2) the description of the tests on non-stationary surface combustion carried out in the shock tube; (3) the description of the tests carried out on Multi-Jet Test Engine No. 2.

Analytic studies of (1) the burning of a fuel-air mixture enclosed in a cylinder; (2) non-stationary non-viscous flow; (3) the effects of viscosity on certain non-stationary flows are discussed in Section V.

The appendix includes a detailed description of (1) the electronic circuits used in the instrumentation of Multi-Jet Test Engine No. 2 and (2) the tests performed with Test Engine No. 2.

SECTION II

MULTI-JET TEST ENGINE NO. 2

A Multi-Jet engine consists essentially of a matrix of many small pulse-jet tubes equipped with valves which control the opening and closing of the inlets and outlets of these tubes (Cf. Figure 1; also Reference 1). Since each of these tubes acts independently of every other tube, the performance of this engine may be obtained by determining the performance of a single tube and then summing to obtain the performance of the complete engine. Multi-Jet Test Engine No. 2 was constructed for the purpose of determining the performance of such a single tube.

Test Engine No. 2 contains a single combustion tube mounted between two rotating-plate valves. This engine was designed so that the effect of variations of the following parameters on engine performance could be determined:

1. Combustion-tube dimensions (lengths from 6 to 15 inches, diameters from 1/4 to 1 inch).
2. Cycle frequency (determined by the number of ports in the valve plates and by the rotor speed).
3. Relative length of the several periods of the cycle (determined by the relative size of the ports in the valve plates and by the phase angle between the two valve plates).
4. Area of openings in combustion chamber during combustion phase (determined by the clearances between the combustion-tube ends and the valve plates).

It was possible to vary the cycle frequency (as a function of rotor speed) during a test period. The remaining parameters could be changed only between tests when the engine was not operating.

Rotating-plate valves (Figure 6 and 7) were selected for use in this engine because of their simplicity and efficiency (Cf. Ref. 1). This valve system consists of a rotor shaft upon which two valve plates containing four ports each are mounted (each rotor revolution corresponds to four cycles). Since the air for this test engine was supplied through a pipe connected to the laboratory air-supply system, it was necessary to prevent the loss of supply air by enclosing the front valve plate within a housing and by installing rotating seals between the valve-plate housing and the rotor shaft. A rear valve-plate housing was also used in the initial tests, but since it was found to serve no useful purpose, it was later discarded. The rotor shaft, rotor-shaft bearings, valve plates, and valve-plate housings of this engine are pictured in Figure 6. (The front valve plate and housing are shown exploded while the rear valve plate and housing are shown assembled.) Note that by sliding the rear valve plate to the appropriate point on the splined rotor shaft it was possible to adjust the distance between the two valve plates so as to correspond to the length of the combustion tube.

Provisions were made for adjusting the clearances between the tube ends and the valve plates to any value between 0 and 1/16 in. Precautions were taken to insure that these clearances could be adjusted accurately and held rigidly for a given test. Spacers having ends parallel to within one minute were used to hold the valve plate faces parallel to the faces of a hub and these hub faces were ground perpen-

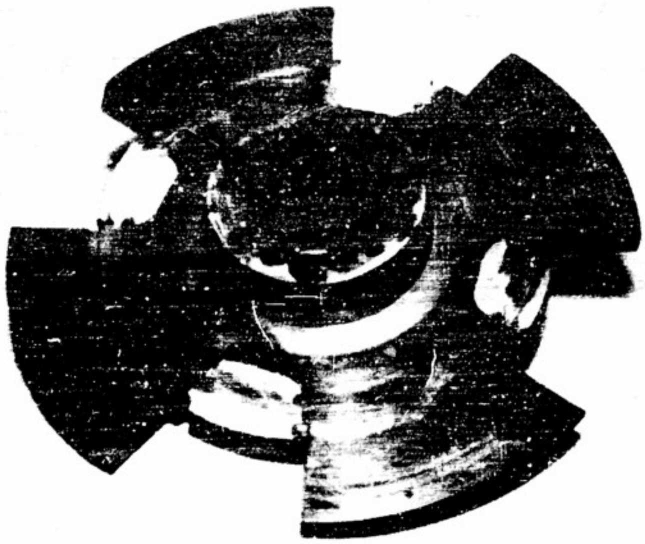

Figure 6. Rotating-Plate Valve - Front View

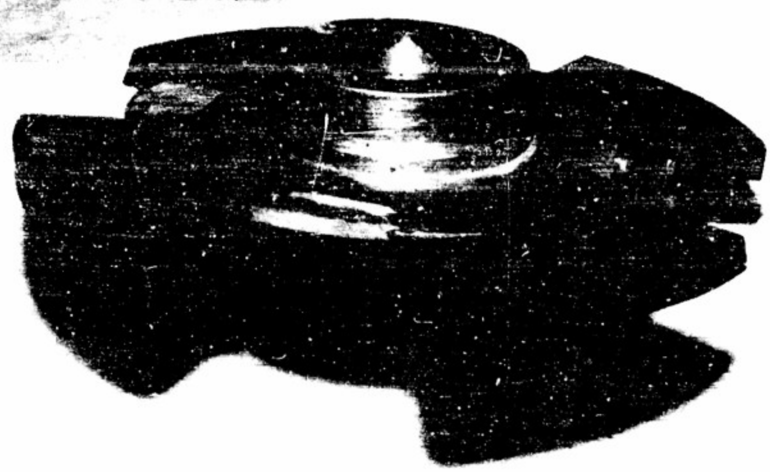

Figure 7. Rotating-Plate Valve - Edge View

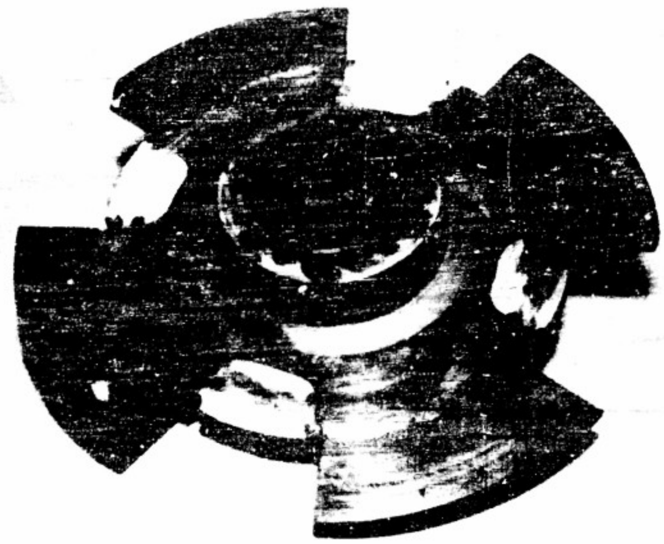

Figure 6. Rotating-Plate Valve - Front View

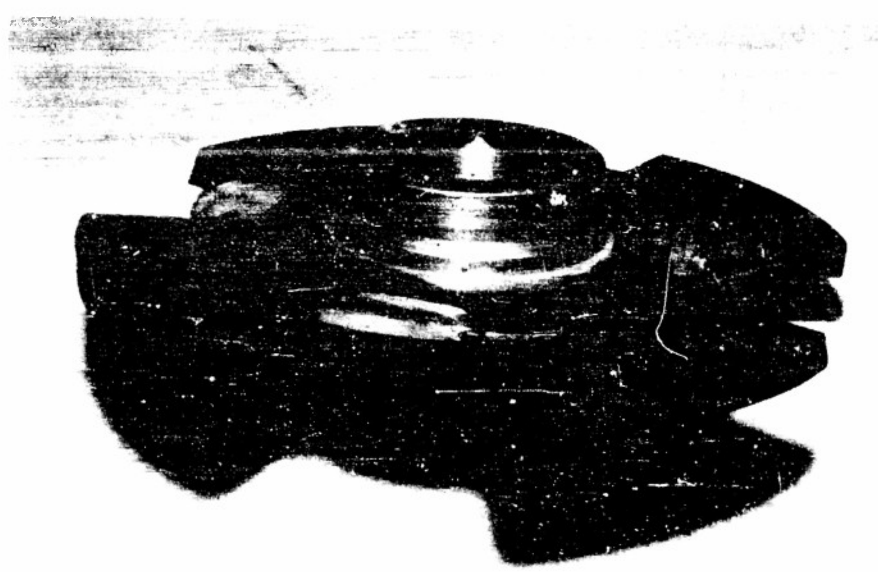

Figure 7. Rotating-Plate Valve - Edge View

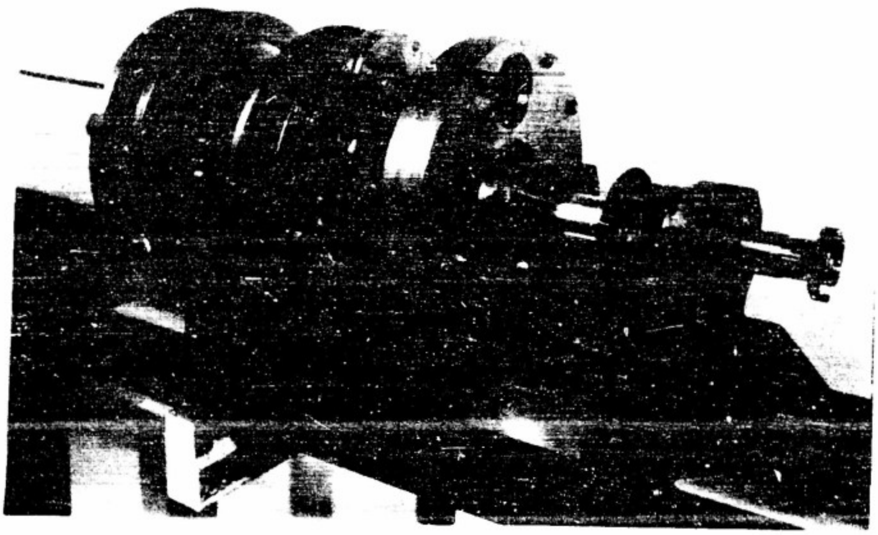

Figure 6. Valves and Rotor Shaft of Multi-Jet Test Engine No. 2

dicular within one minute to the rotor-shaft center line. Facilities were provided for passing water through passages in the valve plates and in their housings, since it was expected that water cooling would be required in order to prevent distortions due to localized heating. Tests indicated, however, that it was not necessary to cool the valve plates or the front valve-plate housing, and consequently only the forward portion of the aft valve-plate housing (that portion which was not discarded as noted above) was water cooled.

The original valve-drive system included two war-surplus 24-volt 90-ampere intermittent-duty aircraft-type dc motors slung beneath the test engine. These drive motors received electrical power from a war-surplus 24-volt 200-ampere aircraft-type dc generator driven by a 10-horsepower ac motor. Mechanical power was transmitted from the drive motors to the rotor by a V belt. The angular speed of the drive motors was controlled by varying the generator field current. This current was supplied by a commercially available 12-volt wet-cell battery charger, and the output of the battery charger was controlled by regulating its ac input with a commercially available voltage divider.

The aircraft-type drive motors were chosen because their light weight allowed the floating of the entire test engine, including drive motors, in order to measure the net thrust directly. However, since these motors were designed only for intermittent duty, they overheated and burned out during the long testing periods. Consequently, this rotor-drive system was replaced by a variable-speed drive system incorporating a Varidrive manufactured by U. S. Motors. Since the weight of the Varidrive prohibited slinging it below the test engine, it was decided not to measure the net thrust of the engine directly. The elimination of this measurement was not serious, however, since the inlet- and exhaust-impulse targets were calibrated satisfactorily.

Attachment of the combustion tubes to the valve-plate housings was accomplished by screwing the tubes into flanged end fittings and then bolting these end fittings to the valve-plate housings (see Figure 9). The front end fitting consisted of a single solid piece of metal, i.e., relative motion between the front end of the tube and the front valve-plate housing was not permitted. The rear end fitting, on the other hand, consisted of a flanged portion and a threaded portion, and these were designed so that the threaded portion could slide axially within the flanged portion, i.e., relative motion between the rear end of the tube and the rear valve-plate housing was permitted. This arrangement permitted the combustion tube to expand as it was heated. The resistances of the heat paths between the tube end fittings and the valve-plate housing were increased by decreasing the contact area between the fittings and the housings. Increasing these resistances reduced the heat transfer rate and increased the temperatures of the tube ends during the tests. A photograph of the combustion tube showing the high frequency pressure gage, the glow plug, and the flanged end-fittings is shown in Figure 9.

The walls of a Multi-Jet engine combustion tube must be heated to a required minimum temperature before the engine can be cycled using surface combustion to ignite the fuel-air mixture during each cycle. This required minimum temperature can be obtained by any one of three

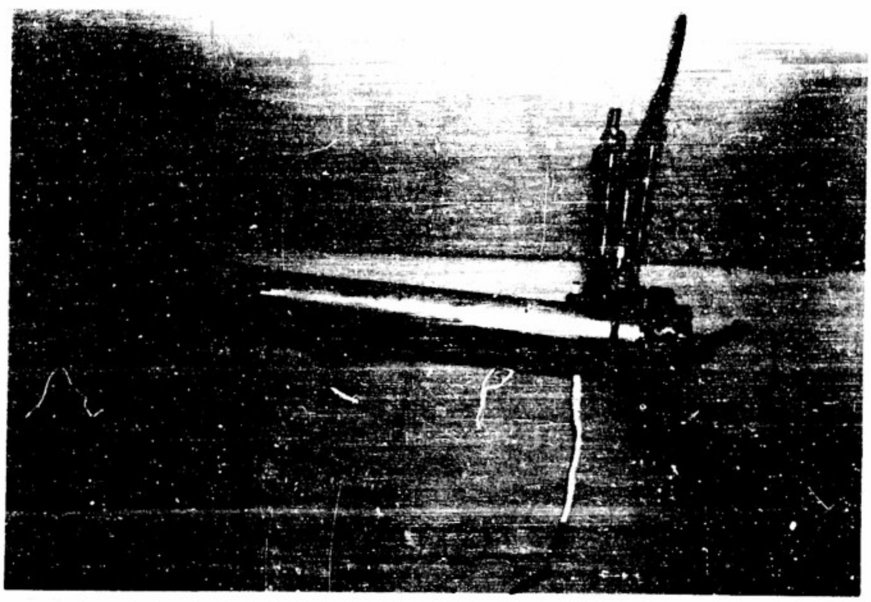

Figure 9. Combustion Tube, Flanged End Fittings, Pressure Gage and Glow Plug

means: (1) by holding a flame ahead of the tube inlet and passing the hot gases through the tube with the valves held in the open position; (2) by operating the engine at reduced air-flow rates and igniting the fuel-air mixture with a spark plug; and (3) by operating the engine at reduced air-flow rates and igniting the fuel-air mixture by means of a glow plug (rather than a spark plug). The third method was found to be more satisfactory than the first two. The first method resulted in slow heating of the combustion tube, unnecessary heating of the inlet valve, and partial obstructing of the air-supply duct. The second method also resulted in slow heating of the combustion tube since the frequency of spark discharge was not high enough to ignite the fuel-air mixture during every cycle.

Air-flow rate was computed from the measured pressure drop across a sharp-edge orifice designed in accordance with specifications of the American Standards Association. In order to simplify the calculations, the air-supply line was arranged so that the pulsations set up by the engine were damped out before they propagated upstream to the metering orifice. The damping was accomplished by a surge chamber (the inlet impulse target) and a throttle valve installed between the orifice and the engine. A given throttle-valve setting held the air-flow rate constant since the average pressure downstream of the throttle valve did not vary appreciably during a test, and the pressure upstream of the throttle valve was held constant by a pressure regulator in the air-supply system.

Several methods of introducing fuel into the combustion chamber were considered: (1) steady injection of fuel into the air-supply duct at a point far upstream from the engine where the air-flow rate is steady; (2) injection of fuel at a constant supply pressure directly into the combustion chamber at a point immediately behind the inlet valve; (3) periodic injection of fuel directly into the combustion chamber; (4) steady injection of fuel into the air-supply duct at a point immediately upstream from the inlet valve; and (5) periodic injection of fuel into the air-supply duct at a point immediately upstream from the inlet valve. Periodic injection at the high cycle frequencies which were realized was considered impractical. Steady injection at a point upstream from the inlet valve was accompanied by flame holding and by burning within the inlet valve-plate housing, and this method was also considered unsatisfactory. Consequently, the second method was used during most of the tests, even though the possibilities existed that fuel-air mixing was not complete and that some fuel was wasted. Note that the pressure variations within the combustion chamber were such that the fuel-injection rate was greatest during the scavenge phase and smallest during the late portion of the combustion phase and the early portion of the exhaust phase. Fuel-flow rates were measured with a Fischer-Porter flowmeter. The propagation of pressure fluctuations from the combustion chamber to the flowmeter was prevented by the damping action of the pressure drop and the volume in the fuel-supply line. A diagram of the air-flow and fuel-flow lines is given in Figure 10.

The time-averaged impulse of the entering and leaving fluids was measured directly. Two methods exist for the determination of these impulses: (1) the time-averaged impulse may be measured directly with

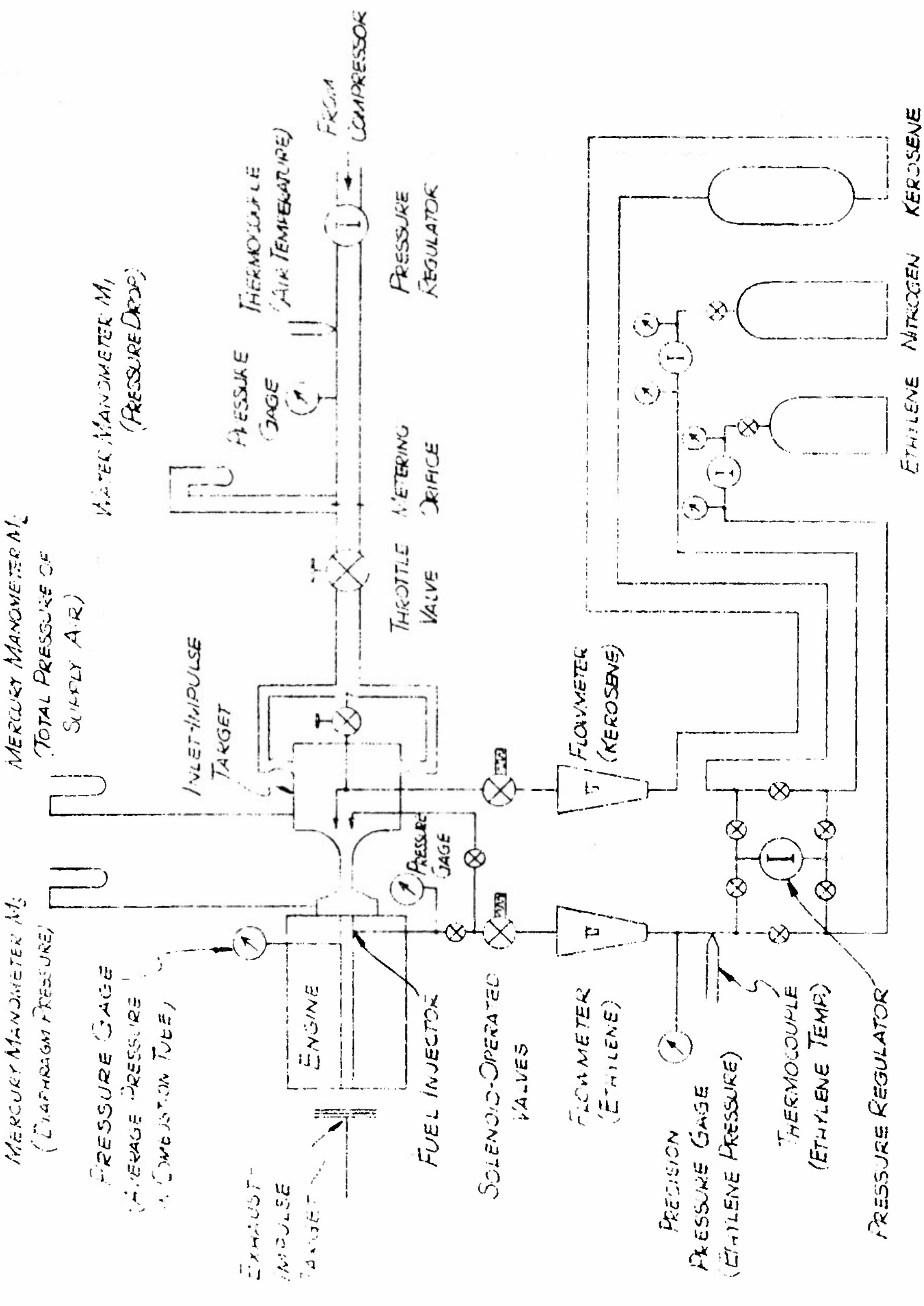

FIGURE 10
FUEL-FLOW AND AIR-FLOW DIAGRAM

the aid of impulse targets; and (2) velocity, temperature, and pressure profiles may be measured as a function of time, and the time-averaged impulses may then be calculated from these measured quantities. The first of these methods was used in the present study since it appeared to be the simplest of the two existing methods. The two impulse targets were mounted on two separate sets of glycerin-supported pontoons in order to minimize measurement errors due to friction. The arrangement of the four carriers for the inlet impulse target is pictured in Figure 11. Each carrier consists of a tank, a float, and the glycerin needed to fill the space between the tank and the float. Motion (in a direction parallel to the engine axis) of the floats relative to the tanks is restricted by strain-gage force pickups as shown in Figure 12. A photograph of the strain-gage force pickup is shown in Figure 13. The original exhaust impulse target is shown on the left in Figure 14. Calibration of this target indicated that it did not function properly. Satisfactory results were obtained, however, after a flat plate covered with fifteen layers of wire net (see Figure 15) was installed in place of the original aft impulse target. This flat plate impulse target was designed and installed according to the information obtained from Reference 2. A photograph of this target mounted on its carriers is shown in Figure 16. In order to prevent the destruction of the exhaust target by the exhaust gases, water was run over the galvanized steel wire mesh covering the target. This water was turned off momentarily when thrust measurements were made.

Air was supplied to the inlet impulse target (Figure 17) through

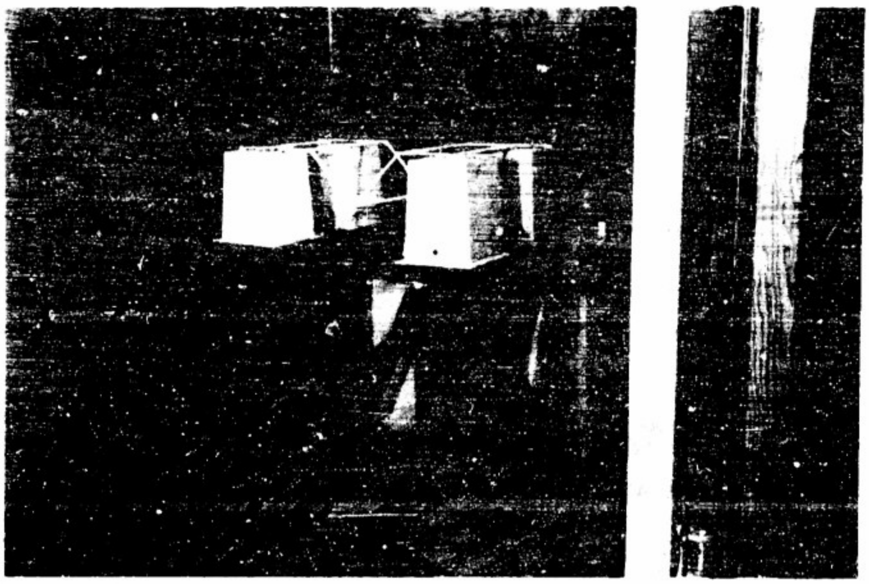

Figure 11. Carriers for Inlet Impulse Target

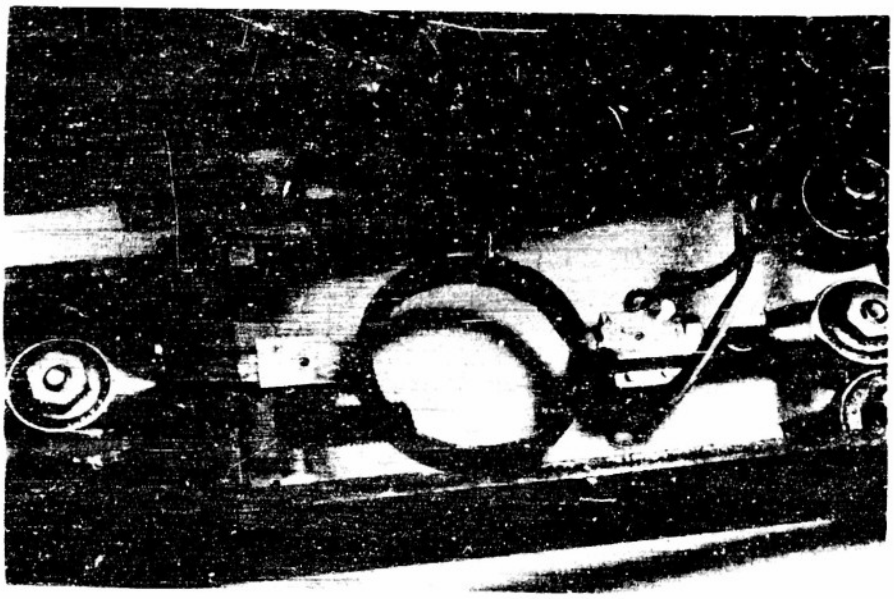

Figure 12. Mounting for Strain Gage Force Pickup

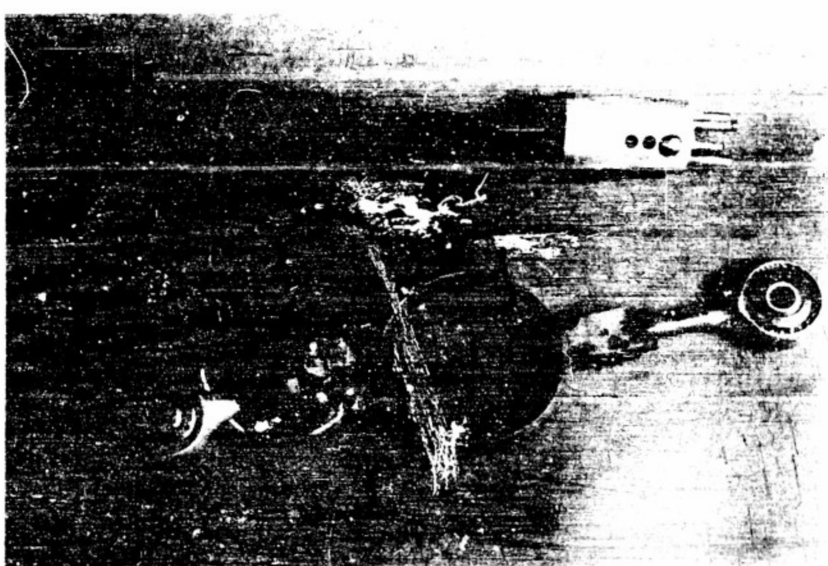

Figure 13. Strain Gage Force Pickup

Figure 14. Layout of Multi-Jet Test Engine No. 2 and the Impulse Targets

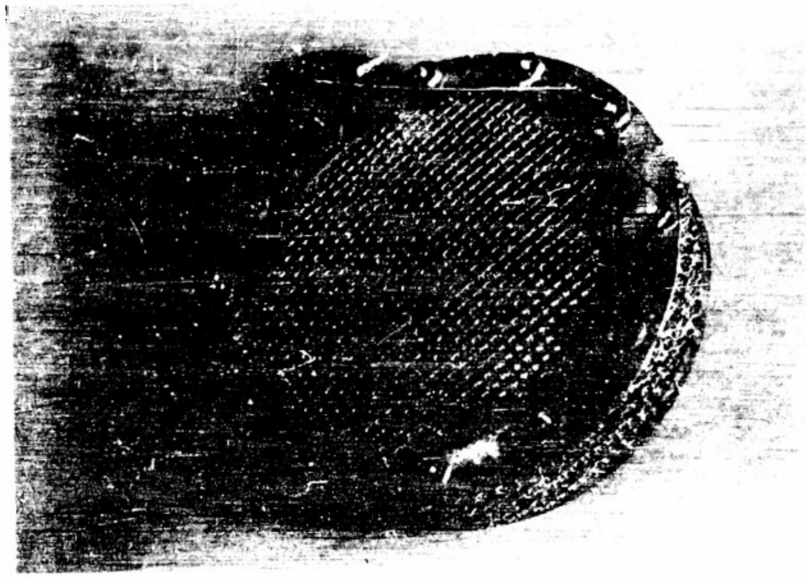

Figure 15. Exhaust Impulse Target

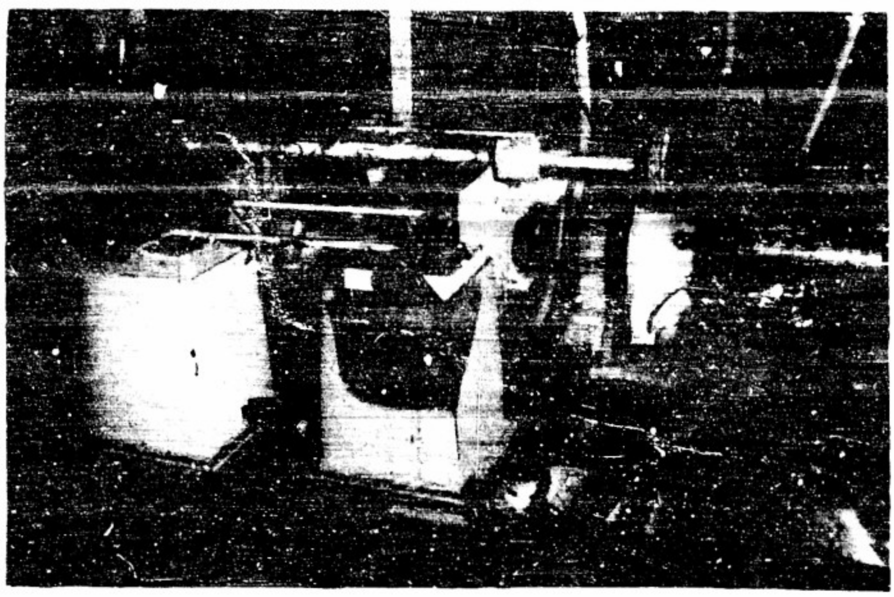

Figure 16. Exhaust Impulse Target and its Carrier

two large flexible hoses arranged so as to direct the air into the target at right angles to the engine axis. A flexible air-tight connection was required at the joint between the inlet valve-plate housing and the inlet impulse target in order to permit unrestricted motion of the inlet target with respect to the engine without incurring any loss of supply air. Two types of flexible joint were considered: (1) a flexible metal bellows, and (2) a diaphragm-type bellows incorporating a rubber-impregnated cloth diaphragm. A metal bellows having sufficient flexibility could not be found, and consequently the second type of bellows was used. This bellows consisted of a circular diaphragm with a hole cut in the center. The outer periphery of the diaphragm was attached to the inlet valve-plate housing, and the inner periphery was attached to the inlet impulse target (Figure 18). The pressure force acting on the diaphragm was balanced by two reactions -- one reaction acting at each periphery of the diaphragm. The magnitude of each of these reactions was related analytically to the magnitude of the pressure force acting on the diaphragm. Since the reaction on the inner periphery was transmitted to the strain-gage force pickup attached to the inlet impulse can, the magnitude of this reaction was calculated and then subtracted from the measured force on the inlet impulse target in order to obtain the magnitude of the inlet impulse. This system was calibrated by applying a known pressure to the inlet target while the air flow to the engine was blocked off. The resulting calculated reaction force equaled the measured force within experimental error. Checks with pulsating flows of cold air indicated that the inlet-impulse measurements were accurate within six percent.

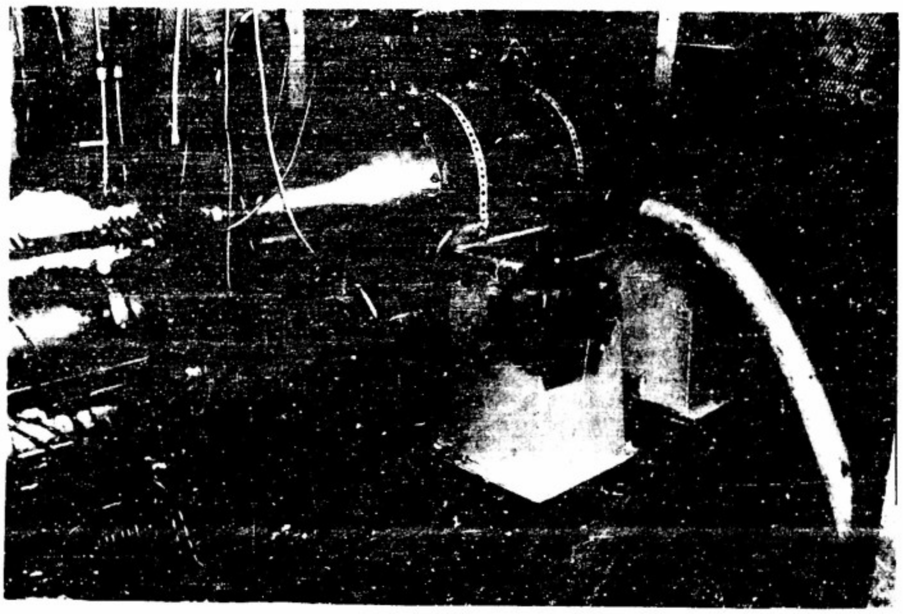

Figure 17. Inlet Impulse Target

FIGURE 18

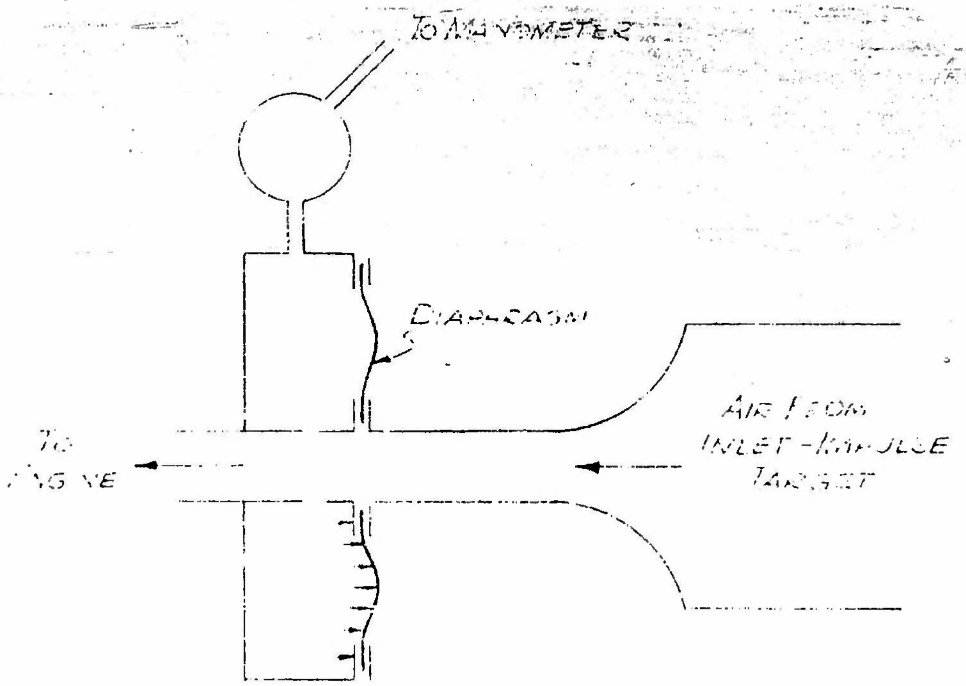

FLEXIBLE JOINT
CONNECTING INLET IMPULSE TARGET
AND ENGINE

A diagram of the engine, showing the arrangement of the impulse targets, force rings, pontoons, combustion tube, and drive motors, is given in Figure 19. A photograph of the engine is shown in Figure 20.

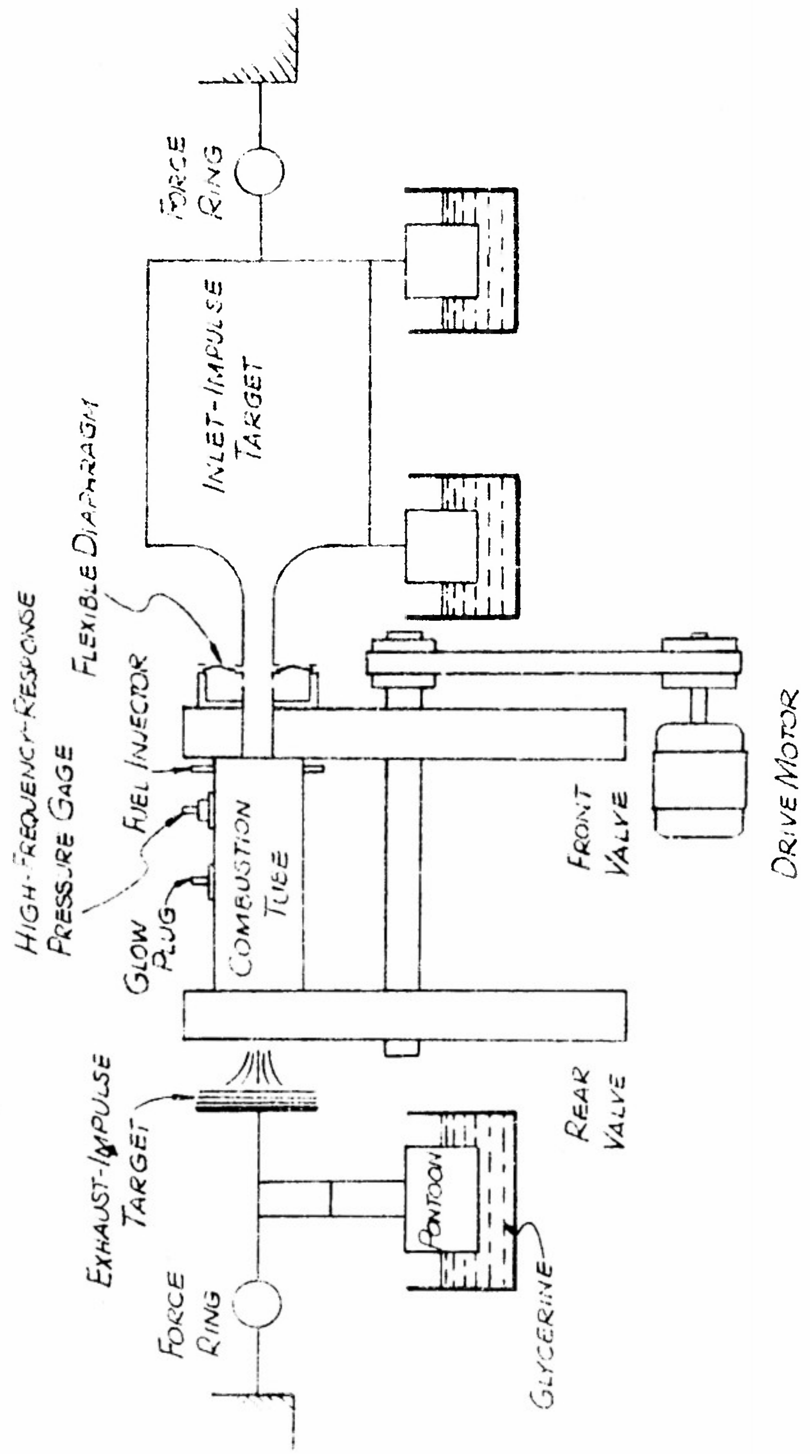

FIGURE 19

MULTI-JET TEST ENGINE NO. 2

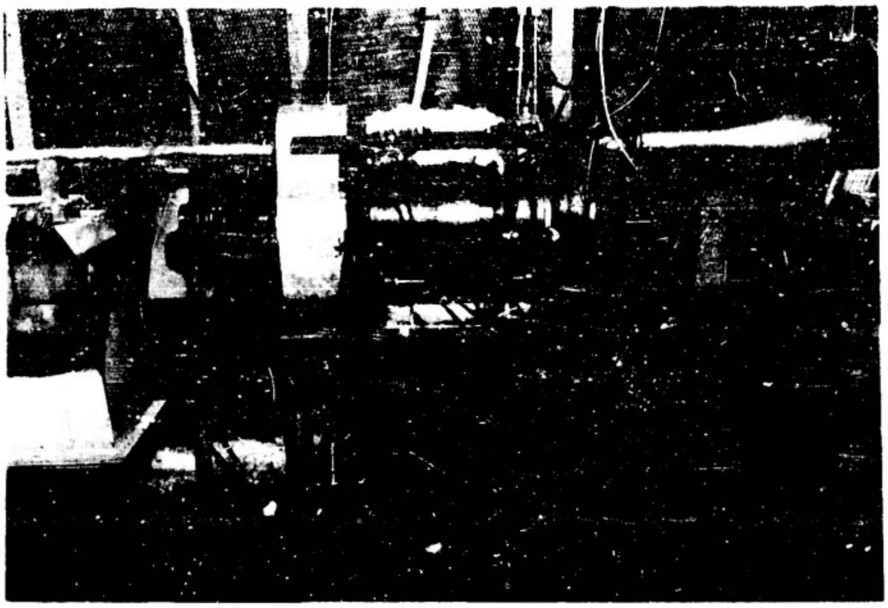

Figure 20. Multi-Jet Test Engine No. 2.

SECTION III

INSTRUMENTATION FOR MULTI-JET TEST ENGINE NO. 2

3.1 Introduction

For use in conjunction with Test Engine No. 2, instruments were assembled which facilitated (1) the development of an engine which operated on the Multi-Jet cycle, and (2) the obtaining of the performance characteristics of a Multi-Jet engine. (See Section 4.3 for details of the program objective.) The engine-development phase required that combustion-chamber pressures be measured and related to the valve-opening and valve-closing times; the performance-testing phase required that the engine thrust and fuel consumption be measured accurately.

The following quantities were determined from measurements made during the tests:

1. Pressure in the combustion chamber
2. Angular speed of the valve plates
3. Angular position of the valve plates
4. Relative length of the several phases of the cycle
5. Forces acting on the impulse targets
6. Rate of fuel flow
7. Rate of air flow
8. Temperature of the combustion-chamber wall
9. Temperature of the valve-plate housing
10. Temperature of the rotor bearings
11. Temperature of the high-frequency-response pressure pickup.

Photographs of the instrument panels are included in Figures 21

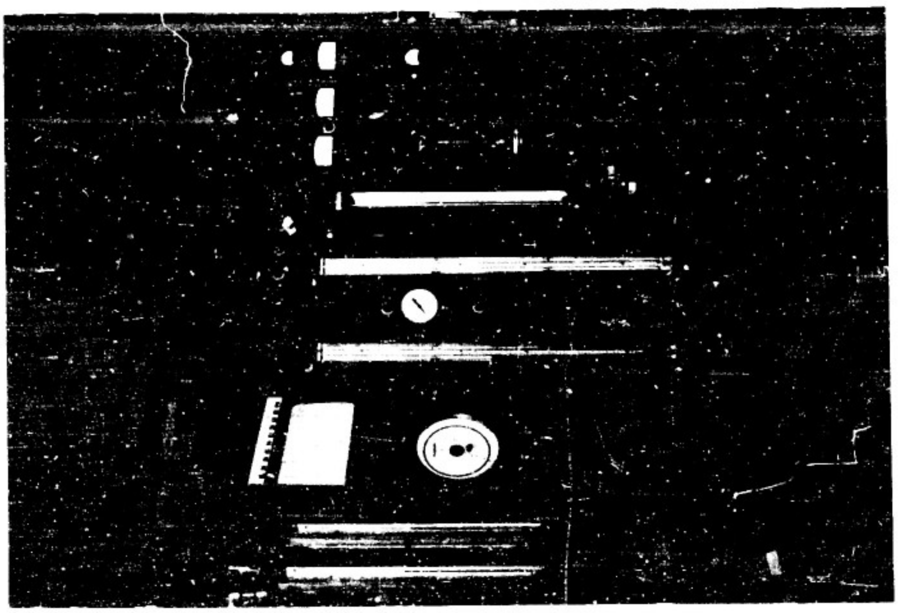

Figure 21. Instrument and Control Panel for Test Engine No. 2 (Left Side)

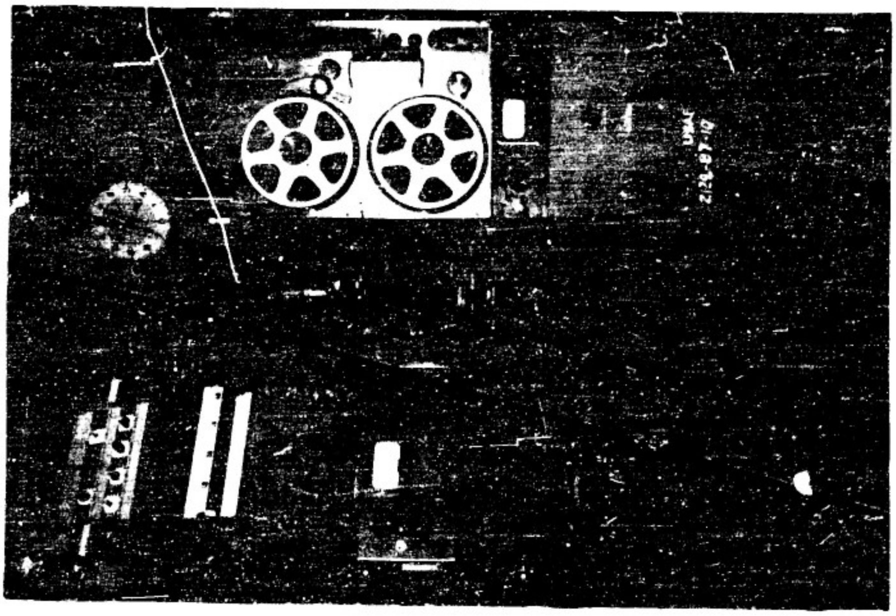

Figure 22. Instrument and Control Panel for Test Engine No. 2 (Right Side)

and 22. Detailed descriptions of the electrical circuits employed in the instrumentation used in the Multi-Jet tests are contained in the Appendix.

3.2 Measuring Combustion-Chamber Pressures

Providing instrumentation for measuring combustion-chamber pressures as a function of time was one of the most difficult (and most important) of the instrumentation problems encountered during this program. Although several good pressure pickups were available commercially, most of these were not suited for this test program because they did not meet all of the following requirements: (1) measure pressures from 0 to 150 psig; (2) respond accurately to frequencies from 0 to 10,000 cycles per second; (3) function properly with the diaphragm exposed to gases at 3000°F; and (4) possess a diaphragm with diameter small enough to permit mounting of the pickup diaphragm flush with the inside of 3/8-in. combustion chamber. (It was necessary that the diaphragm be mounted flush with the inside of the combustion chamber in order to avoid introducing on the combustion-chamber wall irregularities which would reflect pressure or expansion waves passing axially through the combustion chamber.)

A 14-mm-diameter water-cooled variable-capacitance-type pressure pickup (Cf. Ref. 3) manufactured by Photocon Research Products of Pasadena was selected and used. This pickup has a free-diaphragm diameter of approximately 3/8 inch. Although a smaller free-diaphragm diameter was desired, this pickup was acceptable for investigating pressures in the large combustion tubes (in those tubes having diameters equal to or greater than 5/8 inch) and in the square tubes.

Although pressure pickups of this type had been used frequently in piston and rocket-type engines, the problem of holding pickup component temperatures at a safe level during use on a Multi-Jet combustion tube proved relatively difficult. Test durations were greater than are encountered in rocket engine tests; combustion-chamber wall temperatures were higher than are encountered in piston-engine tests. Consequently, the pressure pickup was damaged by heat on several occasions during the test program. The problem was solved by modifying the cooling system so that water could be passed through a jacket surrounding the pickup as well as through holes penetrating the diaphragm, and the pickup was used in subsequent Multi-Jet tests without further heat damage.

The electrical output of the pressure pickup was fed into an oscilloscope whose sweep was triggered at the same point during each engine revolution by instruments measuring the angular position of the valve plates. Thus, if the engine was firing regularly, the oscilloscope beam would continuously retrace its path, and a stationary pattern would register on the oscilloscope screen. Photographs could be taken of this screen in order to provide permanent records of the pressure-time diagram.

This pressure pickup was calibrated periodically during the contract period. Shortly after the pickup was received, it was installed in the wall of the shock tube (see Figure 28, Section 4.2), and its response characteristics were checked. The rapidity of response and the damping were found to be appropriate for the present application. Shock waves having known pressure ratios were passed over the pickup diaphragm, and the calibration curve obtained in this manner was compared with the calibration curve obtained by applying static pressures to the diaphragm. Since these two calibration curves agreed within the limits of expected experimental error, subsequent calibrations of the high-frequency-response pressure pickup were obtained by applying only static pressures to the diaphragm.

3.3 Determining Angular Speed and Angular Position of Valve Plates

In order to facilitate the development of an engine operating on the Multi-Jet cycle, means for determining (1) the valve-opening and valve-closing times relative to the several portions of the pressure-time diagram and (2) the cycle frequency must be available. Consequently, instrumentation for obtaining these data were selected and assembled.

It was decided to relate the angular positions of the valve plates with the several portions of the pressure-time diagram by dimming the oscilloscope beam whenever the valve-plate rotor reached a specified angular position. This dimming was accomplished as follows: A variable-reluctance magnetic impulse generator was attached near each valve plate in such a manner that the generator could detect the passing of the leading and trailing edges of the valve-plate blades, and the generator signals were timed (by locating the generator appropriately) so that the oscilloscope beam was dimmed four times during each engine cycle -- once each time that either end of the combustion tube was half open or half closed. A determination of other rotor postions (e.g., the time when the aft end of the combustion tube begins to open) could be accomplished by interpolating linearly between the known locations.

It was necessary to differentiate between the four signals being sent out during each engine cycle, i.e., it was necessary to determine which signal belonged with which valve-plate position. This differentation was accomplished by making one of the signals longer than the other three. A photograph of the oscilloscope beam trace, showing the four signals sent out by the valve, is presented in Figure 23.

For convenience in observing the pressure-time diagram, provisions were made for starting the sweep of the oscilloscope beam by means of one of the above-mentioned valve-position signals.

The rotor speed (related directly to the cycle frequency) was obtained by measuring the impulse production rate of the impulse generator. This speed was indicated by a voltmeter and recorded by a recording potentiometer.

3.4 Recording, Storing, and Reviewing Combustion-Chamber Pressure-Time Histories

In order to facilitate the test program, it was desirable that a record of the combustion-chamber pressure vs. time variations be obtained for reference use after the completion of an engine test. The oscilloscope-camera records were not sufficient for this purpose since photographs of this type could be taken only periodically. Consequently, a tape recorder was purchased and used to record the desired pressure-time histories. The tape recorder selected possessed characteristics which permitted (1) the recording of absolute as well as relative pressures and (2) the superposing of impulses indicating valve-plate position on the pressure-time record.

In order to determine the magnitude of pressure-pickup output,

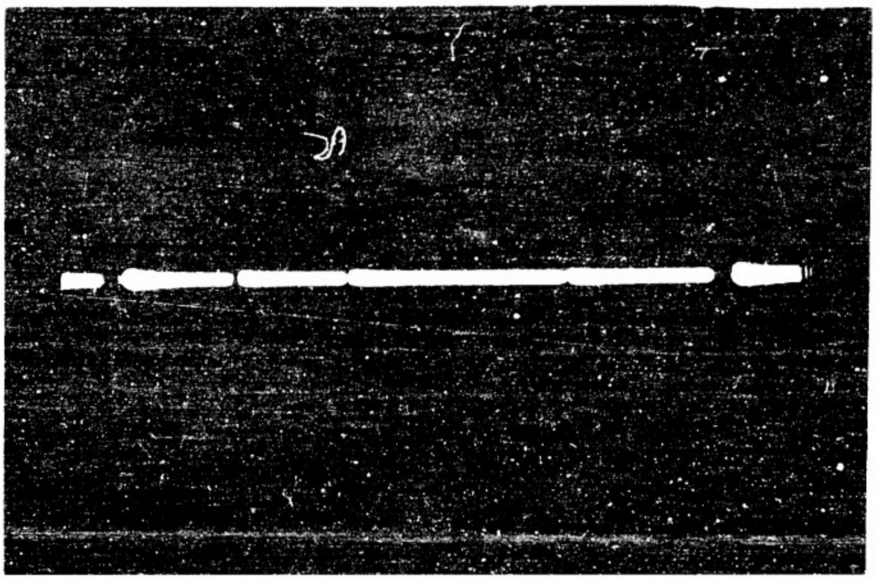

Figure 23. Oscilloscope Trace Modulated by Valve Timing Marks

equipment which permitted the recording of known calibrating voltages on the tape was assembled, and the output of the high-frequency-response pressure pickup was compared with these known calibrating voltages.

Data obtained during motor tests and stored on the tapes were reviewed by playing back the record and feeding the output of the player into an oscilloscope. In this manner the pressure-time diagrams and the valve-opening and valve-closing times could then be reviewed visually, and photographic records could be made by photographing the oscilloscope screen.

3.5 Measuring Temperatures, Forces, and Flow Rates.

Instruments were provided also to facilitate the recording of data from which quantities such as engine thrust, fuel-flow rate, air-flow rate, and miscellaneous temperatures were calculated.

Forces on the impulse targets were measured by means of force rings which incorporated strain-gage bridges. (Special force rings were fabricated to ADC specifications by Micro Test Inc.[1] of Los Angeles, California.) The outputs of these force rings were recorded on a self-balancing recording potentiometer, and the net thrust was calculated by subtracting the magnitude of the inlet impulse from the magnitude of the exit impulse.

The fuel-flow rate was measured with a Fischer-Porter flow meter. The temperature of the fuel in the flow meter was measured with the

---

[1] Micro Test Inc., 657 No. Spaulding Ave., Los Angeles 36, California

aid of a copper-constantan thermocouple, and the pressure in the meter was measured with a dial manometer. Corrections to the measured fuel-flow rate were made for fuel temperature and pressure deviations from standard conditions.

The air-flow rate was measured with the aid of a sharp-edge orifice designed in accordance with American Standards Association specifications. Pressure differential across the orifice was indicated by a water manometer; pressure upstream of the orifice was measured with a Bourdon-tube gage; and temperature upstream of the orifice was measured with the aid of a copper-constantan thermocouple.

Temperatures of the rotor bearings, the valve-plate housings, and the base of the high-frequency-response pressure pickup were measured in order to determine whether or not these temperatures were being held within safe limits. Chromel-alumel and copper-constantan thermocouples facilitated these measurements.

The temperature of the combustion-tube wall was measured in order to determine the relationship between this temperature and combustion-tube wall surface-ignition characteristics. Platinum and 87%-platinum 13%-rhodium thermocouples were used for these measurements. All thermocouple outputs were recorded on self-balancing recording potentiometers.

SECTION IV

EXPERIMENTAL TESTS

4.1 Experimental Tests Involving Multi-Jet Test Engine No. 1.

Since several questions of a qualitative nature relating to the operation of Multi-Jet test engines remained unanswered at the beginning of the present contract period, and since Multi-Jet Test Engine No. 2 was not scheduled to be put into operation until the seventh month of this contract period, Multi-Jet Test Engine No. 1 was reassembled and subsequently used in qualitative studies related to the Multi-Jet engine development program. The simplicity of this engine facilitated the quick obtainment of useful qualitative answers. However, this simplicity, together with the lack of adequate instrumentation, also precluded the extraction of accurate quantitative data. A photograph of Multi-Jet Engine No. 1 is shown in Figure 24. Figure 25 shows the engine together with its control panel and safety box.

In tests performed during the previous contract period, the combustion-chamber walls were heated to the minimum temperature required for initiation of surface combustion by passing a burning ethylene-air mixture through the combustion tube while the valves were held in the open position. Since this method was slow and resulted in undesirable heating of the inlet valve, the feasibility of operating the engine with spark- or glow-plug ignition and with reduced air-flow rates in order to heat the combustion-chamber walls to the minimum temperature required for initiation of surface combustion was investigated during the present contract period. Tests indicated that satisfactory heating was obtained with both types of plugs but that more

Figure 24. Multi-Jet Test Engine No. 1

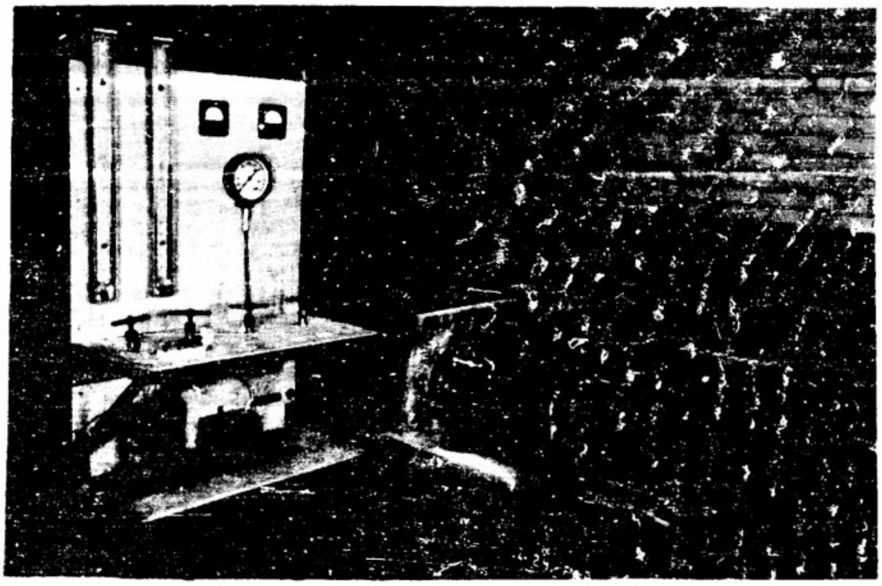

Figure 25. Multi-Jet Test Engine No. 1, Its Control Panel and Its Safety Box

rapid heating was obtained from glow-plug ignition (a continuous ignition source) than from spark-plug ignition (an intermittent ignition source). Glow-plug ignition was used therefore during the tube-heating period in all tests made with Test Engine No. 2.

The original volume between the front valve plate and the front valve-plate housing of Test Engine No. 1 was 45 cubic inches. During operation of the engine, a combustible fuel-air mixture entered and burned within the front valve-plate housing, heating the front valve plate and the neighboring engine components to excessive temperatures. Although experimental evidence was not available due to the lack of adequate instrumentation, it is believed that this burning in the front valve-plate housing appreciably impaired engine performance. The burning within the housing has been eliminated by reducing the volume between the valve plate and the valve-plate housing.

Originally, the combustion tubes were mounted in and attached to the rest of the engine by means of high-temperature-resistant refractory cements. It was found, however, that these cemented joints did not withstand the pressure forces encountered during the engine tests. Consequently, a new technique for mounting the tubes was sought, and threads cut into the outer surfaces at the ends of the Metamic tubes were found to be satisfactory. Axial expansion of the tubes was permitted by allowing the collar into which the aft end of the tube was screwed to slide (with only a small clearance) relative to the rear-valve-plate housing.

It was found also that Metamic may be cut, drilled, and tapped with standard metal-shop tools and practices, a desirable property.

A combustion tube constructed from a round Metamic tube is shown in Figure 26. It shows the ends threaded to receive the flanged end fittings, the 0.60 inch diameter hole drilled to receive the high frequency pressure pickup with a milled flat portion to receive the base of the pickup and a 1/4 inch hole drilled and tapped to receive the flow plug.

Combustion-chamber wall temperatures of 2700°F have been attained without any apparent detrimental effects on the Metamic combustion tubes, and peak combustion temperatures have been obviously higher. This property is also desirable, since calculations indicate that high thrust-to-weight ratios are obtained if high peak combustion temperatures can be utilized.

It has been noted that Test Engine No. 1 operated more satisfactorily with a combustion tube having a cross-sectional area of approximately 0.30 square inch than with a tube having a cross-sectional area of approximately 0.25 square inch. Similar observations were made while operating Test Engine No. 2 (Cf. Section 4.3).

In another investigation, a commercial high-frequency-response water-cooled pressure pickup was mounted on the combustion tube. The water cooling was found to be adequate when the combustion-tube wall was heated to 2300°F. The pressure pickup was attached originally to the Metamic combustion tube by means of bolts screwed into holes tapped in the combustion-tube wall. However, these screws melted at high combustion-tube wall temperatures. Attaching the pressure pickup to the combustion tube by means of a stainless-steel U bolt eliminated this problem. When the pressure pickup was mounted on a 5/8-inch-

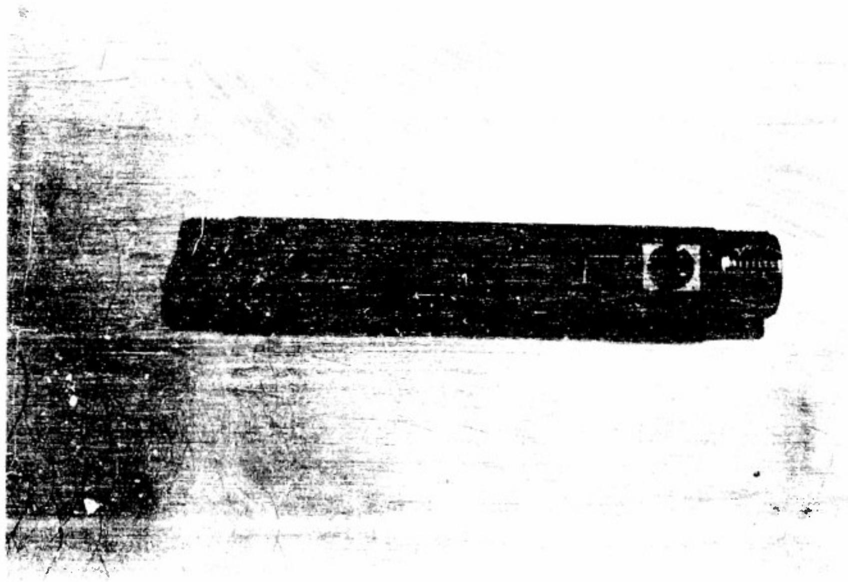

Figure 26. Metamic Combustion Tube

diameter combustion tube, a gas-tight seal between the pickup and the combustion tube was not maintained. A gas-tight seal was maintained, however, when the pickup was mounted on a square tube. (The square combustion tube permitted the use of plane joints. In Test Engine No. 2, when the pressure pickup was mounted on the 1-inch-diameter tubes, a flat surface was milled on the tube wall in order to allow the use of plane joints.) Springs which were inserted between the pressure-pickup flange and the tie-down nuts held this flange against the combustion tube even when the metals in the several components of the assembly expanded nonuniformly.

The feasibility of operating this engine with liquid hydrocarbon fuel has been investigated. After installing a pneumatic atomizing nozzle immediately upstream of the front valve, the engine was cycled using kerosene which had been atomized by the nozzle as a fuel. In order to heat the combustion-chamber walls to a temperature which would sustain surface combustion, the engine was cycled burning an ethylene-air mixture ignited by a glow plug. It was possible then to substitute a liquid fuel (kerosene) for the gaseous fuel (ethylene) and to cycle the engine burning a kerosene-air mixture ignited by the hot combustion-chamber walls. Tests indicated, however, that, in order to sustain surface combustion, a higher wall temperature is required with kerosene than with ethylene.

Tests have been made with a clover-leaf reed valve and a venturi carburetor installed at the inlet end of the combustion tube. With a clover-leaf reed valve located at the inlet end of the combustion tube and a rotating-plate valve located at the exhaust end, the adjustment of the compression-phase and combustion-phase length ratio and of the expansion-phase and scavenge-phase length ratio is accomplished automatically by the reaction of the clover-leaf reed valve to pressure forces. It was anticipated that this automatic proportioning of the phase lengths would facilitate a determination of the phase lengths permitting static operation of the engine and yielding optimum specific fuel consumption. It was anticipated also that the carburetor would eliminate the need for manual fuel-flow control. Preliminary tube-wall heating using a gaseous fuel (such as ethylene) and a continuous ignition source (such as a glow plug) was found to be unnecessary. Heating of the tube walls with a liquid fuel (gasoline) and an intermittent ignition source (spark plug) was accomplished satisfactorily. Manual control of the fuel-flow rate was found as expected, to be unnecessary. Pressure-time diagrams of the type reproduced in Figure 27, emphasizing that the length of the combustion phase could be decreased appreciably below the lengths previously used, have been obtained. In Figure 27, pressure increases downward while time increases from left to right.

4.2 Test Equipment for Studying Non-Stationary Surface Combustion.

The combustion phase of the Multi-Jet engine cycle was found to be the most difficult phase to analyze theoretically. Moreover, no detailed information concerning the ignition and burning of a combustible mixture which has been brought suddenly into contact with a heated solid surface was found in the available literature. Consequently, the length of the combustion phase (and the conditions which would favor rapid ignition and rapid burning) could not be predicted.

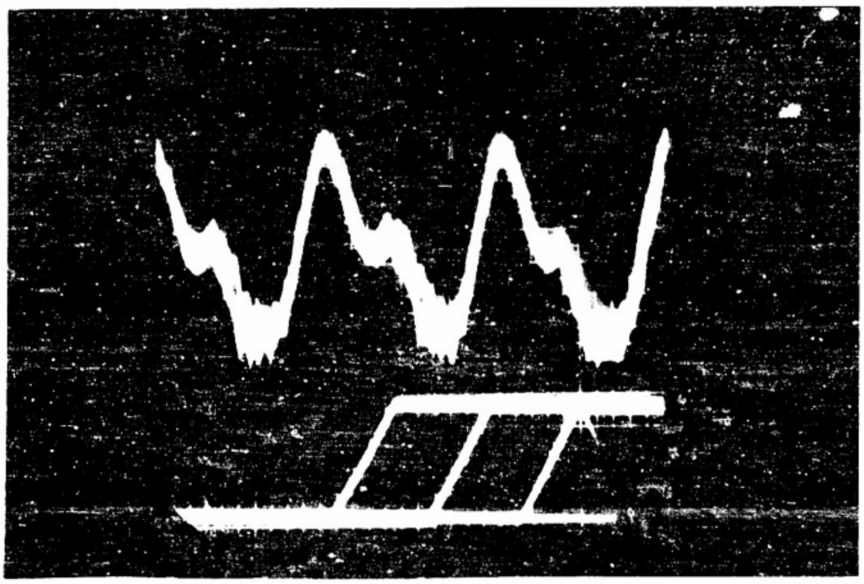

Figure 27. Pressure Time Diagram. Multi Jet Test Engine No. 1 with Reed Type Inlet Valve.

This information would be extremely useful, however, when developing an engine of the Multi-Jet type, and therefore, equipment for studying experimentally the ignition of a combustible mixture which has been brought suddenly into contact with a heated solid surface was assembled.

The test facilities consisted essentially of a test section attached to a shock tube. The shock-tube is pictured in Figure 28. (Both the shock tube and test section possessed square cross-sectional areas.) A heated surface (an electrically heated nichrome strip) constituted the lower inside surface of the test section, and the two sides of the section were comprised of observation windows. (See Figure 30.) The high-pressure side of the shock tube contained compressed air, and the low-pressure side contained a combustible fuel-air mixture. The combustible mixture was accelerated and passed over the heated surface by the action of a shock wave generated within the shock tube. The wave diagram is shown in Figure 32. The resulting phenomena were photographed employing three techniques: (1) high-speed photography, using a steady arc light and the schlieren technique; (2) snap-shot photography, using a spark light and the schlieren technique; and (3) high-speed photography, using light from the flame itself. The schlieren system is shown in Figure 29.

Most of the equipment used in conjunction with the shock tube was constructed originally as part of the instrumentation for Multi-Jet Test Engine No. 2. The shock tube itself was constructed of a standard steel square tubing which had been used first to calibrate the high-frequency-response pressure gage.

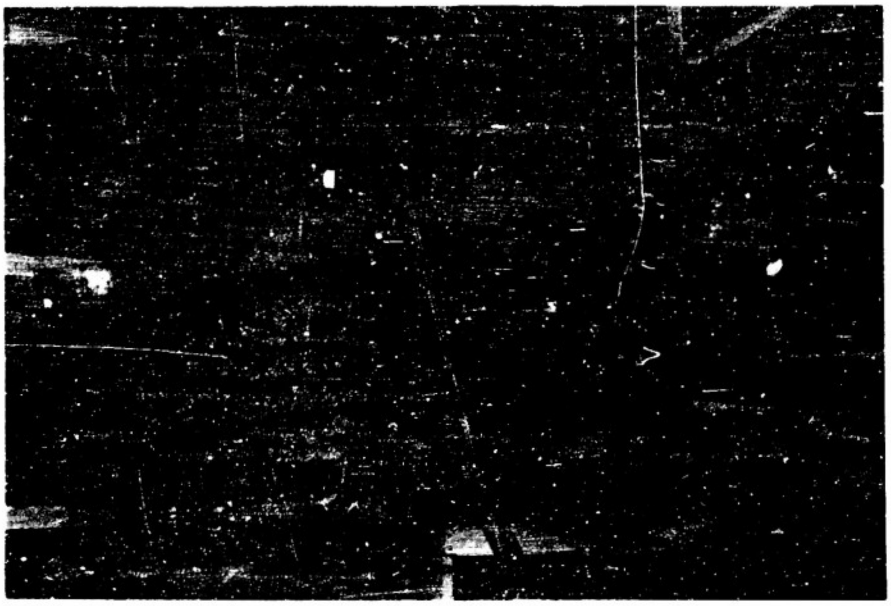

Figure 29. Layout of the Schlieren System

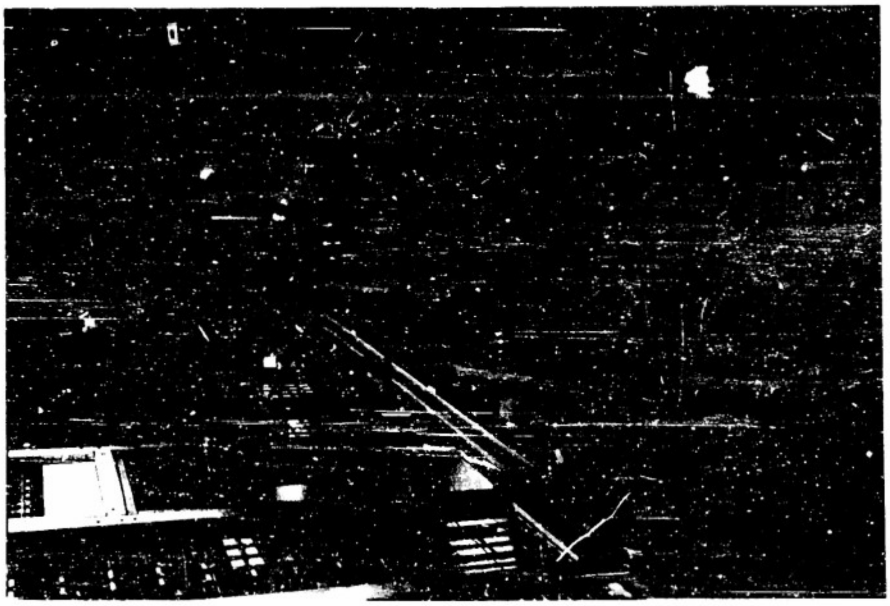

Figure 28. Layout of the Shock Tube

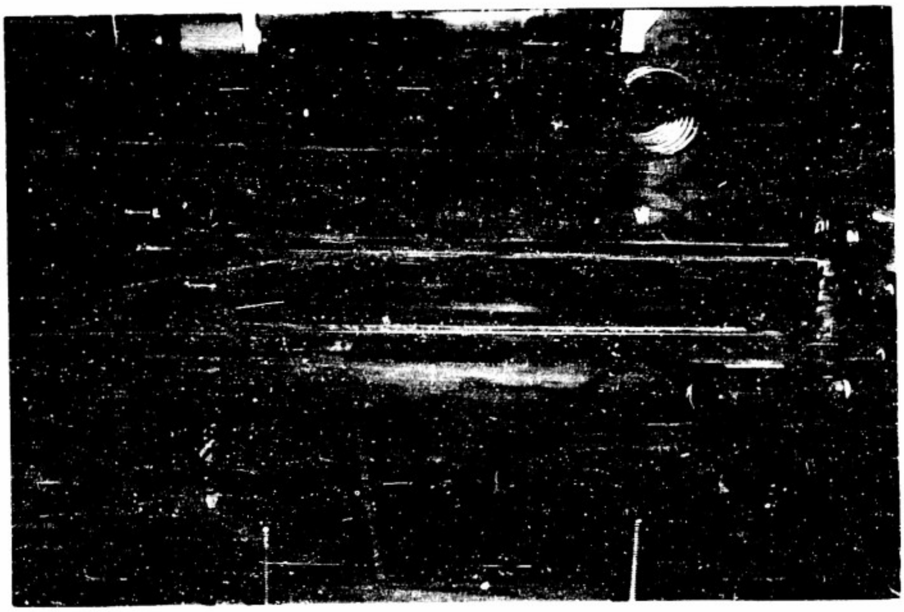

Figure 30. Test Section Showing the Heater Strips

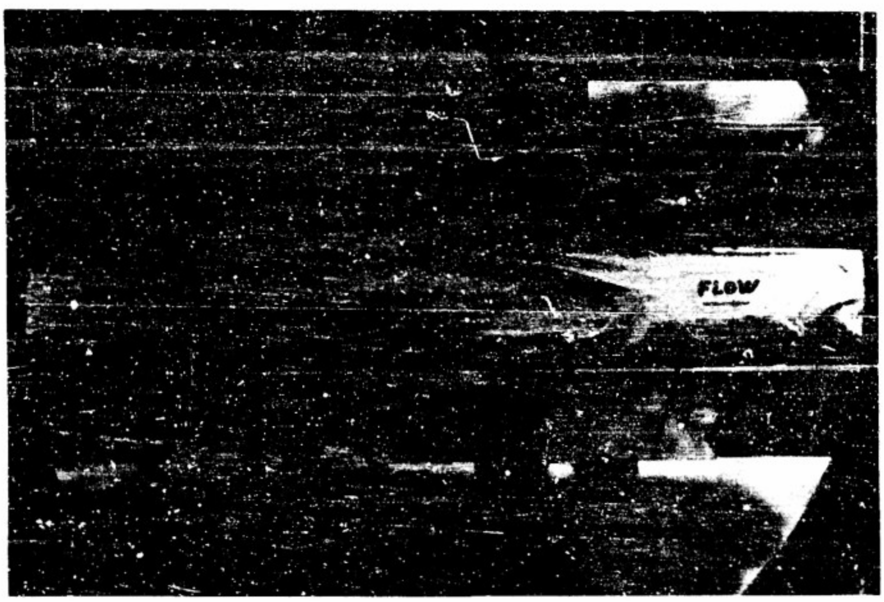

Figure 31. Spark Schlieren Photograph of the Flame

FIGURE 32

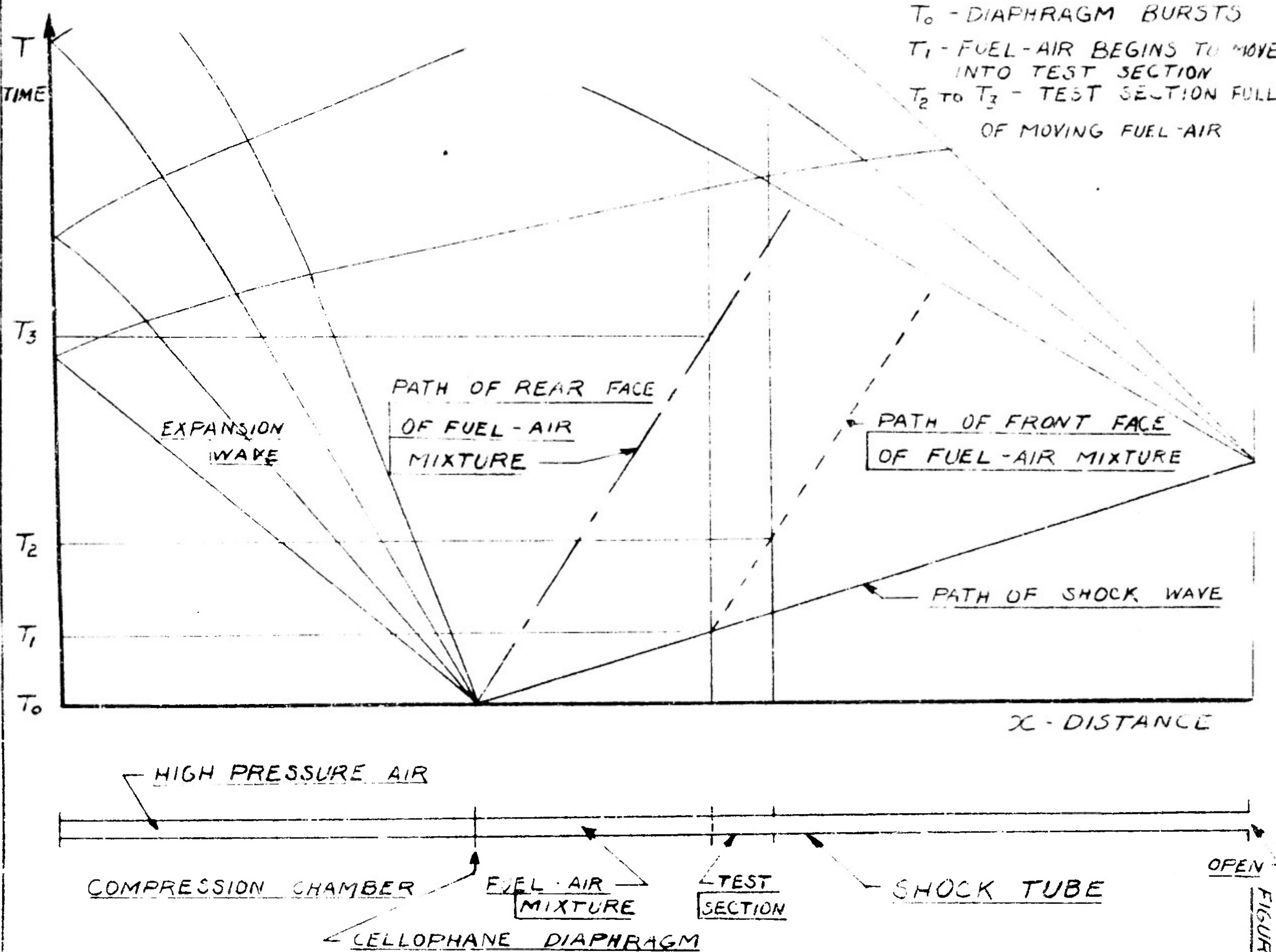

SHOCK TUBE AND WAVE DIAGRAM

The success of the Multi-Jet Engine (as for all constant volume combustion engines) depends to a large extent on the existence of very rapid burning. During the preliminary design studies (Cf., Reference No. 1) it was decided to use the surface combustion phenomenon in order to ignite the fuel-air mixture and burn it rapidly. It was assumed that as the combustible mixture moved into the tube the hot combustion-tube walls would heat those layers of the mixture adjacent to the walls to the ignition point. The mixture would burn then with a cylindrical flame travelling radially inward. Such a flame would have to travel only through the radius of the tube. The mixture that entered the tube first would be ignited first, and an oblique flame front would be formed at a small angle α with the combustion tube wall. A sketch of this phenomenon is shown in Figure 33. A number of questions which arose could not be answered analytically. It was necessary to know (1) the conditions under which ignition of the fuel-air mixture would occur and (2) the time-dependent shape and location of the flame front so that the Multi-Jet combustion-tube configuration could be determined. It was necessary also that the fuel-air mixture be ignited before the combustion tube was closed and that it be allowed to burn only after the tube was closed. A large value of combustion tube length as compared with Z and a large value of α would cause the mixture to burn at constant pressure (i.e., before the tube

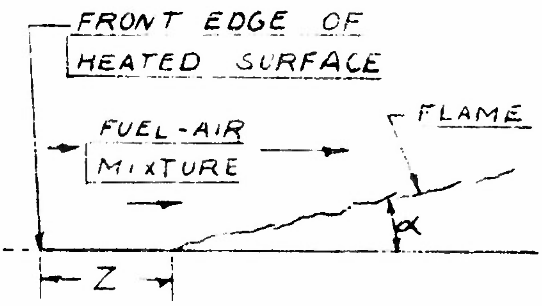

FIGURE 33 FLAME FORMATION

could be closed). Also, a tube length smaller than the distance Z would produce no ignition before the combustion tube was closed by the valves.

The shock tube as described above was capable of reproducing in two dimensions a close approximation of the conditions occurring in the Multi-Jet combustion tube as the combustible mixture travelled into and through the tube. High-speed photographs taken using light from the flame itself indicated that a combustion zone formed and decayed immediately adjacent to the heated surface. This combustion zone was of the type described above. High-speed photographs taken using a steady arc light and the schlieren technique could not be analyzed because random density gradients (produced by the heat of the carbon arc light source) existed in the schlieren field. Snap-shot photographs taken using a sychronized spark light and the schlieren technique were inconclusive since the trigger and synchronizing circuits were not operating consistently. However, density gradients which were interpreted to be the result of combustion were photographed. A typical photograph is shown in Figure 31.

The results of the preliminary study indicated that, with realistic improvements in photographic techniques, the ignition of a combustible mixture which has been brought suddenly into contact with a heated solid surface can be studied experimentally with relatively simple equipment. A few photographs such as shown in Figure 31 were taken, but sufficient data could not be obtained since practically all of this contractor's efforts were concentrated upon the testing with Test Engine No. 2. Very little effort would be required, however, in order to put the equipment into operation and to obtain information useful in determining the design of the Multi-Jet engine combustion tubes.

4.3 Experimental Tests Involving Multi-Jet Test Engine No. 2.

The primary objective of experimental tests involving Multi-Jet Test Engine No. 2 was to determine the specific fuel consumption of a Multi-Jet engine as a function of tube geometry, relative phase lengths, cycle frequency, valve leakages, and fuel-air ratio. The development of an engine which will operate on the Multi-Jet cycle, produce net thrust, and lead itself to quantitative testing constitutes the first step in such a program. The completion of this first step consumed most of the time remaining in this contract period after assembly of Test Engine No. 2 was completed.

Valve configurations which were tested in this engine are summarized in Table 1. The sum of the exhaust- and scavenge-phase durations is proportional to the angle subtended by the open portion of the exhaust-valve plate; the sum of the scavenge- and compression-phase durations is proportional to the angle subtended by the open portion of the inlet valve; the sum of the compression- and burning-phase durations is proportional to the angle subtended by the closed portion of the exhaust valve; and the sum of the burning- and exhaust-phase durations is proportional to the angle subtended by the closed portion of the inlet valve. The tests in which each of these valve configurations was used are noted at the top of the table.

Phase lengths and tube geometries which were tested in this engine are summarized in Table 2. The desired phase lengths were obtained by

TABLE I

CYCLE CONSTANTS DETERMINED BY CONFIGURATIONS OF VALVE PLATES TESTED IN ENGINE NO. 2

TEST	1-26	27-34	35-52	53-58	59-
EXH + SCAV	45	45	45	42.5	50.9
SCAV + COMP	45	49	39	34.5	34.5
COMP + BURN	45	45	45	47.5	39.1
BURN + EXH	45	41	51	55.5	55.5

selecting the appropriate valve plates and attaching them to the rotor shaft in the appropriate angular relationship.

Three methods of fuel injection were attempted: (1) injecting at constant pressure and at a point immediately upstream from the front valve into a tube having the same diameter as the combustion-tube; (2) injecting at constant pressure into the combustion tube at a point immediately downstream from the inlet valve; and (3) injecting far upstream from the inlet valve (i.e., where the air flow is steady).

The first of these methods was used in tests 1 through 14, the third was tried in tests 46 and 50, and the second was used in all other tests. It was observed in tests 1 through 14 and 46 and 50 that the combustible mixture was burning within the front valve housing before it entered the combustion tube, whereas in all other tests no burning occurred within this housing.

The burning of the fuel-air mixture at the front valve could be due either to the fact that the valve is enclosed in a housing where the combustible mixture can collect and burn, or to the poor valve timing encountered in the early tests (e.g., a long pulse compression phase would allow the compression wave to move out of the front end of the tube, carrying a flame which ignites the combustible mixture and causes it to burn within the inlet valve housing). Injection of fuel directly into the combustion tube eliminated the presence of a combustible mixture in the inlet valve housing and therefore prevented any flameholding there. The problem of flameholding at the inlet valve should not be encountered in the flight model of the Multi-Jet Engine, which will contain a multiplicity of tubes, since there will be a con-

TABLE 2

TUBE GEOMETRICS & RELATIVE PHASE LENGTHS
TESTED IN ENGINE NO. 2

TEST NO.	1-5	6-17	18-26	27-34	35-37	38-40	41-46	47-51	51	52	52	53-58	59-68	69-
EXHAUST	17.5	5	10	10	13	8	17	22	24	20	18	20.5	14.4	18.7
SCAVENGE	27.5	40	35	35	32	37	28	23	21	25	27	22.0	34.5	34.5
COMPRESS	17.5	5	10	14	7	2	11	16	18	14	12	12.5	-2.0	2.0
BURN	27.5	40	35	31	38	43	34	29	27	31	33	35.0	39.1	37.1
TUBE L	6	6	6,9	9	6	6	9,12	12	12	12	12	12	12	12
TUBE I.D.	5/8	5/8	5/8	5/8, 1" 1/2 SQUARE	1" ROUND 9/16 SQ.	1" ROUND 9/16 SQ.	1	1	1	1	1	1	1	1

tinuous flow of air around the valve.

The leading edges of the valves used in tests 1 to 26 were not bevelled. Starting with test 27, the leading edges were bevelled in order to give the valve plates a streamline cross-section in the direction of rotation (see Figures 6 and 7, Section II).

The air-supply duct for tests 1 to 14 is shown in Figure 34. During these tests the inlet impulse target was attached directly to the front valve housing, and no thrust measurements were made. The air-supply duct between the inlet impulse target and the inlet valve housing for tests 15 to 56 is shown in Figure 35. The thin rubber membrane used at the joint between the inlet impulse target and the inlet valve housing was not successful since it could not hold the high pressures existing in the air supply line. Starting with test 57, therefore, a diaphragm was installed at the joint between the impulse target and the engine (see Figure 36). A description of this diaphragm and of the calibration of the inlet impulse target is given in Section II.

Since all the test results from Test Engine No. 1 were obtained with a round Metamic tube 5/8 inch in diameter and 6 inches long, it was decided to install a similar tube in Test Engine No. 2 during the first test runs. The heating rate was fair on these first tests. After installing a 9/16-inch square tube 6 inches long with the pressure pickup mounted 2 inches from the inlet valve, it was observed that the heating rate was reduced appreciably. This was probably due partly to the cooling effect of the water-cooled pressure gage and partly to the smaller cross-sectional area of the square tube. This

FIGURE 34

AIR-SUPPLY DUCTING TO ENGINE
FOR TESTS 1 THROUGH 14

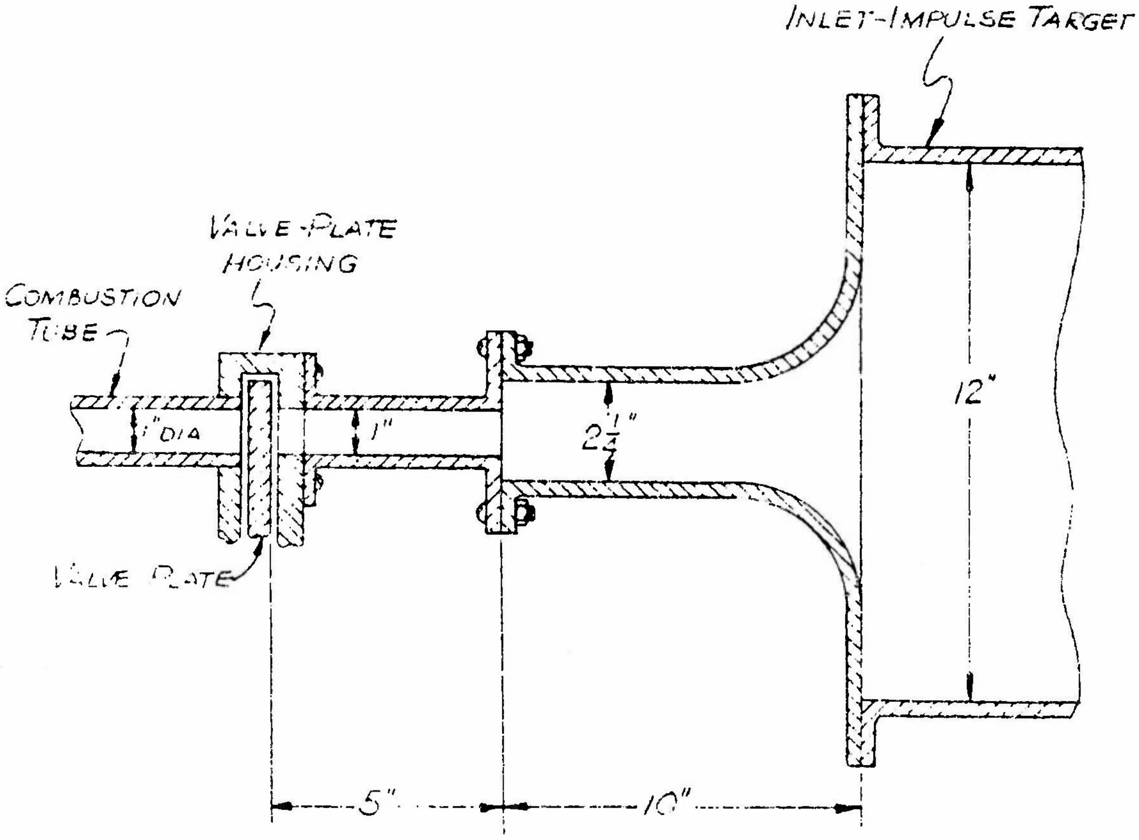

FIGURE 35

AIR-SUPPLY DUCTING TO ENGINE FOR TESTS 15 THROUGH 56

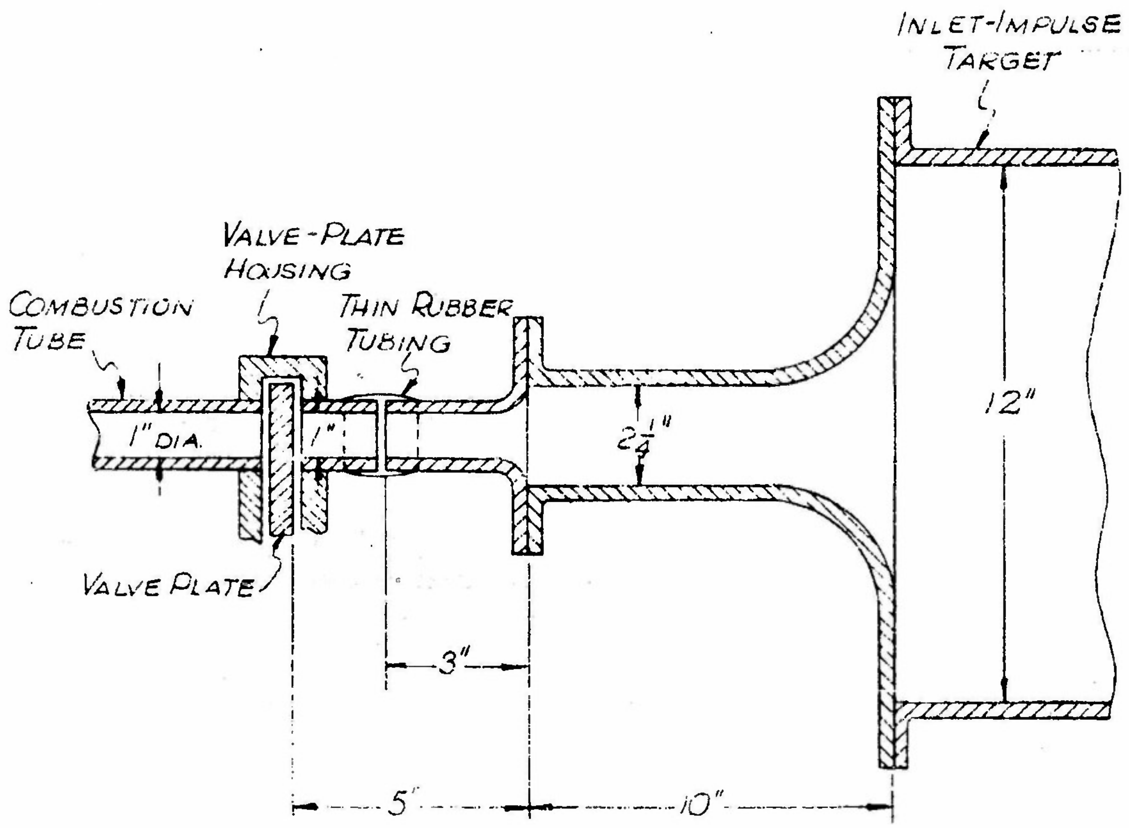

FIGURE 36

AIR-SUPPLY DUCTING TO ENGINE
FOR REMAINDER OF TESTS STARTING FROM TEST 57

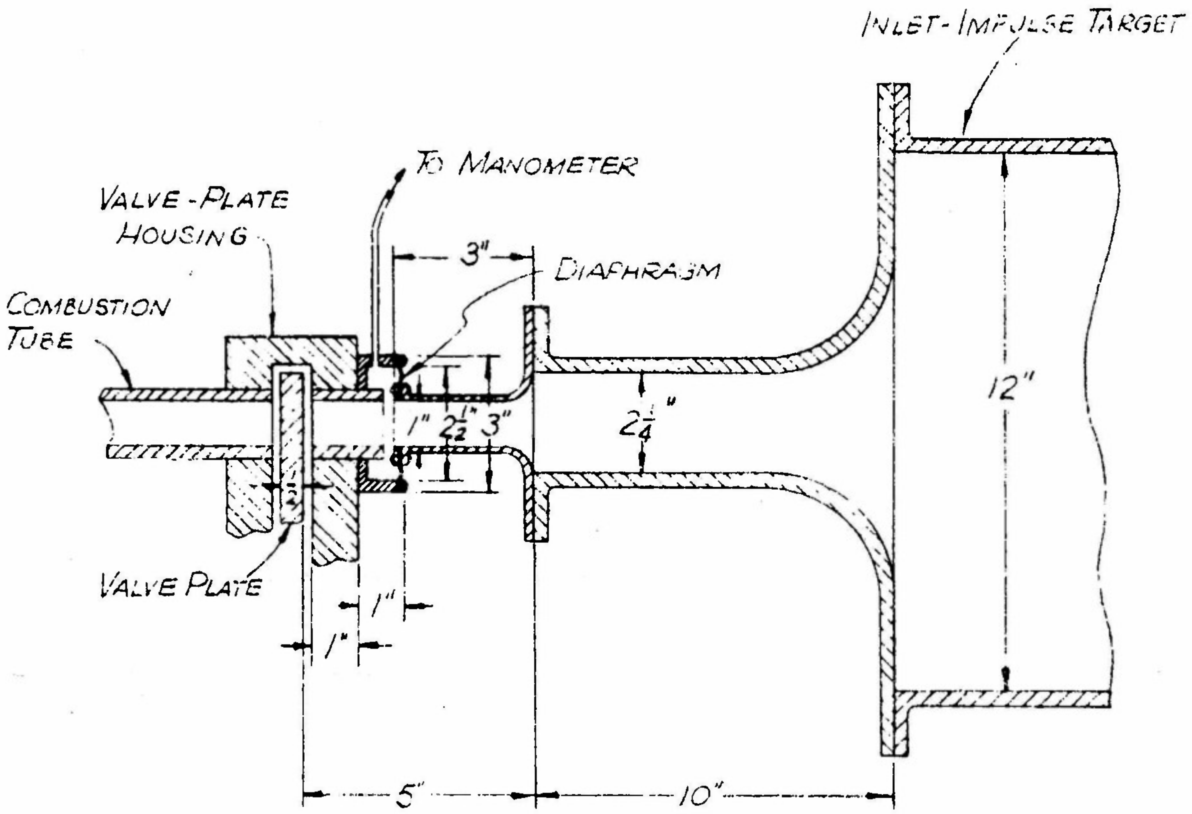

problem was alleviated somewhat by increasing the tube length to 9 inches, but the heating rate was still too low. The best heating rate was obtained when a 1-inch-diameter tube was installed in the engine. The improvement can be explained by the balance of heat transfer to the tube and heat losses from the tube. The heat release in the tube is proportional to D^2L (where D is the tube diameter and L is the length). The heat transfer to the walls is proportional to the surface area (or DL). The heat losses occur at three points: (1) at the tube ends (heat lost is proportional to D), (2) from the walls (heat lost is proportional to DL), and (3) at the water cooled high-frequency response pressure pickup (heat lost is constant). Therefore, it can be seen that increasing the tube diameter and tube length will increase the heating rate. All subsequent testing was performed in 1-inch-diameter tubes. Furthermore, a tube length of 12 inches was used so that the results of tests employing different valve configurations could be compared more easily. It is probable that the poor heating rate of the small tubes was aggravated by the inefficient Multi-Jet cycle realized at that time. Once an efficient Multi-Jet cycle is found, better heating characteristics may be obtained even with the small combustion tubes.

Pressure-time histories during some of the early tests in a 1-inch-diameter tube 6 inches long indicated that burning occurred only during every other cycle when relatively high combustion-chamber pressures (pressure ratio ≈ 4) were realized. A typical example of this unexpected combustion phenomenon is described by Figures 37 and 38. The first figure is a photograph of the pressure-time diagram as

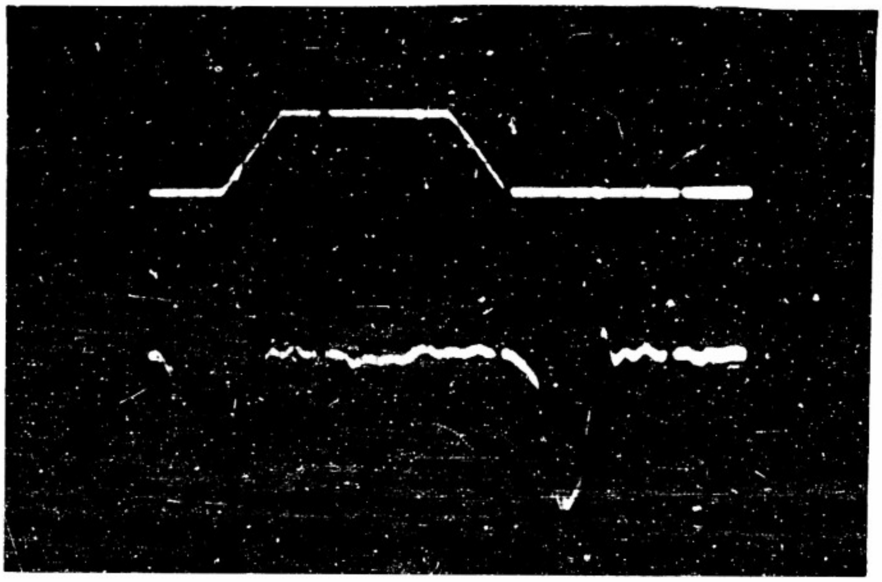

FIGURE 37 PHOTOGRAPH OF PRESSURE-TIME AND REFERENCE-VOLTAGE DIAGRAMS

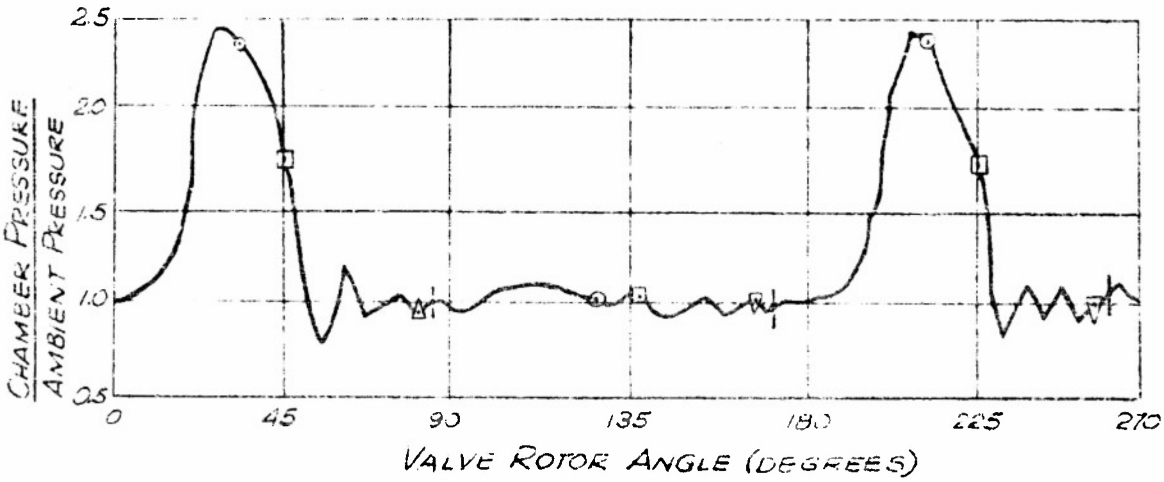

⊙ EXHAUST VALVE STARTS TO OPEN
⊡ INLET VALVE STARTS TO OPEN
△ EXHAUST VALVE STARTS TO CLOSE
| INLET VALVE STARTS TO CLOSE

COMBUSTION TUBE - 1" I.D.
6" LONG - STAINLESS STEEL (304)

PULSE COMPRESSION: BURN : EXHAUST : SCAVENGE = 1:22:4:18

FIGURE 38 PRESSURE-TIME DIAGRAM

seen on the oscilloscope screen, and the second figure is an enlarged sketch of the diagram presented in Figure 37.

The valve timing is indicated in Figure 37 by light and dark spots on the trace. The bright spot indicates the time at which the exhaust end of the tube is half open, i.e., this spot is an index of the beginning of the exhaust phase. The dark spot indicates the time at which the exhaust end of the tube is half closed, i.e., this spot is an index of the beginning of the compression phase. The times at which the valves begin to open or close are indicated directly in Figure 38.

An inspection of these figures reveals that the valve at the inlet end of the combustion tube opened during the first cycle before the pressure within the inlet end of the tube had decreased to a value less than that which existed within the inlet duct. Such a pressure differential would cause gases to move in the upstream direction during the early portion of the scavenge phase and would prevent, thus, a combustible mixture from entering the combustion tube during the scavenge and compression phases of this cycle. Consequently, burning would not occur during the second cycle. Scavenging the combustion tube of burned gases and charging this tube with combustible gases could take place during the second cycle, however, since the supply pressure would be greater now than the combustion-chamber pressure at the beginning of the scavenge phase of this cycle. The third cycle would now repeat the first cycle, i.e., burning would occur, combustion-chamber pressure would rise, scavenging would not occur properly, and the cycle would end with the combustion chamber filled with a noncombustible mixture.

The maximum combustion-chamber pressure observed in cases where burning occurred during every other cycle exceeded appreciably the maximum combustion-chamber pressure observed when burning occurred during every cycle. These observations substantiate the belief that the exhaust time is too short whenever burning occurs only during every other cycle. The duration of the exhaust phase, which is required in order to produce a combustion-chamber pressure smaller than the pressure in the inlet duct at the time the inlet valve begins to open, increases as the maximum combustion-chamber pressure increases.

Maximum combustion-chamber pressures from 2 1/2 to 4 atmospheres have been observed in the cases where burning occurred during every other cycle. This difference in maximum pressures depended upon the values of parameters such as air-flow rate, fuel-flow rate, and cycle frequency.

Lengths of the pulse-compression, combustion, expansion, and scavenge phases were in the ratios 1 : 22 : 4 : 18 for the test (test 40) during which Figure 37 was photographed. In an attempt to improve the scavenging process and to learn more about the conditions which lead to burning only during every other cycle, the length of the exhaust phase relative to the other phases of the cycle was increased.

A typical example of the pressure-time history obtained during a test run of a cycle having increased exhaust time is presented in Figures 39 and 40. The lengths of pulse compression, combustion, expansion, and scavenge were in the ratios 1 : 1.8 : 1.37 : 1.43 for the test (test 47) during which this figure was photographed. Although

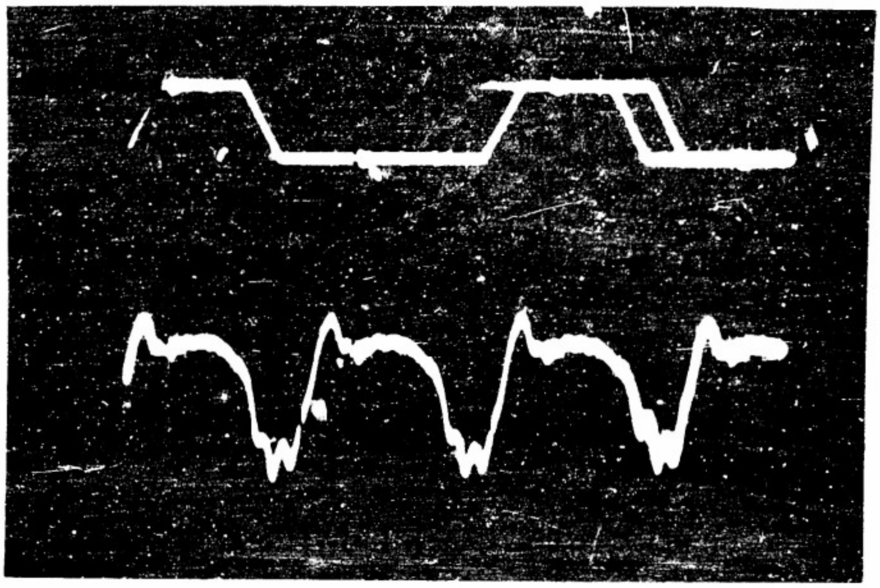

Figure 39. Photograph of Pressure Time and Reference Voltage Diagrams (Test Run 47)

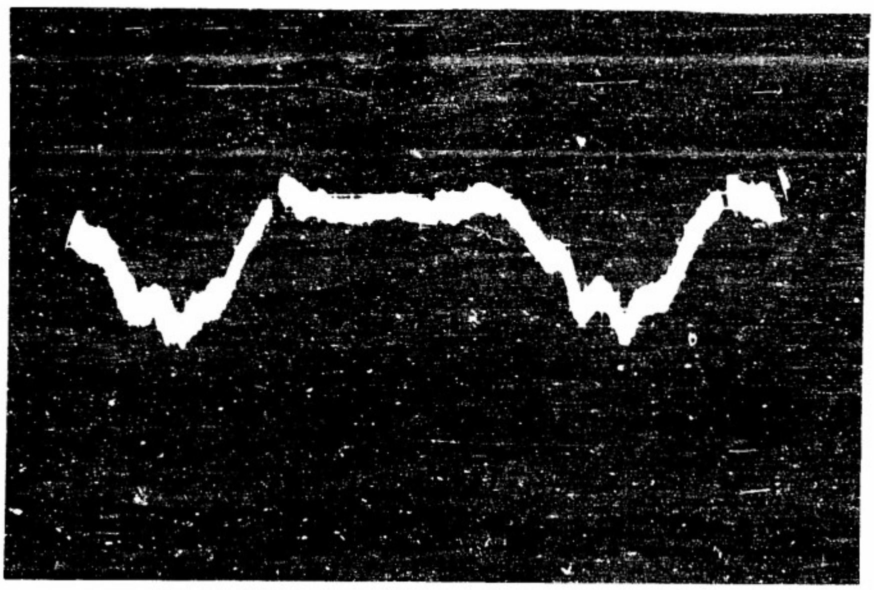

Figure 40. Photograph of Pressure Time Diagram (Test Run 47)

firing was obtained in every cycle, peak pressure ratios greater than four could not be obtained with the various valve configurations tested in tests 41 to 58. However, a significant advance was made during these tests when Test Engine No. 2 was operated using relatively high air-flow rates (scavenge-phase air-flow velocities of approximately 400-500 ft/sec) with no decrease in combustion-tube wall temperature and with cyclic ignition of the fresh charge by non-stationary surface combustion. Thrust measurements made during all the above tests still indicated that no net thrust was obtained.

Computations of the ideal cycle, which were made during the previous contract period (reported in Reference 1), indicate that the Multi-Jet Engine must be operating at peak cycle pressures of more than 4 in order to obtain any appreciable net thrust. See Figures 41 and 42 which are reproduced from Reference 1. Therefore, further tests on Test Engine No. 2 were pointed in the direction of obtaining higher maximum cycle pressure ratios.

In order to determine whether some of the fuel-air mixture is passing completely through the tube during the scavenge phase without burning at constant volume, the air mass flow is calculated by two methods: (1) from the measured pressure drop across the standard orifice, and (2) from the density of the air in the tube during each cycle and the frequency of the cycle. It is assumed that supply pressure and temperature exist in the combustion tube before combustion begins. The second method of calculation should give a result which is higher than the actual value (since the temperature of the gases in the tube will actually be greater than the supply temperature assumed

FIGURE 41

IMPULSE FUNCTION

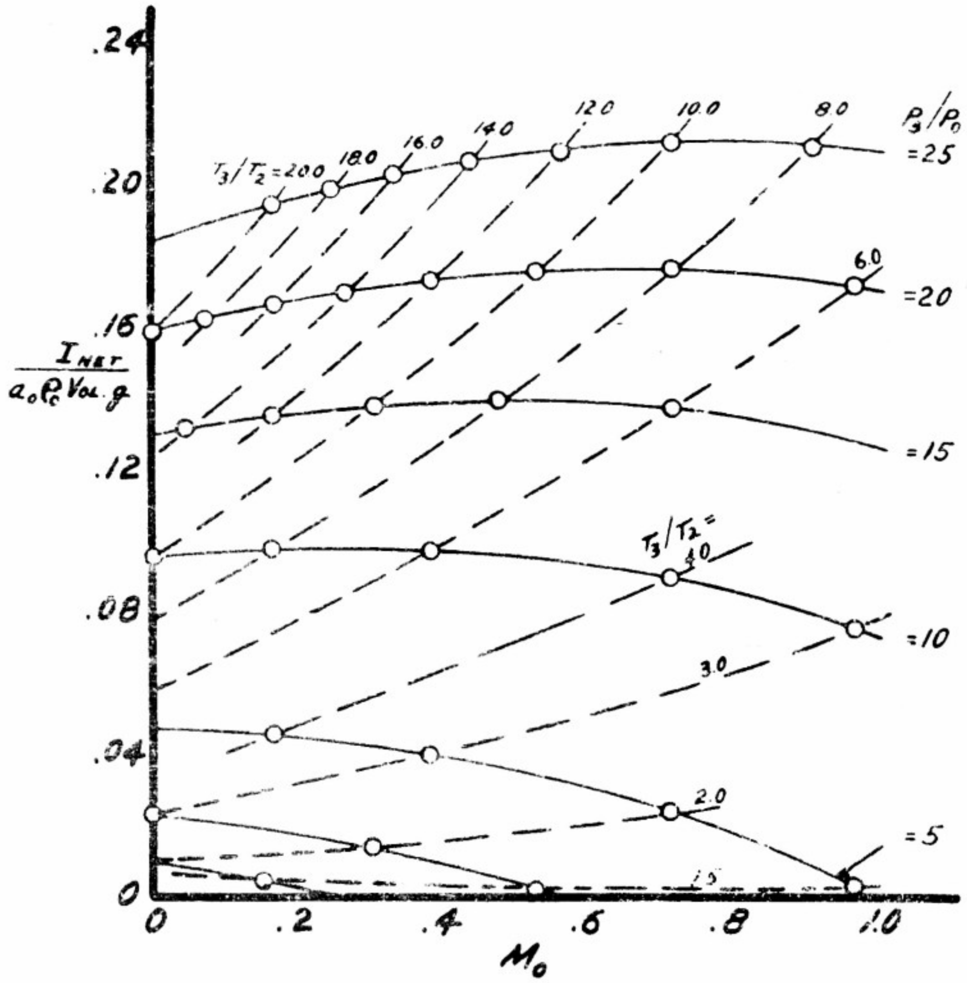

I	= impulse	P_3	= peak cycle pressure
a_o	= vel. of sound in ambient air	P_o	= pressure of ambient air
ρ_o	= density of ambient air	M_o	= Mach Number of vehicle
Vol	= volume of combustion chamber	T_3	= temp. of fluid after burning
g	= acceleration of gravity	T_2	= temp. of fluid before burning

FIGURE 42

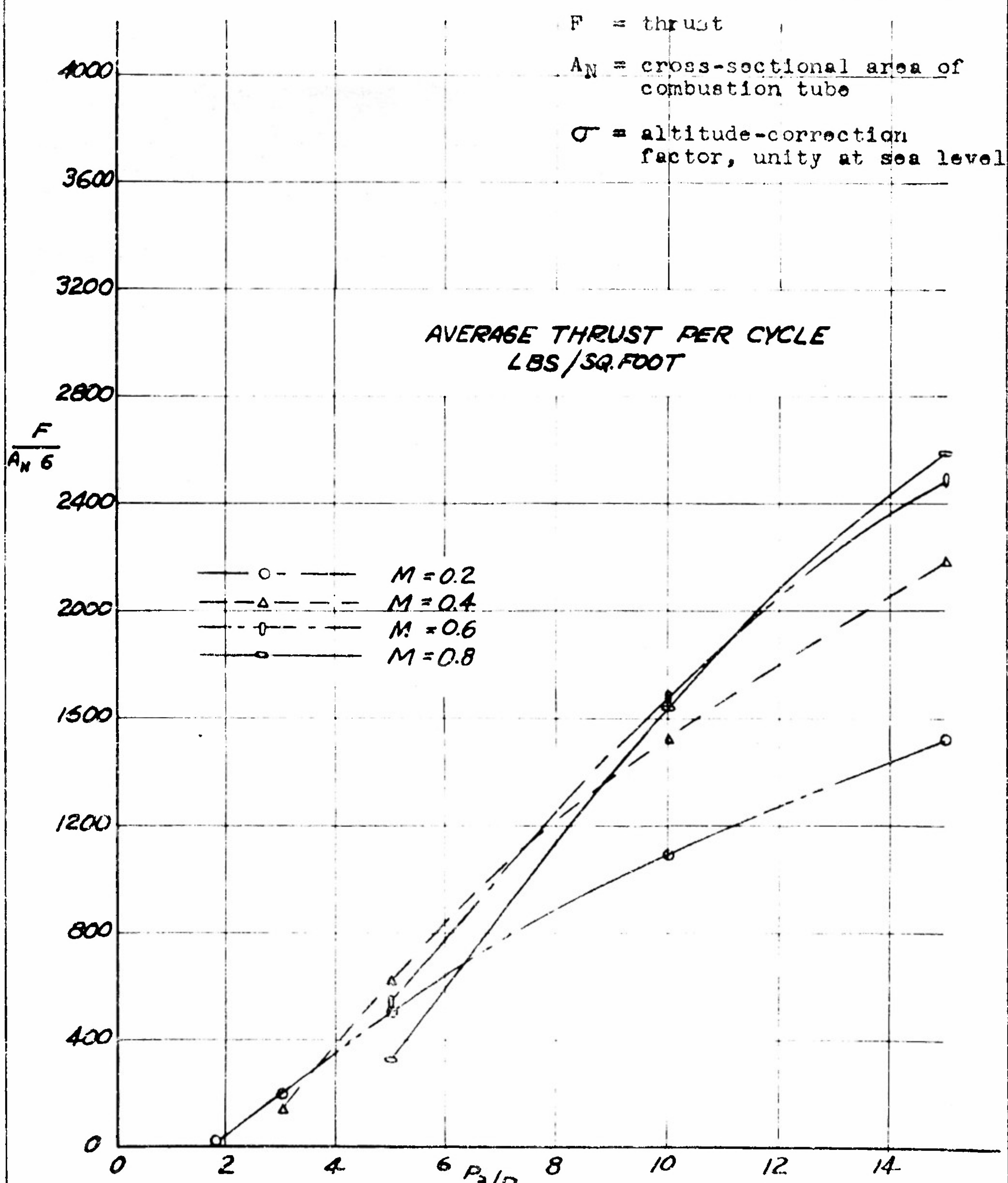
F = thrust
A_N = cross-sectional area of combustion tube
σ = altitude-correction factor, unity at sea level
AVERAGE THRUST PER CYCLE
LBS/SQ.FOOT
$\frac{F}{A_N \sigma}$
M = 0.2
M = 0.4
M = 0.6
M = 0.8
P_3/P_6
0
400
800
1200
1600
2000
2400
2800
3200
3600
4000
2
4
6
8
10
12
14

in the above computations).

However, calculation of the mass flow by the first method gave a larger result than the second method, indicating that more air is supplied to the engine than can be received by the combustion tube. It was concluded that some fuel-air mixture was passing completely through the combustion tube before the tube could be closed. The ejection of this air would lead also to low values of net thrust.

It was believed also that a large percentage of the mixture was burning before the tube could be closed. In order to decrease the stay time of the fuel-air mixture in the tube before the tube is closed, the pulse compression phase was eliminated from the valve configuration. It was assumed that some burning was occurring before the tube was closed (this burning would be occurring at constant pressure), thus reducing the maximum cycle pressure and the efficiency of the engine. The lengths of expansion, scavenge and burning were in the ratios 1 : 2.1 : 2.4.

The above configuration was tested in tests 59 to 66, and a peak cycle pressure ratio greater than 4 was obtained. Pressure ratios varied from 5 to 6.5, depending on the test conditions. A photograph of a high pressure cycle (test 64) is shown in Figure 43. Although the specific fuel consumption was high ($\approx$ 8 to 10), this configuration was the first to give any appreciable net thrust. A net thrust of 1.30 pounds per square inch of combustion tube flow area was obtained. Calculation of mass flow by the method described above still indicated that fuel-air mixture was being lost before the tube was closed. This fact would indicate that scavenge time could be reduced.

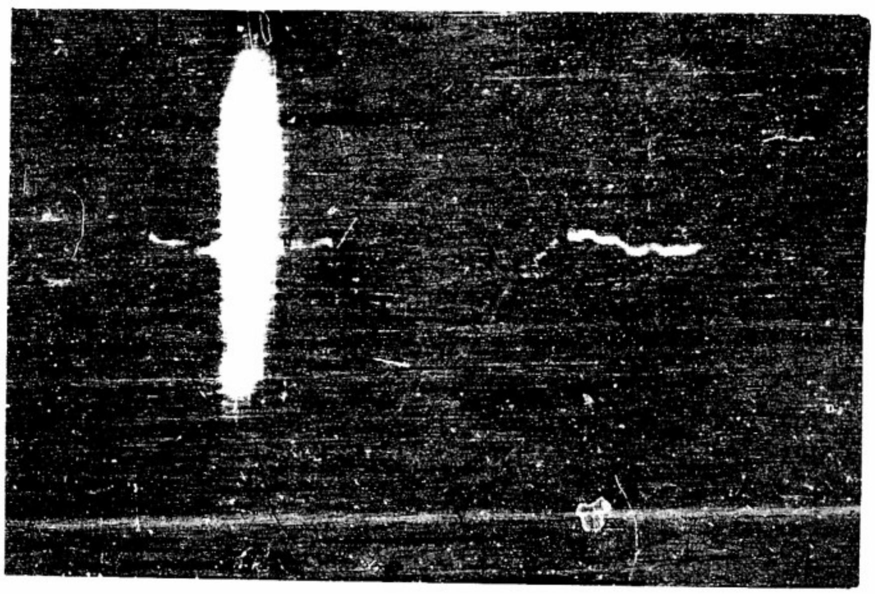

Figure 43. The Pressure-Time Diagram for Peak Cycle Pressure Ratio of 6.5

Stainless steel (Type 302) combustion tubes with 1/4 inch thick walls were used during most tests in the last month of the contract period. Usually more than one run could be made if the tube temperatures were carefully watched during the test run. However, during some of the test runs the tube temperature reached a value that caused the tube to fail. A photograph of such a failure is shown in Figure 44. It shows that the tube failed under stress due to pressure rather than due to softening and melting. This fact would indicate that high pressures were obtained in the combustion tube.

Figure 45 shows a typical pressure diagram obtained during tests 59 to 68. It shows (1) a rapid rise of pressure as soon as the tube is closed (the double valve-timing mark indicates when the tube is only half closed) and (2) a high pressure plateau indicating that combustion is completed and that the stay time of the mixture within the tube is too long. It can be seen, therefore, that the combustion time can be reduced appreciably. Such a reduction should result in a configuration that will produce a greater value of net thrust.

It was decided then to try a valve configuration that included a short pulse-compression phase. The ratio of exhaust : scavenge : pulse compression : burning was 1.00 : 1.77 : 0.11 : 2.12. The tests performed with this configuration showed that it was not as efficient as the configuration without pulse compression. Since the new configuration was obtained by changing the phase angle between the inlet and exhaust valves, the ratios of the cycle phase lengths could not be kept constant for the two configurations. Further tests are required in order to reach definite conclusions.

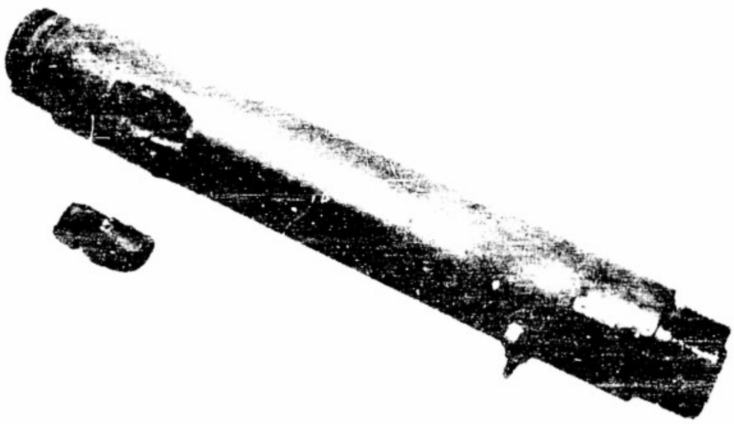

Figure 44. Stainless Steel Combustion Tube Showing High Temperature and High Pressure Failure

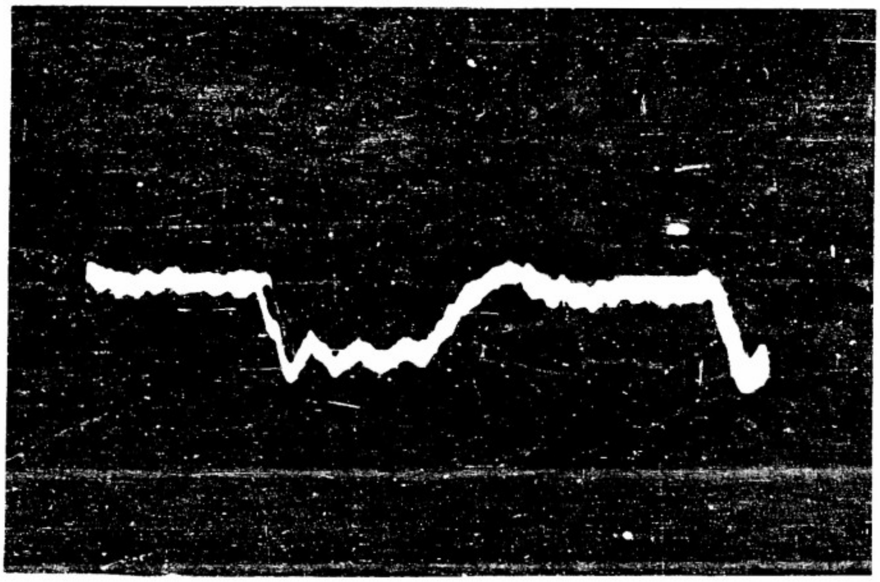

Figure 45. Pressure-Time Diagram Indicating a Long Burning Phase

A systematic investigation of the effect of valve clearances on the efficiency of the cycle was not completed, since a working configuration of the Multi-Jet Engine was not obtained until late in the contract period. However, peculiar pressure diagrams obtained during various test runs, such as shown in Figures 46 and 47 seemed to indicate that leakages were present.

Figure 46 shows a photograph of one cycle. The dark spots indicate the times at which the ends of combustion tube are either half open or half closed. The large dark spot indicates the time at which the inlet end of the combustion tube is half open (the beginning of scavenge); the next spot (time increases to the right) indicates the beginning of pulse compression; the third indicates the beginning of burning; and the fourth indicates the beginning of exhaust. It can be seen that during the burning phase (when the tube is closed at the front and rear) the pressure starts at a high level and drops almost to atmospheric pressure level. During the pulse compression phase the pressure rises considerably before the tube is totally enclosed. This high pressure during pulse compression would cause the fuel-air mixture flowing into the tube at the inlet to reverse itself, thus preventing the tube from being completely filled with fresh fuel-air mixture during that particular cycle.

Usually the cycle shown in Figure 46 is followed by a cycle that looks normal. This is shown in Figure 47. The dark spot in the second or normal cycle indicates the start of exhaust. In the phase immediately ahead of this dark spot, which is the burning phase, the pressure rises rapidly then levels off indicating that combustion is

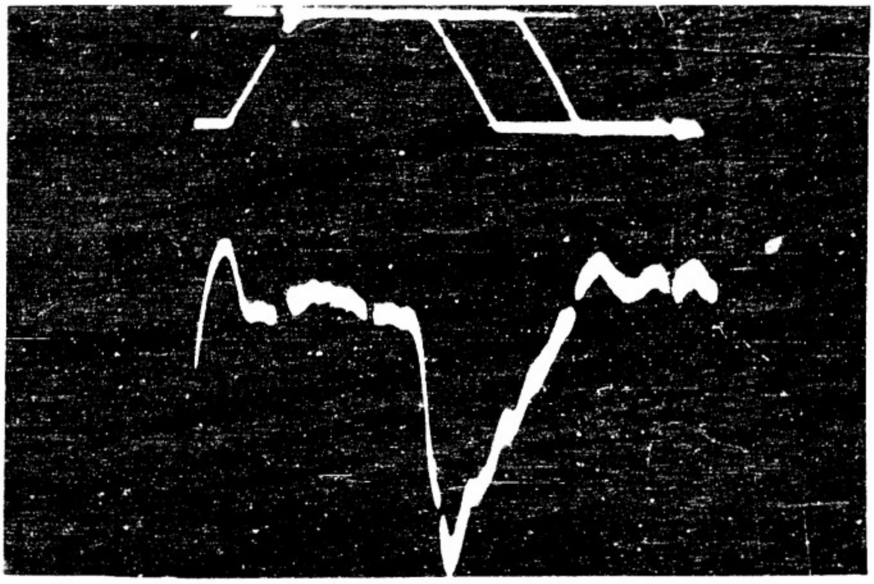

Figure 46. Pressure Time Diagram Indicating Leakage in the Tube

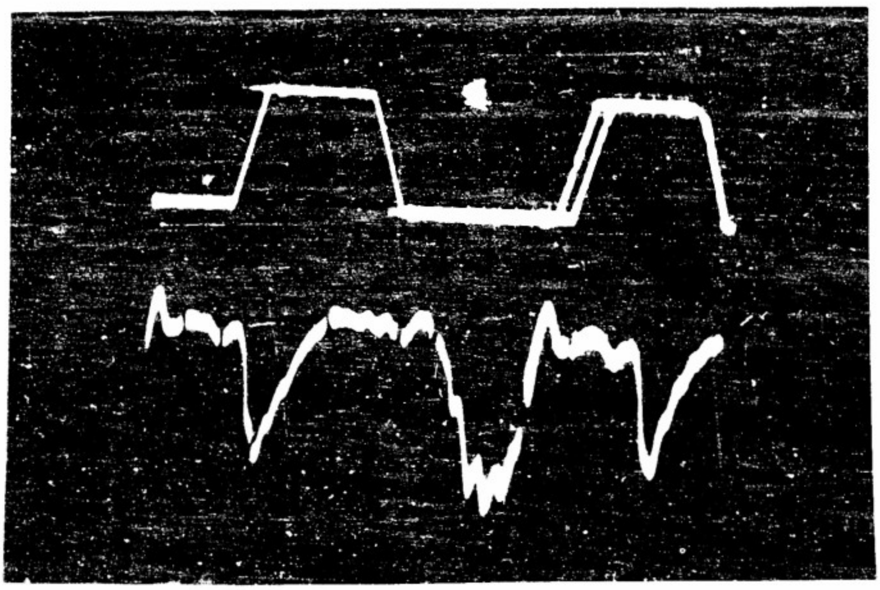

Figure 47. Pressure-Time Diagram Indicating Leakage in the Tube

completed. Previous to this phase, during pulse compression and scavenge, there is little or no pressure rise. Using these observations the following hypothesis can be formulated. Looking at Figure 47, during the first cycle the high pressure rise occurring during pulse compression causes the tube to be only partly filled with new fuel-air mixture. Returning now to the first cycle the mixture in the tube burns rapidly (at present it is not clear what triggers the mixture during pulse compression) as the tube closes to start the burning phase. When the tube is opened then, during the exhaust and scavenge phases, the pressure in the air supply system causes scavenge to proceed now without any interference from a pressure rise due to pulse compression. Thus, in the second cycle combustion proceeds as expected and the pressure rises during the burning phase. At first glance it appears that no leaking is occurring during the second cycle indicating that perhaps the clearances are smaller for the particular valve blades now closing the tube (perhaps due to valve plate wobble; Cf. Section III). However, since during the second cycle better scavenging occurred there is a greater percentage of fuel-air mixture present than in the first cycle. Then if the leakages are not present a higher pressure should be observed or if the leakages are present then the pressure will rise rapidly, the mixture will start to leak out of the tube, the pressure will tend to drop, more mixture will burn, the pressure will tend to rise; this loss and gain of pressure will occur until the exhaust valve opens when the pressure will drop immediately to atmospheric. The above is only an hypothesis and cannot be substantiated definitely by the test results. However, at the completion of these tests an investigation of the valve clearances showed that they were of the order of 1/32 inch or more. By reducing the clearances to the order of 0.005 inch and repeating the run a pressure diagram given in Figure 40 was obtained. All of the above pressure diagrams were obtained during Test Run No. 47.

Visual observations of the engine exhaust suggested that the exhaust was being deflected in a direction opposed to the direction of motion of the valve-plate blade across the end of the combustion tube. High-speed motion pictures confirmed this unexpected observation. The trailing edge of the valve-plate blades (1/2 inch thick) acted apparently as a solid wall as it crosses the tube opening and the gases expanded then away from this wall. The aft valve plate was modified consequently, with the result that the surfaces at the trailing edges of the valve-plate blades made then a 45° angle with the center line of the combustion tube and permitted the exhaust gases to expand more freely in all directions.

SECTION V

CYCLE ANALYSIS

5.1 Non-Viscous Non-Stationary Flows

The graphical method introduced by de Haller (Cf. References 4 and 5) for solving certain non-viscous non-stationary flow problems was used to construct characteristic diagrams for flows in a statically operating Multi-Jet engine combustion tube. These diagrams are useful in determining the optimum valve-plate configuration and the optimum rotor speed for a Multi-Jet engine which is operating statically.

The computations for these characteristic diagrams were based on the following assumptions:

1. The cross-sectional area of the combustion tube is constant.
2. Flow passages in which the cross-sectional area changes suddenly with respect to axial distance (the tube ends when the valves are opening or closing) have the characteristics of very short nozzles, i.e., flows through these passages may be described by the equations of steady adiabatic fluid flows.
3. During the scavenge and compression phases, the static pressure at the tube inlet is related to the ambient pressure by the Bernoulli Equation. This assumption implies that during the scavenge and compression phases the static pressure at the tube inlet is less than the ambient pressure.
4. During the scavenge and compression phases, the total temperature of the combustible mixture is constant.
5. The increase in fluid entropy caused by passage of a shock wave through the fluid is negligible. (This assumption is

justified if the shock-wave pressure ratio is less than 2.5.)

6. If, during the exhaust and scavenge phases, the gas velocity at the tube outlet is less than the local velocity of sound in the gas, the static pressure at the tube outlet is equal to the ambient pressure.

7. The conditions of the gas in the combustion tube at the time for which the fluid flows were calculated (i.e., the pressure and the temperature of the gas in the combustion tube at the end of the combustion phase) are the same as computed in Reference 2 for a statically operating Multi-Jet engine.

Since assumption 7 does not describe the conditions of the gas at the end of a typical combustion phase with complete accuracy, it would be necessary to analyze several consecutive cycles of the engine before a diagram which is repeated during consecutive cycles could be attained. These computations, however, would be tedious and, consequently, characteristic diagrams were constructed for only the first cycle -- the contention being that it can be determined from these diagrams which of the several cases investigated should be analyzed in greater detail at a later date.

Since the main purpose of the characteristic diagram is to facilitate the determination of the valve timing which is needed for efficient scavenging of the combustion tube, computations were made for the following two cases:

1. The pressure within the tube at the inlet valve is allowed to decrease to a value smaller than that of the total free stream pressure before the inlet valve is opened. (Note that if the

engine is operating statically, then the total pressure of the free stream equals the ambient pressure.)

2. The pressure in the tube at the inlet valve is allowed to decrease to a value equal to the total pressure of the free stream before the inlet valve is opened.

The characteristic diagrams (Figures 48 and 49) which were constructed describe the exhaust and scavenge phases as follows (see Figure 48 in particular): As the exhaust valve is opened, an expansion wave I forms and travels toward the closed inlet valve. This expansion wave arrives eventually at the inlet valve (decreasing the pressure in the tube at the inlet valve), reflects from the inlet valve as an expansion wave II, and travels back towards the open exhaust valve. If the exhaust flow is sonic, then this expansion wave reflects from the open exhaust valve as an expansion wave III; if the exhaust flow is subsonic, then this expansion wave reflects from the open exhaust valve as a compression wave IV. When the pressure in the tube at the inlet valve has dropped to a value which gives the desired pressure ratio across the inlet valve, the inlet valve is opened and a compression wave V forms and travels towards the open exhaust valve: fluid flows subsequently with a velocity corresponding to a Mach number of approximately 0.6 into the combustion tube. Compression wave IV reaches eventually the open inlet valve (decreasing the Mach number of the entering fluid and, in some cases, reversing the direction of flow); compression wave V reflects from the open exhaust valve as an expansion wave VI and also reaches eventually the open inlet valve (increasing the Mach number of the entering fluid). The net effect of

FIGURE 48
WAVE DIAGRAM FOR FLOW IN A COMBUSTION TUBE DURING INITIAL PERIOD OF OPERATION OF MULTI-JET ENGINE ALLOWING UNDERPRESSURE TO DEVELOP IN TUBE

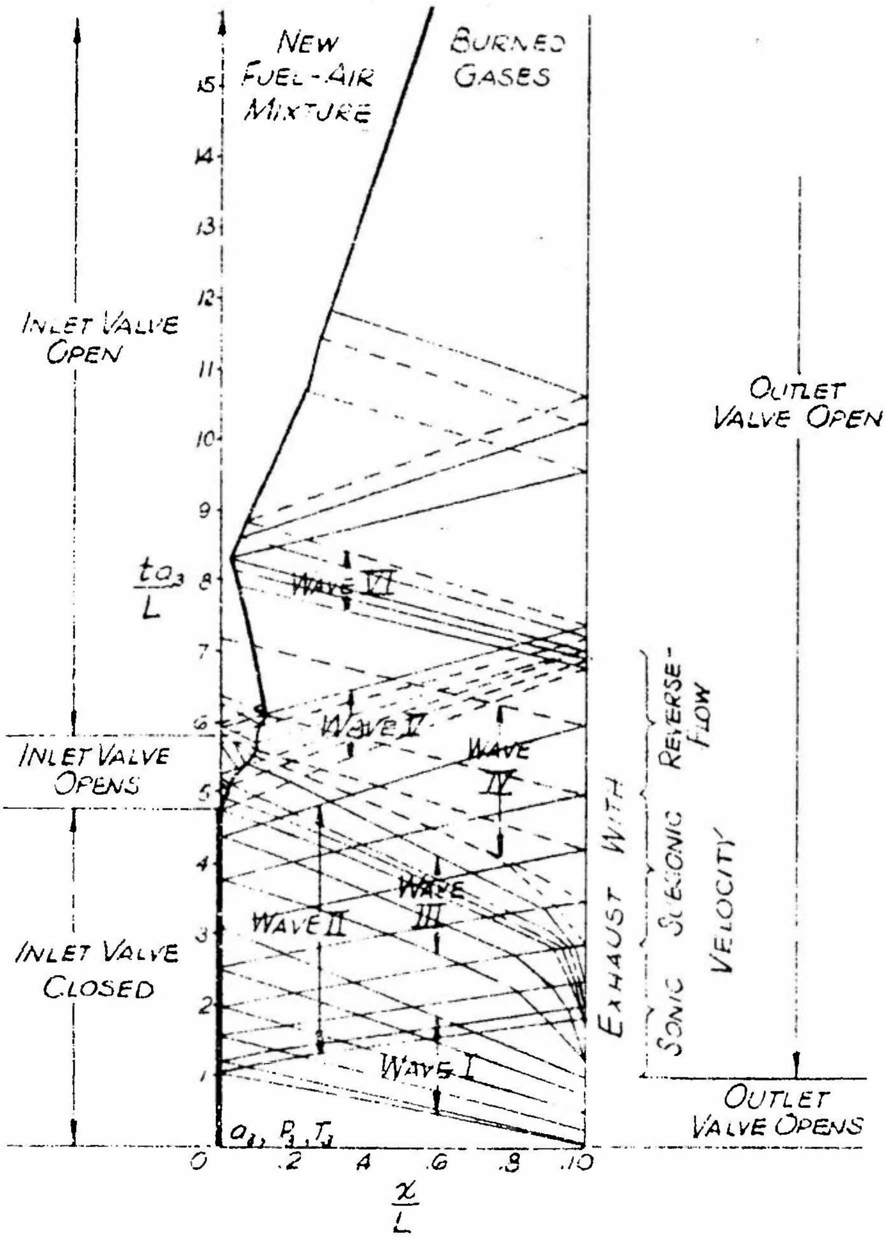

FIGURE 49
WAVE DIAGRAM FOR FLOW IN A COMBUSTION TUBE
DURING INITIAL PERIOD OF OPERATION OF MULTI-JET ENGINE
ALLOWING NO UNDERPRESSURE TO DEVELOP IN TUBE

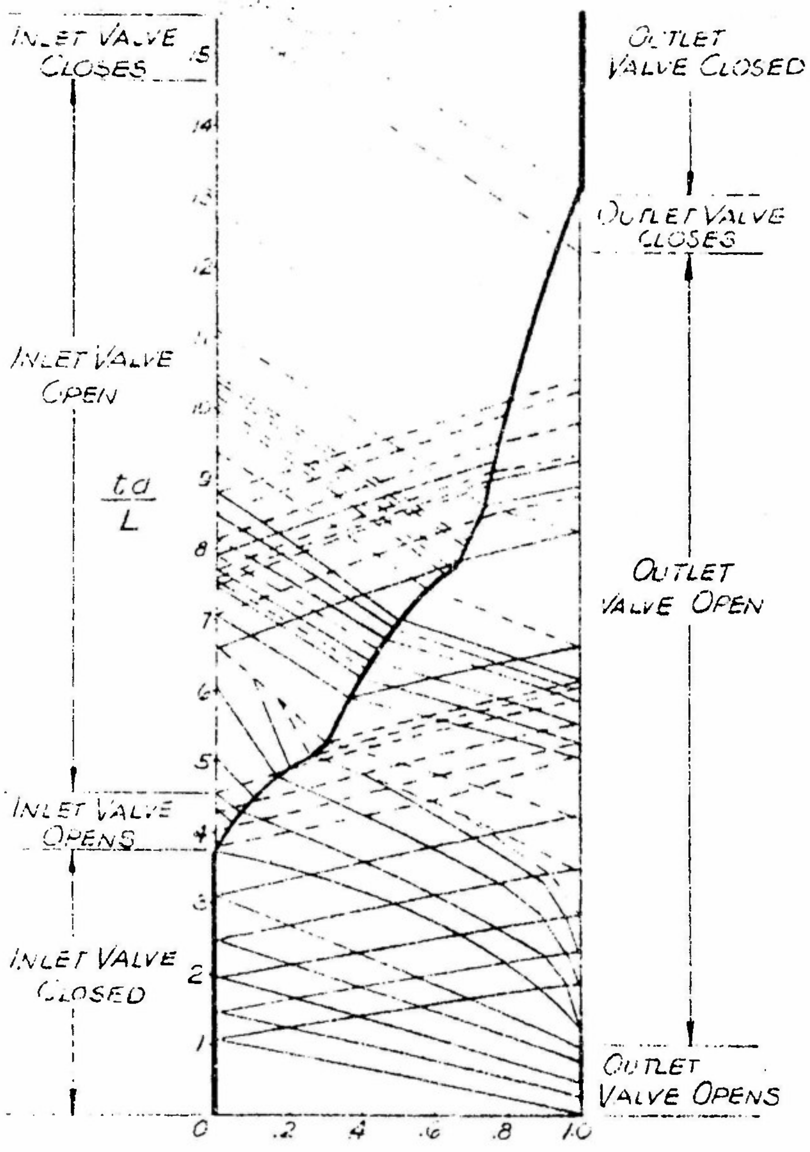

waves IV and VI is to decrease the Mach number of the entering fluid to a value less than 0.6.

If the pressure in the tube at the inlet valve is allowed to decrease to a value equal to 1/2 the total pressure of the free stream before the inlet valve is opened (case 1, Figure 48), then the fluid moves initially into the tube at a Mach number of approximately 0.6. Compression wave IV reverses the flow at the tube inlet; expansion wave VI reverses again the flow at the tube inlet and causes the fluid to move into the tube at a Mach number of approximately 0.3 during the remainder of the scavenge period. Examination of the characteristic diagram reveals that the tube can be scavenged more quickly only if the travel of compression wave IV is delayed or if compression wave IV is eliminated.

If an exhaust tube having a diameter equal to that of the combustion tube is attached behind the exhaust valve, then expansion wave II reflects from the exhaust-tube exit instead of from the combustion-tube exit with the result that the arrival of compression wave IV at the inlet valve is delayed (see Figure 50). Computations for case 1 indicate that an appreciably higher average scavenge velocity is realized if the exhaust tube with a length equal to 62 percent of the length of the combustion tube is used than if no exhaust tube is used.

It should be noted, in Figure 50, that expansion wave I is divided into two parts I(a) and I(b). Expansion wave I(b) is formed by the reflection of the compression wave at the open end of the exhaust tube. The pressure at the tail of expansion I(b) is equal to the ambient pressure. Since there is a time interval between the

FIGURE 50
WAVE DIAGRAM FOR FLOW IN A COMBUSTION TUBE DURING INITIAL PERIOD OF OPERATION OF MULTI-JET ENGINE WITH 62% EXHAUST TUBE

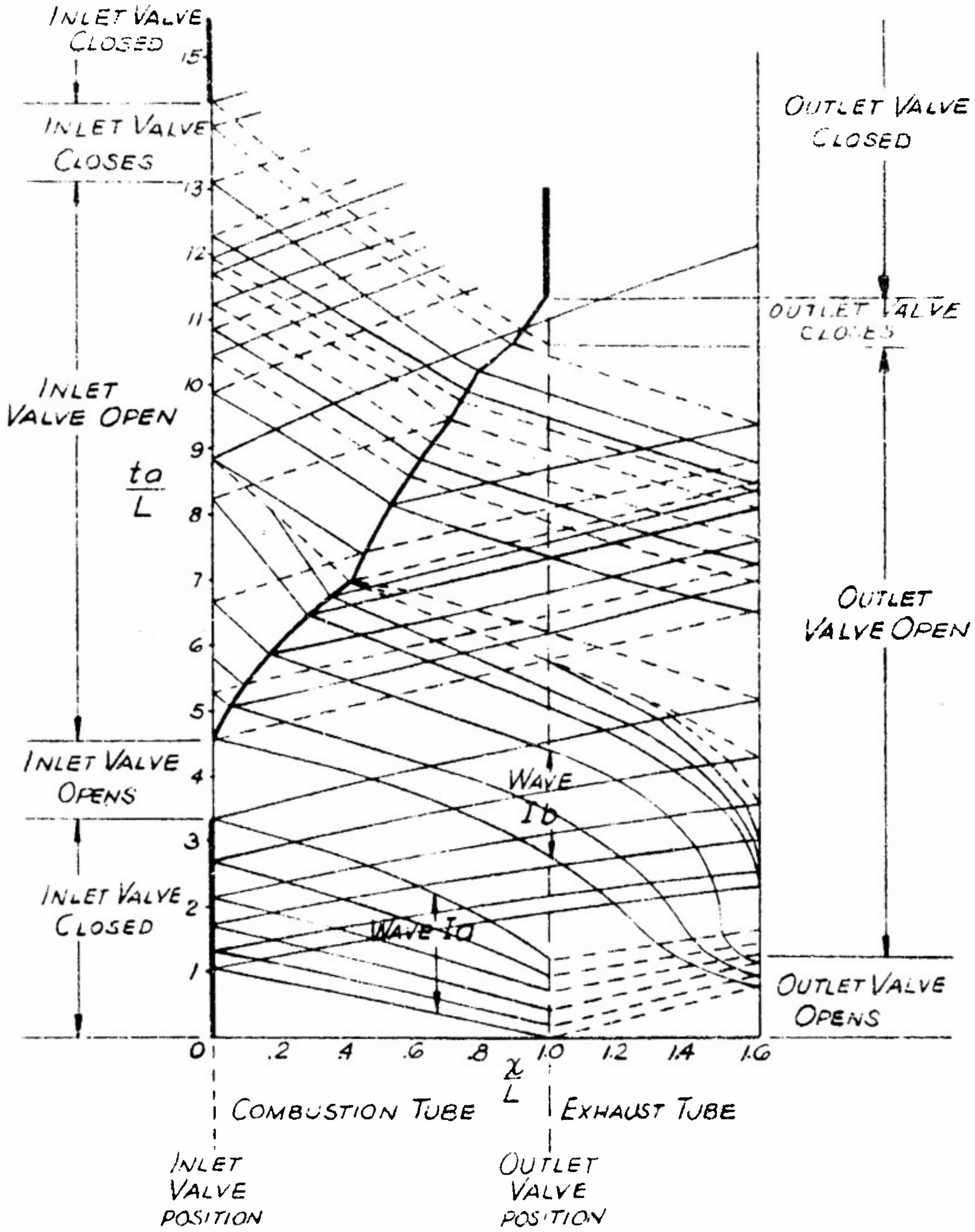

arrival of the tail of expansion wave I(b) and the front of expansion wave I(b) the inlet valve is allowed to open during this interval. No waves are formed by the opening action of the front valve since there is no pressure ratio across the valve as it opens. The length of the exhaust tube is adjusted so that this interval of time is equal to the time required for the inlet valve to open.

Further computations indicate that the average scavenge velocity is of the same order of magnitude for (a) case 1 (Figure 50), with exhaust-tube length equal to 62 percent of the combustion-tube length, and (b) case 2 (Figure 49), with exhaust-tube length equal to zero.

5.2 Results of Preliminary Analytical Study of Combustion in a Closed Cylinder

Combustion in closed cylinders was studied analytically for the purpose of obtaining basic information useful in analyses of jet-propulsion devices involving constant-volume burning in tubular combustion chambers. The calculations were simplified by making the following assumptions:

1. Prior to the instant when ignition occurs, the gas is motionless and its temperature is uniform.
2. At any given time, the pressure within the combustion chamber is uniform.
3. The heat capacity and molecular weight of the gas are constant.
4. The rate at which heat is transferred by conduction is negligible in comparison with the rate at which heat is released by combustion.
5. The unburned gas ahead of the flame front and the burned gas

behind the flame front both are compressed isentropically.

6. The effect of pressure on the normal burning velocity is negligible in comparison with the effect of unburned-gas temperature.

The dependence of (a) the time required for burning and (b) the temperature distribution within the burned gas upon the fluid physical properties, fluid initial temperature, combustion-chamber diameter, combustion pressure ratio, and ignition-source location was determined.

5.2.1 Time Required for Burning. By combining an expression which states that the energy is conserved during the combustion process with the equation of state and an expression which states that volume is constant during the combustion process (remembering especially assumption 4), one can obtain a linear relationship between chamber pressure and mass fraction of burned gas

$$\frac{P}{P_i} = 1 + n(\pi - 1) \qquad (1)$$

where P is pressure, n is mass fraction of burned gas, π is combustion pressure ratio P_e / P_i, and the subscripts i and e refer respectively to the initial state and the end state. By combining an expression which states that mass is conserved during the combustion process with the equation of state and an expression which states that volume is constant during the combustion process (remembering especially assumption 5), one can obtain a relationship between volume fraction of burned gas and mass fraction of burned gas

$$y = 1 - \frac{1-n}{\left[1 + n(\pi - 1)\right]^{1-\sigma}} \tag{2}$$

where y is volume fraction of burned gas, $\sigma = \frac{\gamma - 1}{\gamma}$, and γ is specific-heat ratio (Cf. Ref. 1). These two relations will be used in the following derivation of the equation for the minimum time required for burning completely a combustible gas mixture in a closed cylinder.

A relationship between time, normal burning velocity (the rate at which the flame front advances relative to the unburned gas), chamber pressure, volume fraction of burned gas, and mass fraction of burned gas may be derived if one equates the rate of production of burned gas to the rate of consumption of unburned gas

$$\frac{d\,m_b}{d\,t} = \rho_u \, 3.14 \, S_t \, L \, d \tag{3}$$

where m is mass, t is time, ρ is density, S_t is normal burning velocity, L is combustion-chamber length, d is flame-front diameter (the flame front is assumed to be cylindrical), and the subscripts u and b refer respectively to unburned gas and burned gas. (Density ρ_u is related to the chamber pressure, diameter d is related to the volume fraction of burned gas, and mass m_u is related to the mass fraction of burned gas.) The dependence of d in Equation (3) upon the chamber pressure may be converted to a dependence upon the mass fraction of burned gas by using the equation of state and substituting then from Equation (1) (remember especially assumption No. 5)

$$\frac{D}{4 S_t} \frac{dn}{dt} = \frac{d}{D} \left[1 + n(\pi - 1) \right]^{1-\sigma} \qquad (4)$$

where D is tube diameter. Lengthy mathematical exercises of the type presented on page 4 of Reference 6 are not necessary for the derivation of this equation.

The dependence of d/D in Equation (4) upon the volume fraction of burned gas may be converted to a dependence upon the mass fraction of burned gas by expressing diameter d/D in terms of volume fraction of burned gas g and substituting then from Equation (2). If ignition occurs at the combustion-chamber wall, then $d/D = (1-g)^{1/2}$; if ignition occurs at the combustion-chamber center line, then $d/D = g^{1/2}$.

The dependence of Equation (4) upon the normal burning velocity may be converted to a dependence upon the mass fraction of burned gas by relating empirically the normal burning velocity to the temperature of the unburned gas and substituting then from Equation (1) (remembering especially assumptions 5 and 6). According to Dugger and Simon (Reference 7), the dependence of the maximum normal burning velocity upon the temperature of the unburned gas may be expressed by an equation of the form

$$\frac{S_u}{S_{u_i}} = a + b\left(\frac{T_u}{T_i}\right)^c \qquad (5)$$

where T is temperature and a, b, and c are constants which depend upon the physical properties and initial temperature of the combustible mixture. Combining Equations (1), (4), and (5), rearranging the resulting differential equation, and integrating between the limits $n = 0$ and $n = 1$, one obtains an integral relation for the minimum time required for burning completely a combustible gas in a closed cylinder

$$\frac{t\, S_{u_i}}{D/2} = \frac{1}{2}\int_0^1 \frac{D}{d}\, \frac{dn}{a\left[1 + n(\pi - 1)\right]^{1-\sigma} + b\left[1 + n(\pi - 1)\right]^{1+(c-1)\sigma}} \qquad (6)$$

This equation is the first relation of the two relations which are sought.

5.2.2 Temperature Distribution Within the Burned Gas. The temperature of the burned gas is connected with the temperature of the unburned gas by the relations (recall assumption 5)

$$\frac{T_b(x,1)}{T_u(x,0)} = \frac{T_b(x,1)}{T_b(x,x)} \frac{T_b(x,x)}{T_u(x,x)} \frac{T_u(x,x)}{T_u(x,0)}$$

$$= \left(\frac{P_e}{P_x}\right)^{\sigma} \left[1 + \frac{\pi - 1}{\gamma}\left(\frac{P_i}{P_x}\right)^{\sigma}\right]\left(\frac{P_x}{P_i}\right)^{\sigma}$$

$$= \pi^{\sigma}\left[1 + \frac{\pi - 1}{\gamma}\left\{1 + x(\pi - 1)\right\}^{-\sigma}\right] \tag{7}$$

where the value of x in $T(x, y)$ denotes the particular piece of gas which is under examination ($x = 0$ corresponds to gas which is burned first and $x = 1$ corresponds to gas which is burned last) and the value of y denotes the stage of the combustion process (Cf. Ref. 6). This equation is the second relation of the two relations which are sought.

Keeping in mind that $T_u(x, 0)$ does not vary with x, one can determine easily from Equation (7) that

$$\frac{T_b(0,1) - T_b(1,1)}{T_u(x,0)} = \frac{\pi - 1}{\gamma}\left(\pi^{\sigma} - 1\right) \tag{8}$$

i.e., that, at the instant when combustion is concluded, the temperature of the first-burned gas exceeds appreciably that of the last-burned gas.

5.2.3 Numerical Results. The minimum burning time for an ethylene-air mixture burning at constant volume in a tubular combustion chamber was computed for combustion pressure ratios of 5 and 8 and for (a) ignition at the combustion-chamber wall and (b) ignition at the combustion-chamber center line. For a mixture of ethylene and air initially at 360°K, Dugger and Simon (Reference 7) indicate that the dependence of the maximum burning velocity upon the temperature of the unburned gas may be expressed by an equation of the form

$$\frac{S_t}{S_{t_i}} = 0.12 + 0.88\left(\frac{T_u}{T_i}\right)^{1.74} \qquad (5\text{-}a)$$

so that the minimum time required for burning completely (in a closed cylinder) an ethylene air mixture initially at 360°K is given by the integral relation

$$\frac{t\,S_{t_i}}{D/2} = \frac{1}{2}\int_0^1 \frac{D}{d}\,\frac{dn}{0.12\left[1+n(\pi-1)\right]^{1-\sigma} + 0.88\left[1+n(\pi-1)\right]^{1+0.74\sigma}} \qquad (14a)$$

Equation (6a) was integrated numerically except for small values of α/D ; for small values of α/D , the integrand was expanded in series form, small terms were neglected, and direct integration was employed. The results of these calculations are presented in Table 3.

	Ignition at Wall	Ignition at Center Line
$\pi = 5$	0.39	0.33
$\pi = 8$	0.29	0.24

Table 3. Values of Minimum-Burning-Time Parameter for Ethylene-Air Mixture Burning at Constant Volume in a Tubular Combustion Chamber.

An examination of Table 3 emphasizes two interesting facts. The most important fact is that the time required for a flame to traverse a given distance is appreciably less if burning is at constant volume than if burning is at constant pressure. If burning is at constant pressure, then the parameter $\frac{t\, S_{e_i}}{D/2}$ equals unity. If burning is at constant volume, then this parameter is less than unity; (a) the normal flame velocity increases when the unburned-gas temperature increases as the result of isentropic compression, and (b) the unburned gas is given a velocity in the direction of burning as the result of unburned-gas compression. (It follows immediately that the minimum time required for burning decreases as the combustion pressure ratio increases.) The second interesting fact is that the minimum time required for burning is less if ignition is at the combustion-tube center line than if ignition is at the combustion-tube wall. This situation exists because the normal burning velocity is greatest when burning is nearly completed (i.e., when the unburned-gas temperature is highest), and because the flame area is greatest when the flame is at the combustion-chamber wall.

The amount by which the temperature of the first-burned gas exceeds the temperature of the last-burned gas at the instant when combustion is concluded was calculated using Equation (8) for a specific-heat ratio of 1.40 and an initial temperature of 650°R. For a combustion pressure ratio of 5 this temperature difference equals 1090°R, whereas for a combustion pressure ratio of 8 this temperature difference equals 2640°R. This calculation indicates that, for combustion in a closed cylinder, structural elements which are located near the ignition source will attain a higher temperature (and will possess consequently a lower tensile strength) than similar structural elements which are located far from the ignition source.

The reason why the temperature of the first-burned gas exceeds that of the last-burned gas become apparent if one considers the manner in which the temperature rises occur. The temperature of the first-burned gas rises first as the result of combustion and then as the result of compression; the temperature of the last-burned gas rises first as the result of compression and then as the result of combustion. The temperature rise due to combustion is the same for both cases; the temperature rise due to compression is greatest when the temperature at beginning of compression is greatest. It follows immediately that the temperature of the first-burned gas exceeds that of the last-burned gas.

5.2.4 Conclusions. The preliminary analytical study of combustion in a closed cylinder yielded the following results:

1. The minimum time required for burning may be cal ulated if the combustion pressure ratio, the initial fluid temperature, the cylinder diameter, and the ignition-source location are known.
2. The time required for a flame to traverse a given distance is appreciably less if burning is at constant volume than if burning is at constant pressure.
3. The time required for burning is less if ignition is at the combustion-tube center line than if ignition is at the combustion-tube wall.
4. The temperature distribution within the burned gas at the instant when combustion is concluded may be calculated if the combustion pressure ratio and the initial fluid temperature are known.
5. The temperature of the first-burned gas exceeds appreciably the temperature of the last-burned gas at the instant when combustion is concluded.

Since it is useful to have information concerning the time required for burning and the temperature of the structural components of the combustion chamber when developing a jet-propulsion device, the results of this preliminary analytical study have particular usefulness in the present Multi-Jet development program.

5.3 Results of Preliminary Analytical Study of Effects of Viscosity on Certain Non-Stationary Pipe Flows.

The effects of viscosity on certain non-stationary pipe flows were studied analytically for the purpose of obtaining basic information useful in analyses of jet-propulsion devices involving non-stationary fluid flows in straight tubes. After neglecting derivatives with respect to distance in the direction of the duct axis in comparison with derivatives with respect to distance in the radial direction and/or derivatives with respect to time, and after assuming that the physical properties of the fluid do not vary either with distance or with time, the following items were determined:

1. The velocity profile in the neighborhood of an infinitely long flat plate when the fluid properties and the free-stream velocity are specified (both the free-stream and the local velocities may be functions of time).
2. The limits within which the results of studies of flow along an infinitely long flat plate may be applied to flow through an infinitely long tube.
3. The effects of viscosity on the mass-flow rate through a tube.
4. The effects of viscosity on mass flow through a tube during a given period.

5.3.1 Velocity Profile for Flow along a Flat Plate. Consider first the case occurring when the fluid is set in motion impulsively and the free-stream velocity is held constant thereafter. Contemplate an infinitely long flat plate along which a fluid is flowing subject to:

1. The general restrictions that derivatives in the direction of the free-stream flow are negligible in comparison with derivatives with respect to distance in the direction normal to the flat plate and/or derivatives with respect to time and that the physical properties of the fluid do not vary either with distance or with time.

2. The boundary conditions:

$$u(0,t)=0 \qquad t>0$$
$$u(\infty,t)=U_0 \qquad t>0 \tag{1}$$

and

3. The initial conditions:

$$u(y,0-)=0 \qquad y\geq 0$$
$$u(y,0+)=U_0 \qquad y>0 \tag{2}$$

where u is velocity in the direction of the free-stream flow, y is distance in the direction normal to the flat plate, and t is time. Fluid flow subject to these restrictions is described by the partial-differential equation

$$\frac{\partial u}{\partial t} = \nu \frac{\partial^2 u}{\partial y^2} \tag{3}$$

where ν = kinematic viscosity. For values of t greater than zero, the expression

$$\frac{u}{U_0} = \operatorname{erf} \zeta \qquad (4)$$

where $\zeta = y/\sqrt{4\nu t}$, satisfies partial-differential Equation (3), boundary conditions (1), and initial conditions (2). Equation (4) describes completely the velocity profile which results when fluid in the neighborhood of a flat plate is set in motion impulsively at $t = 0$ and the free stream velocity is held constant thereafter.

Consider now the case occurring when the fluid is set in motion impulsively and the free-stream velocity is caused then to vary arbitrarily as a function of time. Contemplate an infinitely long flat plate along which fluid is flowing subject to:

1. The general restrictions and initial conditions as described previously, and
2. The boundary conditions

$$\begin{aligned} u(0,t) &= 0 \qquad & t > 0 \\ u(\infty,t) &= U(t) \qquad & t > 0 \end{aligned} \qquad (5)$$

As in the previous paragraph, the fluid motion is described by the partial-differential equation

$$\frac{\partial u}{\partial t} = \nu \frac{\partial^2 u}{\partial y^2} \qquad (3)$$

The solution to partial-differential Equation (3) which satisfies initial conditions (2) and boundary conditions (5) is obtained by the superposition of an infinite number of terms of the type given in Equation (4) and may be written in the form

$$u(y,t) = U_o \operatorname{erf} \xi + \int_0^t \frac{dU}{d\tau} \operatorname{erf} \frac{y}{\sqrt{4\nu(t-\tau)}} \, d\tau \qquad (6)$$

Equation (6) describes completely the velocity profile which results when fluid in the neighborhood of a flat plate is set in motion impulsively at $t = 0$ and the free-stream velocity is caused then to vary arbitrarily as a function of time.

Consider finally the special case occurring when the fluid is set in motion impulsively and the free-stream velocity is caused then to vary linearly with time. This case is a special case of the problem treated in the previous paragraph which occurs when the free-stream velocity is caused to vary linearly with time, i.e., when

$$U(t) = U_o + At$$

Substituting into Equation (6) and integrating (by parts, when necessary), one obtains

$$\frac{u}{U_0} = \left(1 + \frac{At}{U_0}\right) \operatorname{erf} \zeta + \frac{At}{U_0}\left(\frac{2}{\sqrt{\pi}} \zeta e^{-\zeta^2} - 2\zeta^2 \operatorname{erfc} \zeta\right) \tag{8}$$

Equation (8) describes completely the velocity profile which results in the special case occurring when the fluid in the neighborhood of a flat plate is set in motion implusively at $t = 0$ and the free-stream velocity is caused then to vary linearly with time.

Curves of dimensionless velocity u/U_0 are presented in Figure 51 for several values of dimensionless time At/U_0. As At/U_0 approaches -1 (i.e., as the free-stream velocity approaches 0), reverse flow occurs; when $At/U_0 = -1$, the minimum value of u/U_0 is equal to -0.202 and is attained at ζ = 0.407.

5.3.2 Applicability of Results of Studies of Flow Along a Flat Plate to Flow Through a Tube. Since boundary-layer growth along a flat plate may be described with simpler mathematics than boundary-layer growth along a tube surface, it is desirable to use, whenever feasible, the result of studies of flow along a flat plate to describe flow through a tube. This use of the results of studies of flow along a flat plate gives valid results provided that the boundary-layer thickness for the flow along the flat plate is small compared with the tube radius. For the case where the velocity profile is described by the expression

$$\frac{u}{U_0} = \operatorname{erf} \zeta$$

FIGURE 51

DIMENSIONLESS PLOT OF FLUID VELOCITY AS A FUNCTION OF DISTANCE FROM FLAT PLATE FOR SEVERAL VALUES OF TIME

FLUID IS SET IN MOTION IMPULSIVELY AND FREE STREAM VELOCITY IS CAUSED THEN TO VARY LINEARLY WITH TIME.

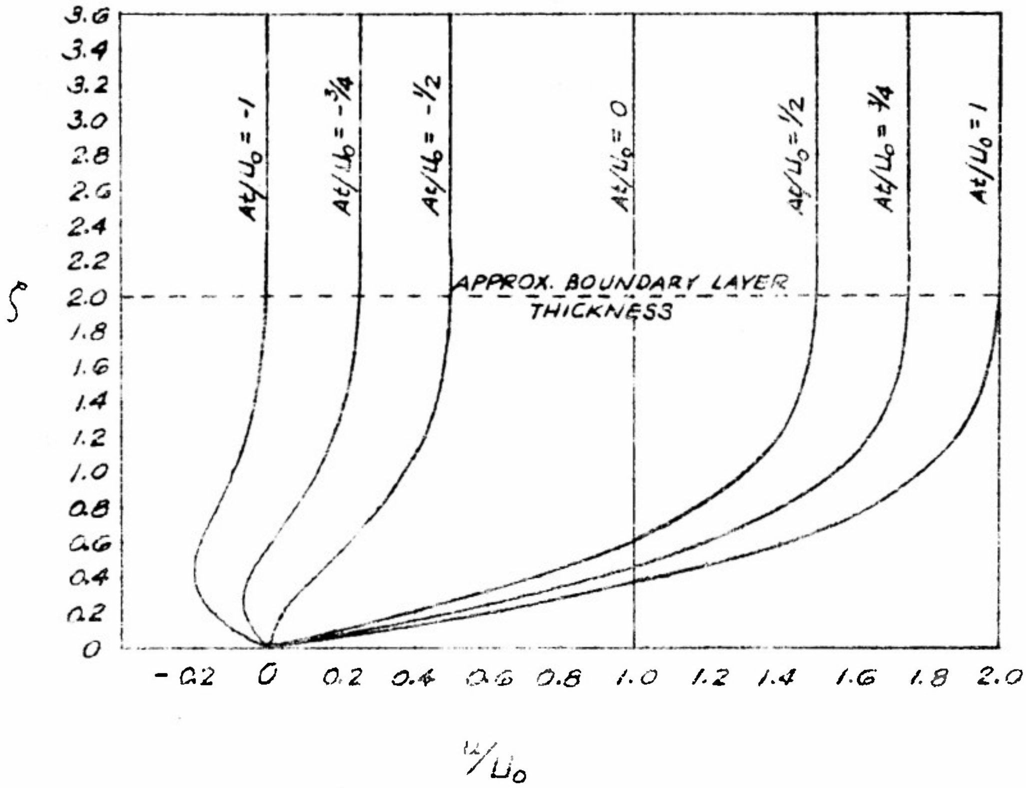

the ratio u/U_o equals 0.995 when $\zeta = 2$. Therefore, the boundary-layer thickness is given approximately in this case by

$$\zeta = 2 \tag{9}$$

For the case where the velocity profile is described by the expression

$$\frac{u}{U_o} = \left(1 + \frac{At}{U_o}\right) \operatorname{erf} \zeta + \frac{At}{U_o}\left(\frac{2}{\sqrt{\pi}} \zeta e^{-\zeta^2} - 2\zeta^2 \operatorname{erfc} \zeta\right) \tag{8}$$

an inspection of Figure 1 reveals that here also the boundary-layer thickness is given approximately by $\zeta = 2$. Hence, if $Z = R/\sqrt{4\nu t}$ (where R is the tube radius) is much larger than 2, then (at least for the two cases mentioned above) the results of the studies of flow along a flat plate may be used to describe flow through a tube of radius R.

Note that R = 0.50 inch and t = 0.001 second correspond to Z = 14 if $\nu = 2.32 \times 10^{-3}$ ft^2/sec (air at 2500°R) and to $Z = 45$ if $\nu = 0.21 \times 10^{-3}$ ft^2/sec (air at 600°R). These values of Z are typical values for a Multi-Jet engine.

5.3.3 Mass-Flow Rate Through a Tube. For flow of a fluid stream with depth $Y = Z\sqrt{4\nu t}$ along a flat plate, the mass-flow rate may be determined readily in dimensionless form from

$$\frac{m}{m'} = \frac{\int_0^{Z} \rho u \, d\zeta}{\rho U Z} \tag{10}$$

where m' is the mass flow rate which could be obtained if the viscosity were zero. For the case occurring when the fluid in the neighborhood of the flat plate is set in motion impulsively at $t = 0$ and the free-stream velocity is caused then to vary linearly with time

$$\frac{m}{m'} = \frac{\int_0^z \left[(U_0 + At)\,\mathrm{erf}\,\zeta + At\left(\frac{2}{\sqrt{\pi}}\zeta e^{-\zeta^2} - 2\zeta^2\,\mathrm{erfc}\,\zeta\right)\right] d\zeta}{(U_0 + At)\,z}$$

$$= \mathrm{erf}\,z - \frac{1}{\sqrt{\pi}\,z}\left(1 - e^{-z^2}\right) + \frac{At}{U_0 + At}\left[\frac{1}{3\sqrt{\pi}\,z}\left(1 - e^{-z^2}\right) - \frac{2}{3} z^2\,\mathrm{erfc}\,z + \frac{2z}{3\sqrt{\pi}} e^{-z^2}\right] \qquad (11)$$

If z is large in comparison with unity, then Equation (11) may be approximated by the simple expression

$$\frac{m}{m'} = 1 - \frac{1}{\sqrt{\pi}\,z}\left(1 - \frac{1}{3}\,\frac{At}{U_0 + At}\right) \qquad (11a)$$

For approximately two-dimensional flow adjacent to an arbitrary bounding surface, the quantity $\frac{m' - m}{m'}$ is directly proportional to the peripheral length L of the bounding surface and inversely proportional to the cross-sectional area Q of the fluid stream. Therefore, since the ratio L/Q equals $1/r$ for flow of a fluid stream with depth Y along a flat plate and equals $2/R$ for flow through a tube having a radius R, Equation (11a) reads for flow through a tube of radius R

$$\frac{m}{m'} = 1 - \frac{2}{\sqrt{\pi}} \frac{\sqrt{4\nu t}}{R}\left(1 - \frac{1}{3}\frac{At}{U_0 + At}\right) \qquad (12)$$

The special case which is obtained when $A = 0$ is the case which occurs when the fluid is set in motion impulsively at $t = 0$ and the center-line velocity is held constant thereafter.

5.3.4 Mass Flow Through a Tube During a Given Period. The mass flow through a tube during a given period may be determined readily in dimensionless form from

$$\frac{G}{G'} = \frac{\int_0^T m\,dt}{\int_0^T m'\,dt} \qquad (13)$$

For the case occurring when the fluid is set in motion impulsively at $t = 0$ and the center-line velocity is caused then to vary linearly with time

$$\frac{G}{G'} = \frac{\int_0^T \rho\left[(U_0 + At) - \frac{2}{\sqrt{\pi}}\frac{\sqrt{4\nu t}}{R}U_0 - \frac{2}{\sqrt{\pi}}\frac{\sqrt{4\nu t}}{R}\frac{2}{3}At\right]dt}{\int_0^T \rho(U_0 + At)\,dt}$$

$$= 1 - \frac{4}{3\sqrt{\pi}}\frac{\sqrt{4\nu t}}{R}\left(1 - \frac{1}{5}\frac{AT^2/2}{U_0 T + AT^2/2}\right) \qquad (14)$$

As in Part 5.3.3, the special case which is obtained when $A = 0$ is the case which occurs when the fluid is set in motion impulsively at $\tau = 0$ and the center-line velocity is held constant thereafter.

Keep in mind the fact that Equation (14) is valid only for large values of the parameter $R/\sqrt{4\nu t}$.

5.3.5 Numerical Results. To indicate quantitatively the effects of viscosity on the several non-stationary pipe flows which were studied, typical numerical results are presented here. If fluid is set in motion impulsively at $\tau = 0$ and the center-line velocity is caused then to vary linearly with time, then for $\tau = 14$

$$\frac{m}{m'} = 1 - \frac{1}{14\sqrt{\pi}}\left(1 - \frac{1}{3}\,\frac{At}{U_0 + At}\right) = 0.96 + 0.01\,\frac{At}{U_0 + At} \qquad (15)$$

$$\frac{G}{G'} = 1 - \frac{4}{42\sqrt{\pi}}\left(1 - \frac{1}{5}\,\frac{AT^2/2}{U_0 T + AT^2/2}\right) = 0.95 + 0.01\,\frac{AT^2/2}{U_0 T + AT^2/2} \qquad (16)$$

and for $\tau = 45$

$$\frac{m}{m'} = 1 - \frac{1}{45\sqrt{\pi}}\left(1 - \frac{1}{3}\,\frac{AT}{U_0 + AT}\right) = 0.99 + 0.00\,\frac{AT}{U_0 + AT} \qquad (17)$$

$$\frac{G}{G'} = 1 - \frac{4}{135\sqrt{\pi}}\left(1 - \frac{1}{5}\,\frac{AT^2/2}{U_0 T + AT^2/2}\right) = 0.98 + 0.00\,\frac{AT^2/2}{U_0 T + AT^2/2} \qquad (18)$$

As in Parts 5.3.3 and 5.3.4, the special case which is obtained when $A = 0$ is the case which occurs when the fluid is set in motion impulsively at $t = 0$ and the center-line velocity is held constant thereafter.

5.3.6 Conclusions. The preliminary analytical study of effects of viscosity on certain non-stationary pipe flows indicated that

1. The results of studies of flow along a flat plate may be used to describe flow through a tube of radius R provided that $R/\sqrt{\nu t} \gg 4$.
2. If the fluid within a tube is set in motion impulsively at $t = 0$ and the center-line velocity is caused thereafter to vary linearly with time, then the decrease in mass-flow rate through the tube due to viscous effects is proportional inversely to $R/\sqrt{\nu t}$ provided that $R/\sqrt{\nu t} \gg 4$.

It is concluded therefore that a large value of $R/\sqrt{\nu t}$ is essential for the attainment of a large mass-flow rate through a jet-propulsion device involving non-stationary fluid flows in straight tubes, i.e., that a large tube diameter and a high cycle frequency is essential for the attainment of a large mass-flow rate through a Multi-Jet engine.

APPENDIX A

ELECTRONIC INSTRUMENTATION

A.1 Measuring Combustion Chamber Pressures.

The following equipment is used to measure combustion chamber pressures:

1. Pressure Pickup, capacitive type, 14mm diaphragm diameter, 0-150 psi range. Model No. 303.(1)
2. Indicator, "DYNAGAGE", DG-101.(1)
   This indicator, when properly calibrated, is sufficient for showing steady-state pressures.
3. Auxiliary Indicator, DuMont 250AH Oscilloscope.
   With this auxiliary indicator, the transients and frequency components up to about 10 kc may be graphically presented for display. If the pressure cycle being examined is of sufficient amplitude and is sufficiently constant as to its recurrent frequency, no further equipment is necessary in order to obtain pressure-time histories. Such, however, is not the case in the Multi-Jet pressure cycles examined, especially during the engine warm-up phase. Additional equipment is required, therefore, in order to synchronize the sweep of the auxiliary indicator with the rotation of the engine shaft and to mark on the pressure-time histories the valve opening and closing times. This synchronizing and marking equipment, together with other related timing equipment, is described in Section A.2 of this appendix.

(1) These instruments are manufactured by Photocon Research Products, 421 N. Foothill Blvd., Pasadena 8, California

The following auxiliary equipment is also required:

1. With the Pickup:

   a. Connecting cable to the Dynagage Indicator(1)

   b. Visual indicator for cooling water flow-rate

   c. Thermocouple for monitoring the outflow water temperature, or the temperature rise of the coolant water.

   d. Thermocouple for monitoring the body temperature of the pickup.

2. With the Dynagage:

   a. Associated power supply--Photocon Research Products Power Supply PS-102 (1)

   b. Auxiliary indicator for display of cyclic pressure voltages.

3. Connections required for the equipment are shown in Figure 52.

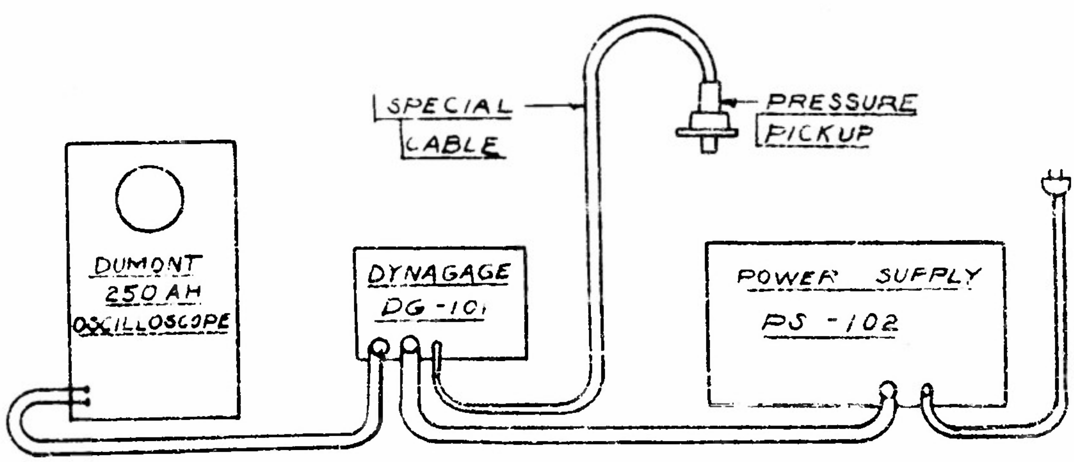

Figure 52. Cable Interconnections Required for Display of Pressure Voltages.

The output of the Dynagage is a medium-impedance negative-going voltage substantially unaffected by external loading, provided that the external load is held to not less than 25,000 ohms impedance.

(1) These instruments are manufactured by Photocon Research Products, 421 N. Foothill Blvd., Pasadena 8, California

Since two loads having respective values of 2 megohms (DuMont 250 AH) and 1 megohm (Bendix TOE-17) are normally used in parallel with the output, their effective combined impedance of 660,000 ohms is appreciably larger than the 25,000 minimum.

In the early stages of the investigations, both recurrent and driven sweep were used for the time base. However, when an external synchronization signal is available, it gives a more satisfactory and stable cycle presentation. Consequently, the timing equipment described in Section A.2 of this appendix was used for almost all of the pressure vs time presentations. Also included in the timing equipment are markers which can be used to vary the trace brilliance in order to show the valve change times or to measure the duration or separation of phenomena which may be observed on the trace.

A.2 Determining Angular Speed and Angular Position of Valve Plates.

Since obtaining pressure time histories and studying valve phasings constituted a major part of the investigation, the choice of the timing system was an important one. Timing signals were needed (1) for synchronizing oscilloscope horizontal sweep with the valve shaft rotation, (2) for marking valve openings and closings on the Oscilloscope trace, and (3) for photographic exposure control in the recording of valve data together with the pressure time histories.

A.2.1 Pulse Generating System for Valve Timing and Oscilloscope Synchronization Marks. A block diagram of the synchronization generating system is shown in Figure 53. This system consists of the following items: two magnetic impulse pickups; a preamplifier; cable leads; a sync-separator which separates positive from negative impulses (see Figure 54 (d) and then inverts the negative ones; and a

PREPARED BY	AEROPHYSICS DEVELOPMENT CORPORATION	REPORT NO 2003-1-R6
CHECKED BY	PACIFIC PALISADES, CALIFORNIA	DATE Oct. 1, 1954

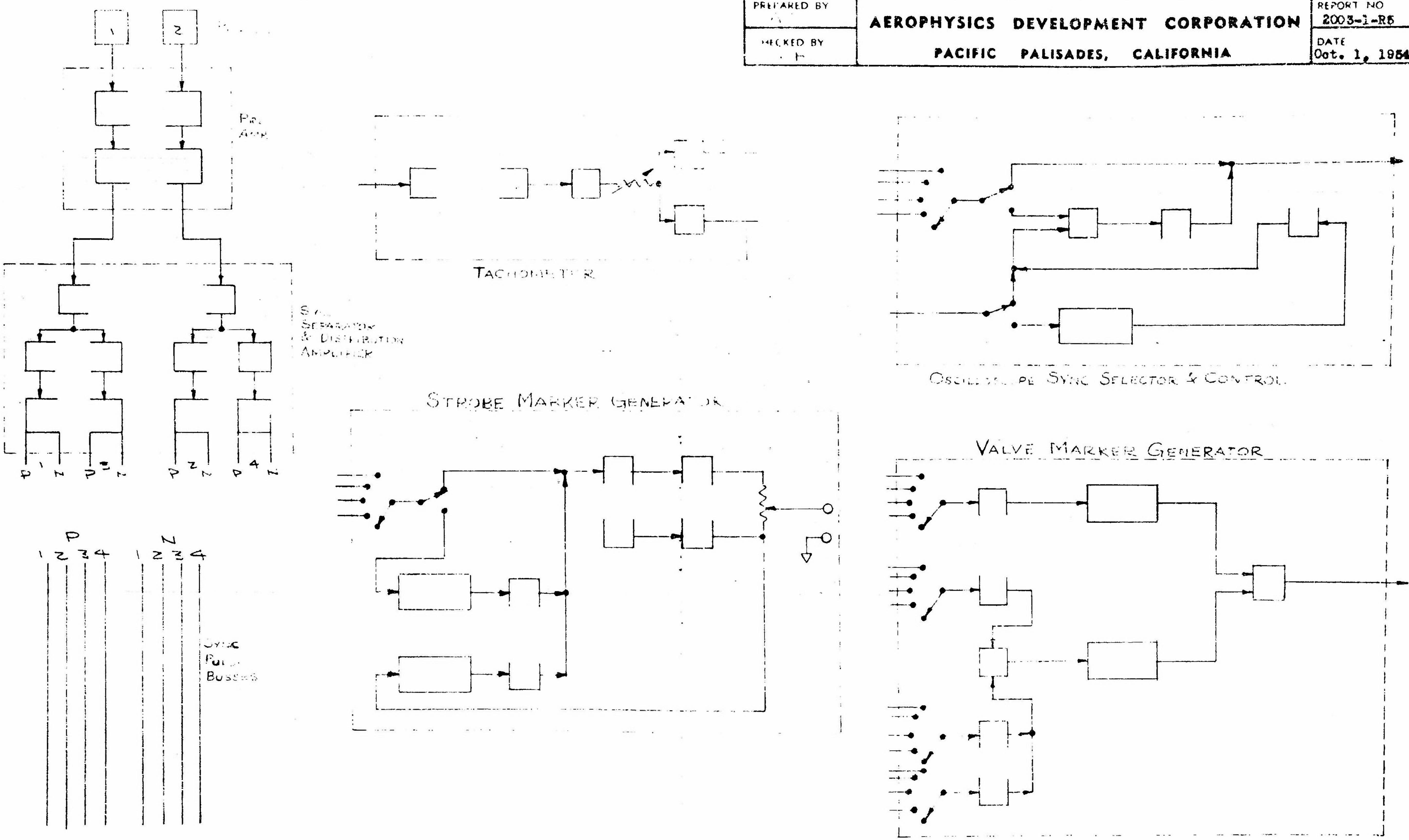

FIGURE 53-TIMING SYSTEM, BLOCK DIAGRAM.

distribution amplifier which provides multiple outputs of either polarity and of power sufficient for driving two or three high impedance inputs from the same source. The block diagram also shows the major units that receive pulses from the distribution amplifier.

During the preliminary design phase of Test Engine No. 2, it appeared that it would not be possible to obtain direct connection of instrumentation equipment to the main shaft. This ruled out the use of synchros and tachometer generators unless chain-and-sprocket or gearing devices were employed to obtain drive. Since it was not desirable that either of these methods be used, a variable reluctance type magnetic impulse generator was chosen to detect engine cycle phase transition times. Two Electro Products Laboratories, Inc. Model 3010 pickups are used -- one for the inlet valve, one for the exhaust valve. Because of the valve housing cooling system configuration, these pickups were placed in the valve housing diametrically opposite the combustion tube opening. The pickups have a positive output when magnetic circuit reluctance decreases and a negative output when this reluctance increases. The Electro Products pickups have an output impedance of about 500 ohms. The wave-form produced is estimated to have a rich harmonic content, extending from about 240 cps to about 48 kcps (for 3600 shaft rpm). During the preliminary design phase it was estimated that cable in excess of 100 feet might be required between the test engine and the control station, thus making it desirable that the source impedance be transformed to a lower value for transmission through a coaxial cable.

When this system was given an initial tryout, trouble was encountered from one source that had been overlooked. The initial choice of pickup radial distance from the shaft center was unfortunate, however, in that it was also the radial distance for the rivets holding the hollow half sections of the valves together. As a result the output signal from the magnetic impulse pickups was not as shown in Figure 54 (a) but instead appeared as shown in Figure 54 (b). The rivets, because of their different magnetic permeability, contributed the three extra impulses following each positive impulse.

The presence of this "rivet noise" in the system would not in itself constitute a serious problem. A suitable circuit would use biased tubes that would not be affected until valve signals of larger amplitude than the rivet signals appeared. Actually, however, the pulses were amplitude modulated by a one-cycle (per shaft revolution) sine wave. The output instead of producing a signal as shown in Figure 54(b) a signal as shown in Figure 54 (c) was produced. Note that amplitude selection can no longer be used, since the one-cycle valve fundamental increases the "rivet noise" during one part of the cycle to a value greater than that of the valve signal impulse during another part of the cycle. The change in amplitude during a cycle was due to valve plate wobble. (This valve plate wobble was later reduced as explained in Section II.) The alternatives were: (1) to modulate the biasing voltage with the same valve wobble signal, or (2) to relocate the pickups radially so as not to pick up rivet noise. The latter step was chosen since it was the quickest and least expensive.

The circuit for the preamplifier, sync-separator, and distribution amplifier is shown in Figure 55. The impulses from the magnetic pickups are fed to a limiting amplifier stage in order to minimize the effect of rpm changes on the impulse amplitude (since the output voltage

FIGURE 54

FIGURE
OUTPUT OF MAGNETIC PICK-UP

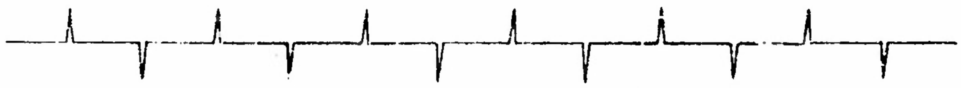

a. DESIRED SIGNAL FROM MAGNETIC PICK-UP

b. SIGNAL FROM MAGNETIC PICK-UP INCLUDING RIVET NOISE

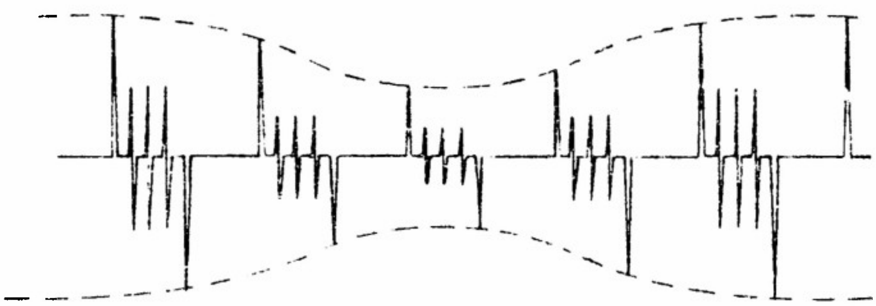

c. AMPLITUDE MODULATION DUE TO VALVE-PLATE WOBBLE

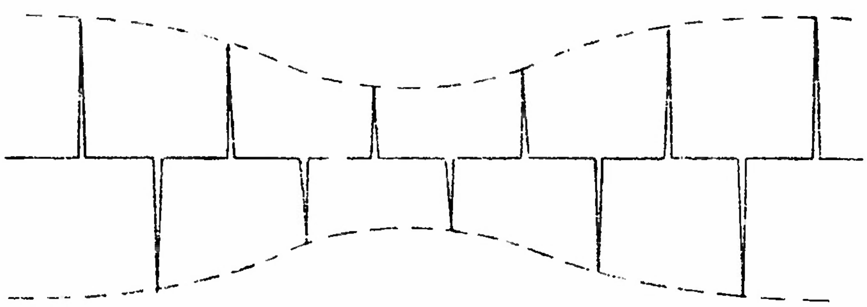

d. SIGNAL FINALLY OBTAINED FROM MAGNETIC PICK-UP

PREPARED BY	AEROPHYSICS DEVELOPMENT CORPORATION	REPORT NO
[illegible]		2003-1-R5
CHECKED BY	PACIFIC PALISADES, CALIFORNIA	DATE
C P H		Oct. 1, 1951

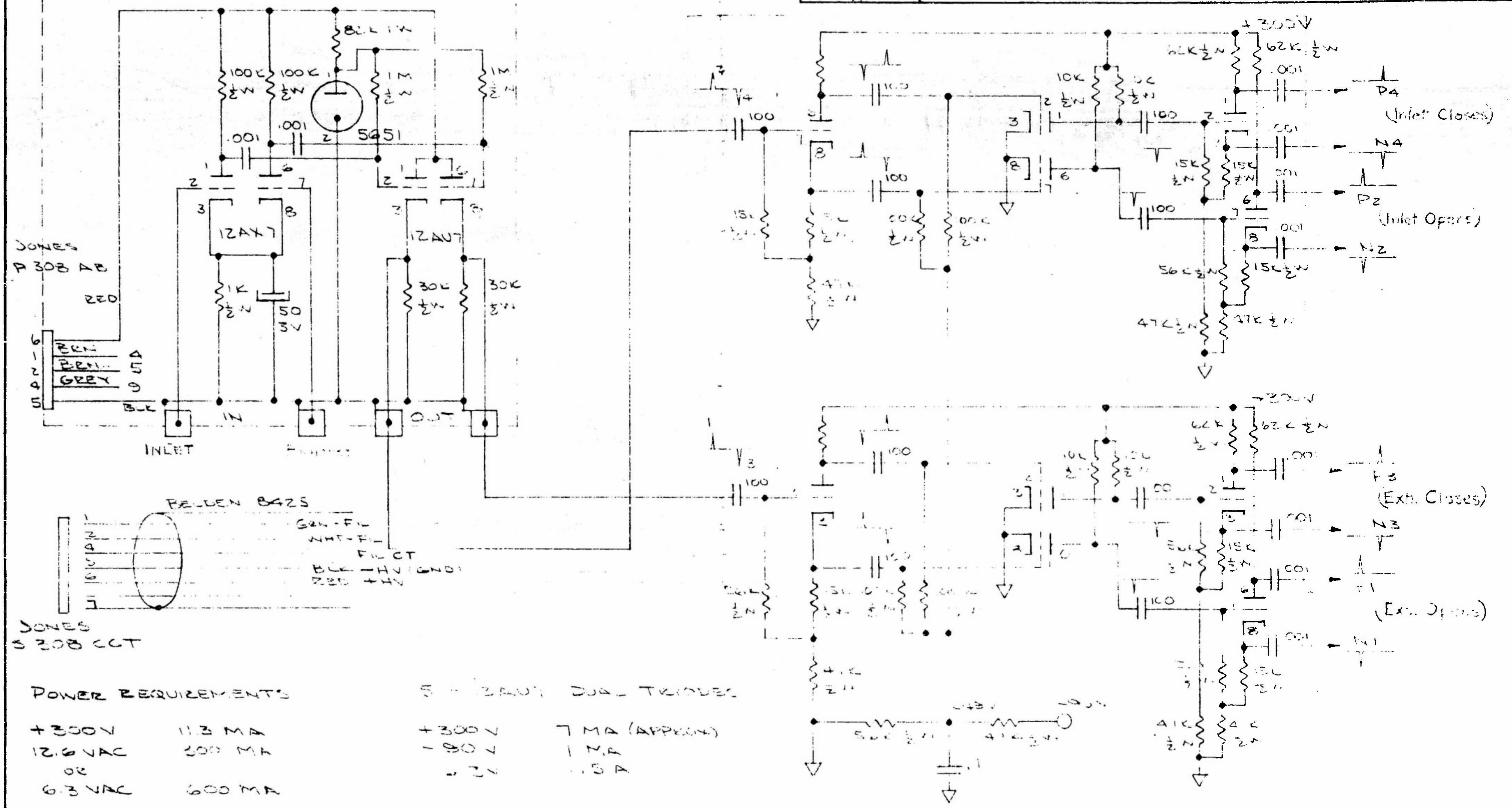

FIGURE 55 SYNC PICKUP AND DISTRIBUTION CIRCUITS.

is a linear function of the valve face speed past the pickup). The limited pulses are then fed through cathode-follower impedance-matching amplifiers to the synchronizing-pulse-separator circuits at the master control station.

For the 12AX7 limiting preamplifiers, the dc grid return is through the pickup winding. These preamplifiers are cathode biased at approximately 1.75 volts by a 1000 ohm resistor shunted by a 50 mfd 3-volt electrolytic capacitor. The load resistors on the limiters are 100,000 ohms each and are returned to +300 volts. Thus, a 3.5 volt peak-to-peak signal input gives maximum output, and no further increase in the output amplitude can be realized.

Capacitance coupling to the next stage is accomplished through 1000 mmf capacitors to the grids of the 12AU7 cathode follower triodes. The grid resistors, 1 megohm each, were returned not to ground but to +89 volts (anode of the 5651 voltage reference tube) in order to hold the cathodes at approximately +100 volts and thereby permit peak-to-peak amplitudes of nearly 200 volts unloaded. Because a 12AU7 cathode voltage of +200 would exceed the cathode-to-filament tube rating, the preamplifier filaments are operated at +150 volts with respect to ground. (Actually, any voltage from +20 to +180 would have been suitable from a design standpoint.) The cathode resistors are 30,000 ohms. The power consumption for the preamplifier alone is 300 volts at 11.3 dcma and 6.3 volts at 600 acma.

Coaxial lines transmit the signals from the preamplifier to the sync separator circuits. Even though the coaxial lines are not properly terminated, no indications of ringing due to reflections within the cable were observed. The sync-separator separates the impulses generated by the valve openings from those generated by the valve closings. In this circuit, the two input stages are connected as phase splitters. Output signals are taken from both plates and from both cathodes of the 12AU7 input tube. The actual separation of the sync pulses is accomplished by the following two 12AU7 tubes. The grids are fixed at a bias well beyond cutoff so that the triode sections are non-conducting until a pulse equalling or exceeding this degree of "beyond cutoff" bias appears. The original amount of bias had to be modified slightly because of the amplitude difficulties that resulted from valve plate wobble. This was accomplished by revising the component values of the voltage divider in the -90 volt circuit. This pair of 12AU7's separated the sync pulses so that each type appeared on a separate terminal.

Because of uncertainty at this point as to the driving needs of the succeeding circuits, it was considered expedient to include a phase splitter in each sync channel, providing both positive-going high-impedance and negative-going low-impedance outputs for each sync impulse. Five 12AU7 medium mu dual triodes are used in the combined sync-separator and distribution amplifier. The power requirement is 300 volts at 7 dcma, -90 volts at 1 dcma, and 6.3 volts at 1.5 aca.

A.2.2 Tachometer. In order to locate a suitable tachometer circuit, a number of circuits found in currently available literature were examined. None of these appeared to meet Multi-Jet testing requirements, and so the following circuit was devised. The input pulses are both "stretched" and amplitude-limited in a single operation by employing one of the available pulses to trigger a flip-flop. This flip-flop controls the next stage, the cathode follower, with an absolute minimum of loading. (Had it been possible to operate from the flip-flop directly and to obtain the exact electrical size of components needed, the cathode follower might have been eliminated.) The purpose of this follower is two-fold. The potentiometer used as a cathode resistor serves as a very convenient means for initially adjusting or calibrating the circuit as well as for touching it up whenever it becomes necessary to change tubes or other circuit components that might affect the output. The tachometer block diagram is presented in Figure 56. At the output of the cathode follower, the square wave of proper amplitude is used alternately to charge and discharge a capacitor through two 1N34 diodes and their associated charge and discharge paths. The quantity of electricity (Q) stored in a capacitor is equal to the product of the capacitance times the electromotive force. Thus, if the capacitor can be made to charge to an arbitrarily fixed amplitude and then to discharge through a meter, we have a rudimentary counting system. An ampere is defined as the current resulting from uniform charge flow past a point such that one coulomb per second passes the point. It follows, then, that if the charge through the meter per shaft revolution can be held constant, the charge per unit time flow of current through the meter is directly proportional to the number of revolutions of the shaft per unit time. In order to obtain a high order of accuracy, it is necessary that (1) the amplitude of the drive (in this case, the flip-flop) be held constant and (2) that the charging and discharging time constants (R x C)

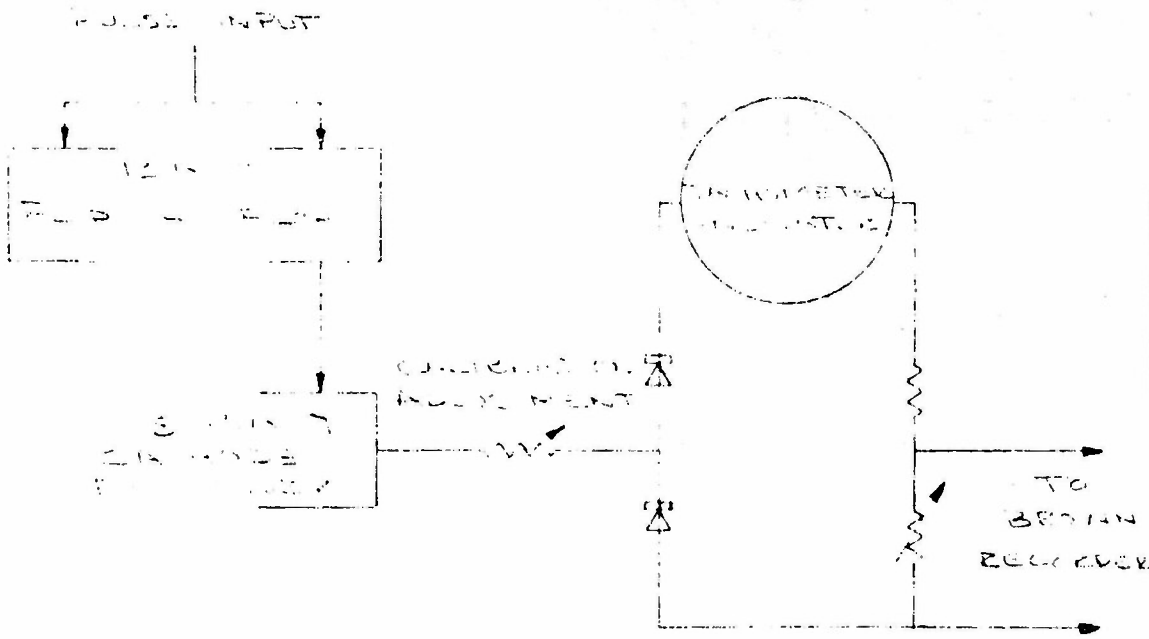

Figure 56. Tachometer, Block Diagram

of the charging and discharging paths be not more than 10 percent of the smallest time available for charging and discharging (in this case the period of the highest number of revolutions per SECOND to be accurately measured). It is further necessary in order to protect the crystals, that the applied pulse amplitude be equal to or, preferably, less than their maximum working back voltage and that the peak charging and discharging current be held below the crystal diode current rating. If such precautions are observed, this system will show a current-to-rpm relationship that is constant to within 0.1 percent. In order to take full advantage of such a linear system, however, a meter having non-linearities of 2 percent or 5 percent of full scale could not be used. Consequently, a 0 - 50 microamp meter represented as accurate to 1/2 percent was used as the indicator. An overlay face showing "RPM x 10^2" was prepared for this meter.

The tachometer circuit is illustrated in Figure 57. The design data for the flip-flop included in this circuit was obtained from a recent publication (see Reference 8). The design has been modified slightly to conform to available power supply voltages and trigger inputs. Also, a switch, a 760 ohm resistor, and a 1520 ohm resistor were included so that the tachometer range could be extended by a factor of two if it became desirable to operate above 5,000 rpm. The 91 ohm resistor is normally a 5 percent tolerance value, and so it is used in conjunction with a 20 ohm rheostat or potentiometer in order to bring the resistance to 100 ohms so that the IR drop may then be 1.00 millivolt per 1000 rpm. The IR drop thus obtained is fed to the Brown recorder to be permanently recorded. The choke in series with

PREPARED BY A.T.	AEROPHYSICS DEVELOPMENT CORPORATION	REPORT NO. 2003-1-R5
CHECKED BY CFH	PACIFIC PALISADES, CALIFORNIA	DATE Oct. 1, 1954

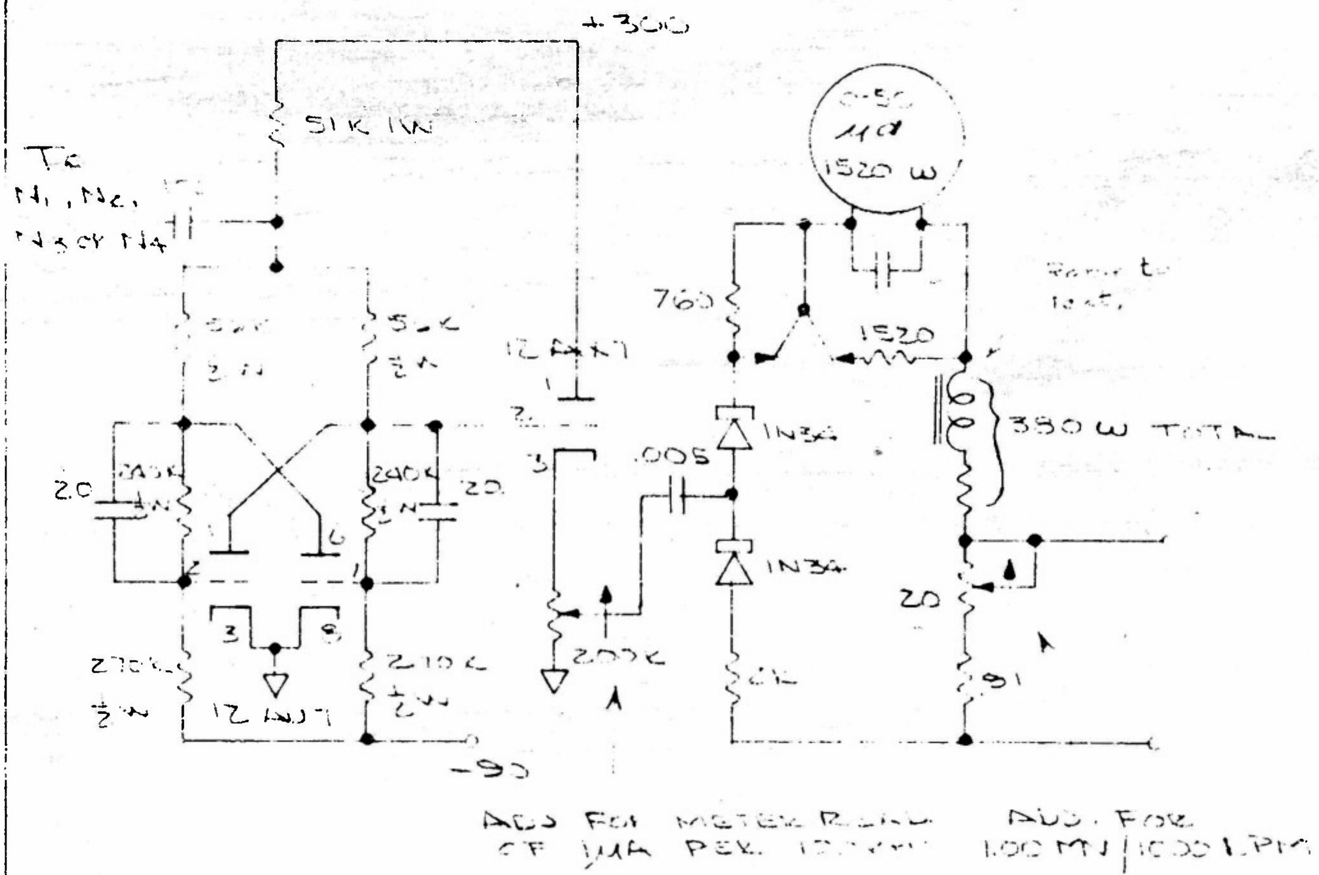

POWER REQUIREMENTS:

+300 V 3.5 MA (MAX)
-90 V 3.6 MA
6.3V 600 MA (FILS)

PANEL CONTROLS:

RANGE SWITCH ONLY

(CHASSIS CONTROLS, CALIBRATION)

BOTH W/ LOCKS

Figure 57. Tachometer, Schematic

the meter movement and the capacitor across the meter movement may be omitted if the counting rate is too high for the meter movement to follow. However, if smooth meter action is desired down to 600 or 800 rpm, some such smoothing device is required.

A.2.3 Oscilloscope Sync Control. It has been previously stated that the pressure cycle was not sufficiently steady, especially during the warm-up period, to provide a steady trace when the pressure build-up voltage was used to synchronize or to trigger the sweep. Consequently, best results were obtained by using "driven" rather than "recurrent" sweep. The purpose of the oscilloscope sync control device, then, is to permit the selection and control of the sync pulses which are to be applied to the "external sync" input in order to perform this sweep triggering service on the oscilloscope.

Reference to the block diagram for this circuit, Figure 58 shows that the purpose of this device is twofold.

(1) S-1 switch permits the selection of any one of the four valve timing signals to trigger the driven sweep. When switch S-2 is in its normal position (as shown), the sweep triggering pulses selected by S-1 go straight through and repeatedly trigger the oscilloscope sweep.

(2) External control of the sync pulses selected by S-1 is provided from the camera shutter release when it is desired that photographic records be taken of the pressure histories being obtained. S-2 then diverts the selected sync pulses to a "gate" which is normally "closed" so that these pulses cannot trigger sweeps of the oscilloscope. When S-3 is

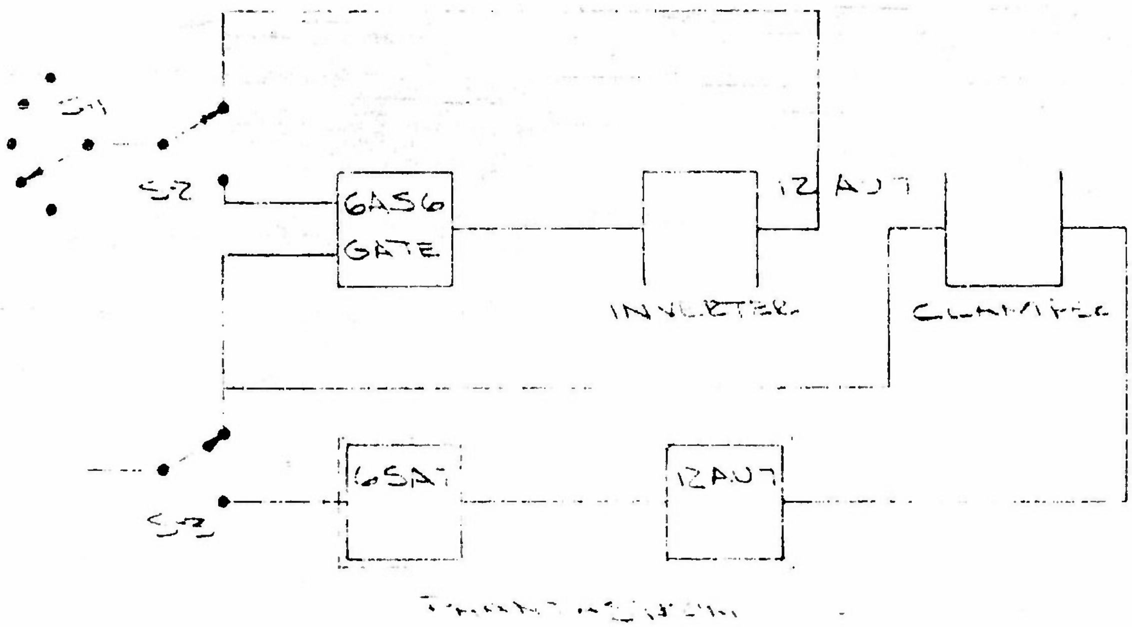

Figure 58. Oscilloscope Sync Selector & Control, Block Diagram

actuated, it triggers a phantastron time-delay generator which provides a pulse of very precise duration. This pulse causes the gate to "open", and its cessation causes the gate to close again. In this manner, from the time that S-2 is first operated, no sync pulses are allowed to trigger sweeps of the oscilloscope until S-3 also is operated. When this occurs, oscilloscope sweeps are triggered by those pulses which appear before the gate is again closed after the "exposure time" is up.

It was considered desirable that composite or multiple photograph exposures be obtained of the engine cycle range, from one cycle only to perhaps ten or more complete engine cycles. While camera shutter speeds in steps covering a part of this range were available, it should be noted that there are two attendant difficulties in the uncontrolled snapshooting of rapidly recurring phenomena:

(1) There is a probability that the shutter will not open until after the sweep has started and has traveled a portion of its normal path, resulting in the loss of part of the cycle to be recorded. In order to overcome this difficulty, the duration of shutter opening can be increased -- which leads to the second difficulty:

(2) There is a probability that at least a portion of a second cycle of the sweep being presented will occur while the shutter remains open. If a steady state phenomenon is being displayed, the portion that is double-exposed will merely burn in a little heavier. However, if there are random

variations to the signal being displayed, then a portion of the trace will be double and very probably ambiguous.

Both of the above conditions assume a perfect shutter. A shutter requiring milliseconds to open and close makes the problem all the more serious. The need for the second function of the sync control circuit -- that of providing a means for feeding the sync pulses to a gate which, when closed, will prevent triggering of oscilloscope sweeps by the pulses -- becomes obvious.

The gate noted above can be set to open, remain open, and then close at any desired times. In Figure 59, the 6AS6 V1 is normally held closed by the plate of V2A (the 12AU7 triode section connected to V1's Grid No. 1). Consequently, sync pulses applied to the suppressor grid do not normally get through to the gate output. However, the gate can be opened by removing the bias on V1's Grid No. 1. This bias can be removed by making the V2A nonconducting, which effectively returns the V1 control grid to ground (zero bias) for the duration of V2A's nonconducting state. Control of V2A is in turn obtained from its grid, which is normally negative with respect to ground by reason of grid current flow. Even though the V2A control grid is normally below ground, the triode section is conducting heavily because it has a slight positive bias. Signal drive for the V2A grid is obtained through a blocking capacitor from the cathode of V4A, which is an output terminal for the phantastron (see References 9 and 10) consisting of V3, V4, and associated circuits. When triggered, the phantastron output appearing at the V4A cathode is a negative-going sawtooth or sloping wave of sufficient amplitude to cut off V4A. This opens gate

PREPARED BY	AEROPHYSICS DEVELOPMENT CORPORATION	REPORT NO.
AT		2003-1-R5
CHECKED BY	PACIFIC PALISADES, CALIFORNIA	DATE
CPH		Oct. 1, 1954

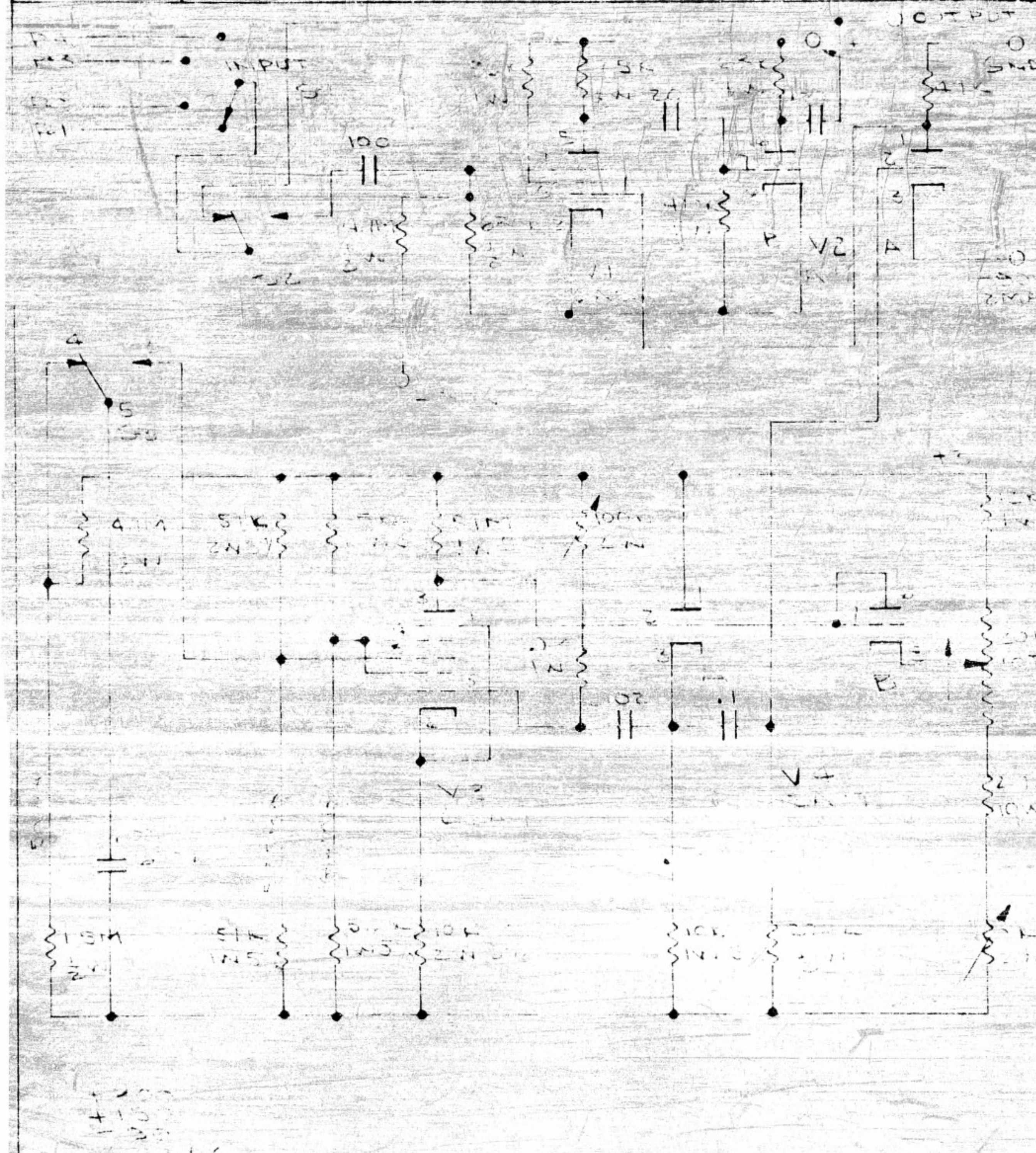

Figure 59. Oscilloscope Sync Selector & Control, Schematic

tube V1 and pass any pulses appearing on Grid No. 3 of V1. Switch No. 3 normally applies +72 volts to a storage capacitor. When this switch is actuated, the +72 volts from the condenser is applied to Grid No. 3 of V3 (the phantastron trigger input), which is normally slightly under 30 volts. This, in effect, applies a pulse of approximately (72 - 29 = +43 volts to trigger the phantastron and thereby open the gate.

A special cable release incorporating switches S_2 and S_3 was built for the camera shutter. The camera is equipped with a special pistol grip device having two camming surfaces which act upon these two microswitches. S_2 operates as soon as the trigger squeeze is started. During the middle portion of the squeeze the shutter is opened (when the camera shutter control is set to B, or bulb). At the end of the trigger stroke S_3 is actuated. Thus, by means of this device it is possible to obtain at will photographs of "n" whole sweeps, where n is an integer subject to the following qualifications:

(1) The oscilloscope is set to produce one sweep for each pulse;

(2) n is the number of sync pulses passed by the gate. (The "open" time for the gate, with the component values shown, may be varied from 0.002 to 0.100 seconds.)

V2B inverts the gated pulses so that the pulses appearing at the output have the same (positive-going) polarity as the input pulses to the contacts of S_1.

Some difficulty in feeding the sync pulse through the cable to S_2 in the pistol grip and back again was anticipated. Space was provided for mounting a relay which could perform the required switching and which could be remotely operated by S_2. However, the circuit functions quite satisfactorily as shown. If a connecting cable longer than 6 to 10 feet is used, the sync pulse should be switched by relay rather than directly by S_2.

A.2.4 Strobe Marker Generator. It was considered desirable to have a marker pulse which could be superimposed on the pressure-time plot as a brilliancy or intensity modulation usable for identification or for time or phase position measurement. Figure 60 presents the block diagram for the strobe marker generator, and Figure 61 presents the schematic for this generator.

S_1 selects the sync pulse which is to trigger the marker. S_2 chooses between instantly started (direct) and delayed pulses. Direct pulse is fed directly to octal socket terminal 5 for the EECO Flip-Flop Z8342. The corresponding output (octal socket terminal 6 of the same socket) is directly connected to octal socket terminal 4 fo the EECO Dual Cathode Follower Z8309. The second output of the flip-flop (octal socket terminal 7 for the Z8342) is directly connected to the other input of the dual cathode follower, octal socket terminal 5 for Z8309. The two cathode follower output terminals (octal pin 6 and 7) are connected to opposite ends of a 100,000 ohm or a 200,000 ohm potentiometer. This same pin 7 is also capacitively coupled (470 to 500 mmf) to the sync pulse input terminal of the marker duration phantastron.[1] Its output is directly coupled to octal socket 5 for the Dual

[1] These two phantastrons are quite similar to the ones heretofore referred to. The principal difference is that in this case negative-going signals are used for triggering. The circuit is found in the third edition of Federal Telephone Radio Corporation's: Reference Data for Radio Engineers, pp 270-271.

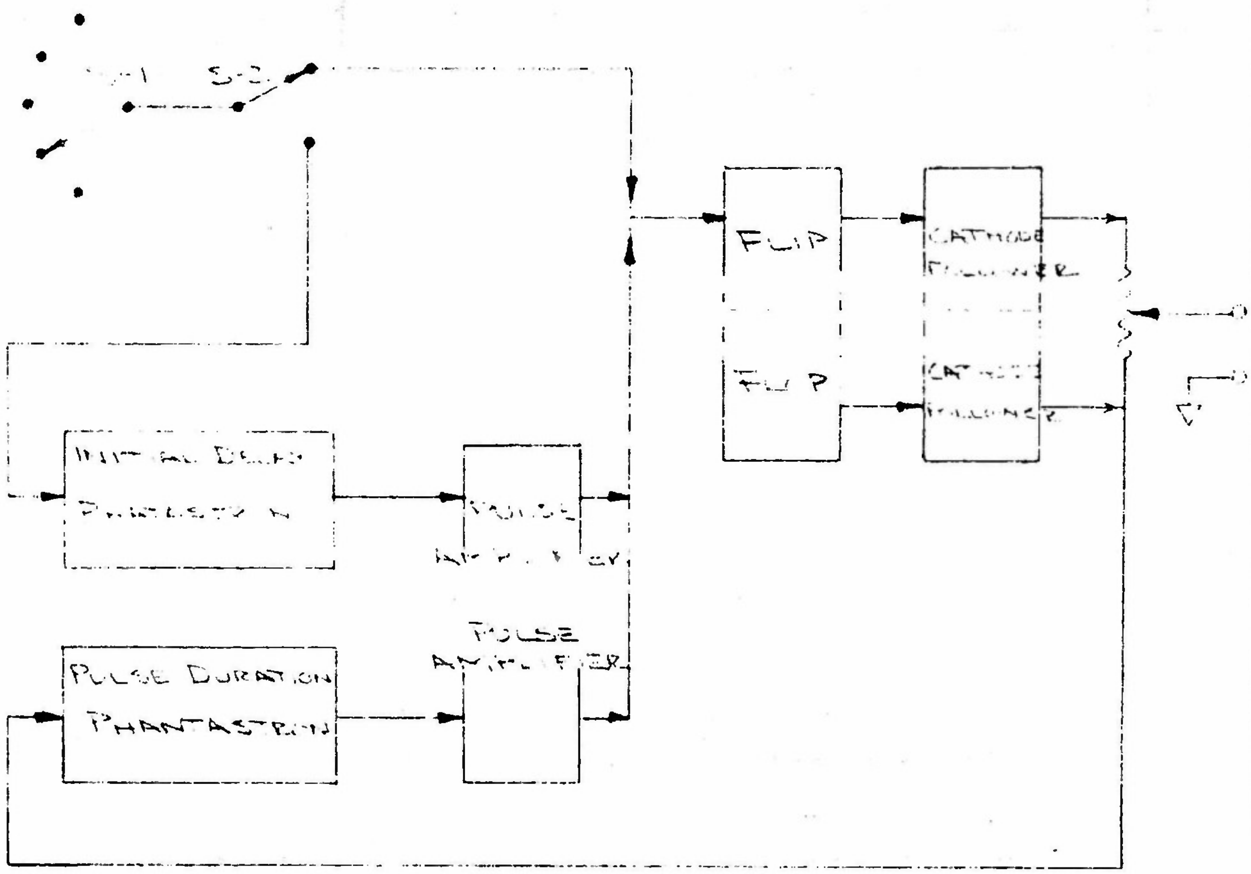

Figure 60. Strobe Marker Generator, Block Diagram

PREPARED BY AT	**AEROPHYSICS DEVELOPMENT CORPORATION**	REPORT NO. 2003-1-R5
CHECKED BY CPH	**PACIFIC PALISADES, CALIFORNIA**	DATE Oct. 1, 1954

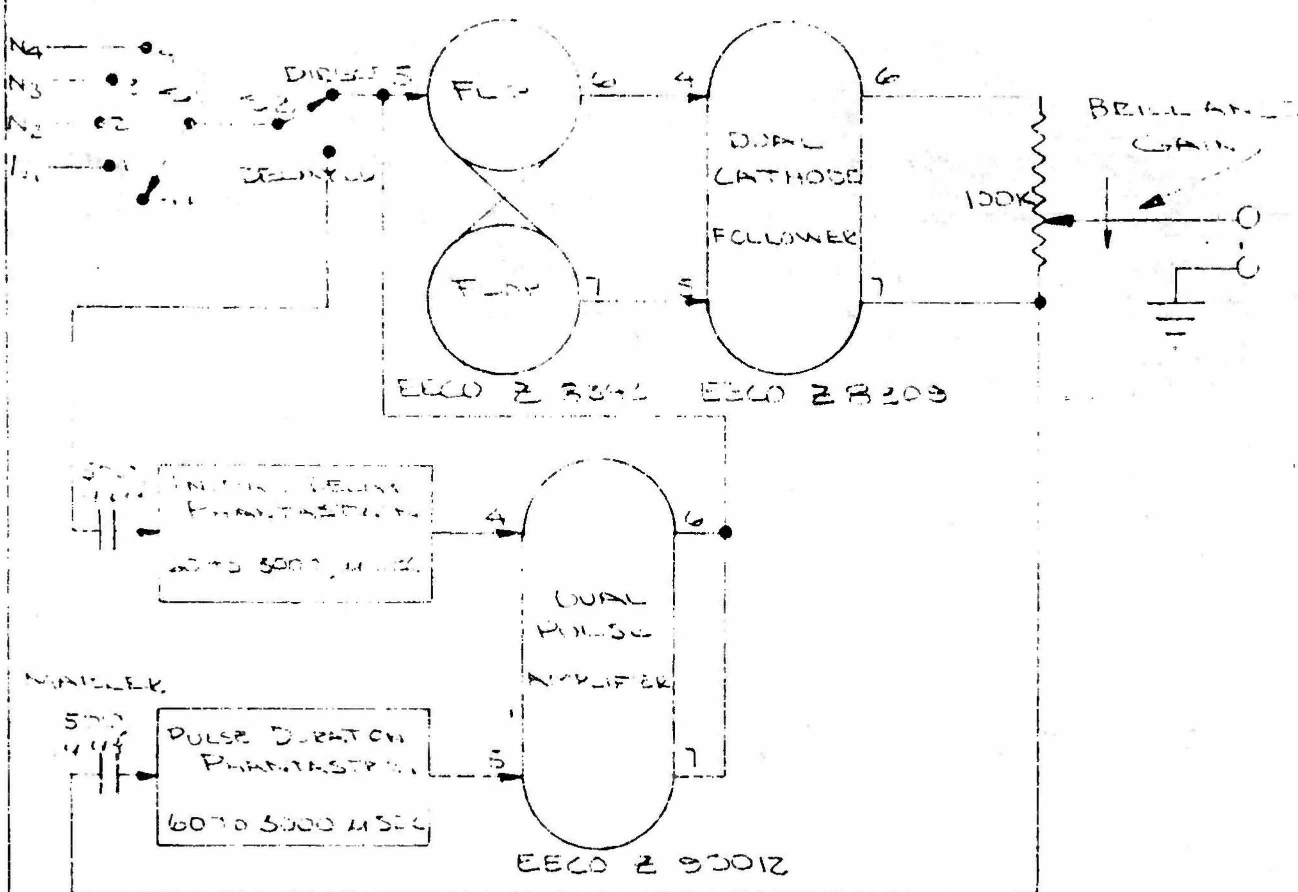

PHANTASTRON [illegible] FROM
REFERENCE DATA FOR RADIO ENGRS
3rd EDITION, pp 270-[illegible]

PLUG INS:
EECO PRODUCTION CO.
867 S. VERMONT
L.A. 5 CALIF.

Figure 61. Strobe Marker Generator, Schematic

Pulse Amplifier EECO Z90012.

The "delayed" switch is capacitively coupled by 500 mmf to the initial delay phantastron input. The corresponding output is directly coupled to octal socket terminal 4 for the dual pulse amplifier. The outputs (terminals 6 and 7) for the Dual Pulse Amplifier Z90012 are directly connected to the flip-flop input (octal socket terminal 5).

The wiring then is continued by applying 6.3 vac to pin 3 and 8 of all octal sockets and by applying +200 volts to socket connection 1 for the Z8342 and to socket connection 2 for the Z90012. Grounds are applied to Z8342 terminal 2, and Z90012 terminal 1. If a 200 volt supply which is balanced to ground is available, the +100 should be connected to Z8309 octal socket terminal 2 and the -100 to terminal 1. In this case the output is taken directly from the movable contact of the potentiometer between terminals 6 and 7 of the socket for Z8309.

If the above voltages are not available, +200 should be applied to octal socket terminal 2, and terminal 1 should be grounded. The output may then be taken from the same point as above, but it must now be capacitively coupled. If the lowest frequency (pulse repetition rate) and the Z input impedance of the oscilloscope are known, the smallest capacitor to use should be:

$$C = \frac{10}{f R}$$

C = farads
f = cps
R = ohms

A.2.5 Valve Marker Generator. For recording the transition points between the four engine cycle positions so that they can be shown on the pressure time history graph, the PWM (pulse width modulation) channel of the Ampex 309 recorder is used.

The input requirements are relatively simple. The level (amplitude) may be anywhere from one to 50 volts. The time requirements are also relatively simple. The pulses must be at least 75 microseconds but less than 1000 microseconds long. There must be a minimum resting time of 75 microseconds between pulses.

Since the valve sequence is determined by mechanical mounting, it was assumed that if positive identification of one valve phase transition was provided, the other transitions could merely be marked. Should identification be required for other transitions, it could be provided either by changing the transition selected by means of a selector switch or by counting forward or backward in the transition sequence to the desired point. Such a marking system would then require two types of pulses differing from each other in duration.

The marker system (a block diagram of this system is shown in Figure 62), then, consists of a wafer-type selector switch which selects the transition pulse to be positively identified and feeds it to the identifying marker generator. The other three transition pulses are first mixed then fed to a second marker generator.

The wafer switch in the upper left hand corner (see Figure 63) selects the transition to be positively identified. V1a inverts the sync pulse and triggers the unique delay phantastron. V1b inverts a second sync pulse and triggers V3. V2 mixes the other two sync pulses and also triggers V3.

V3, since it is triggered by both V1b and V2, mixes the last three sync pulses and triggers the common delay phantastron. These phanta-

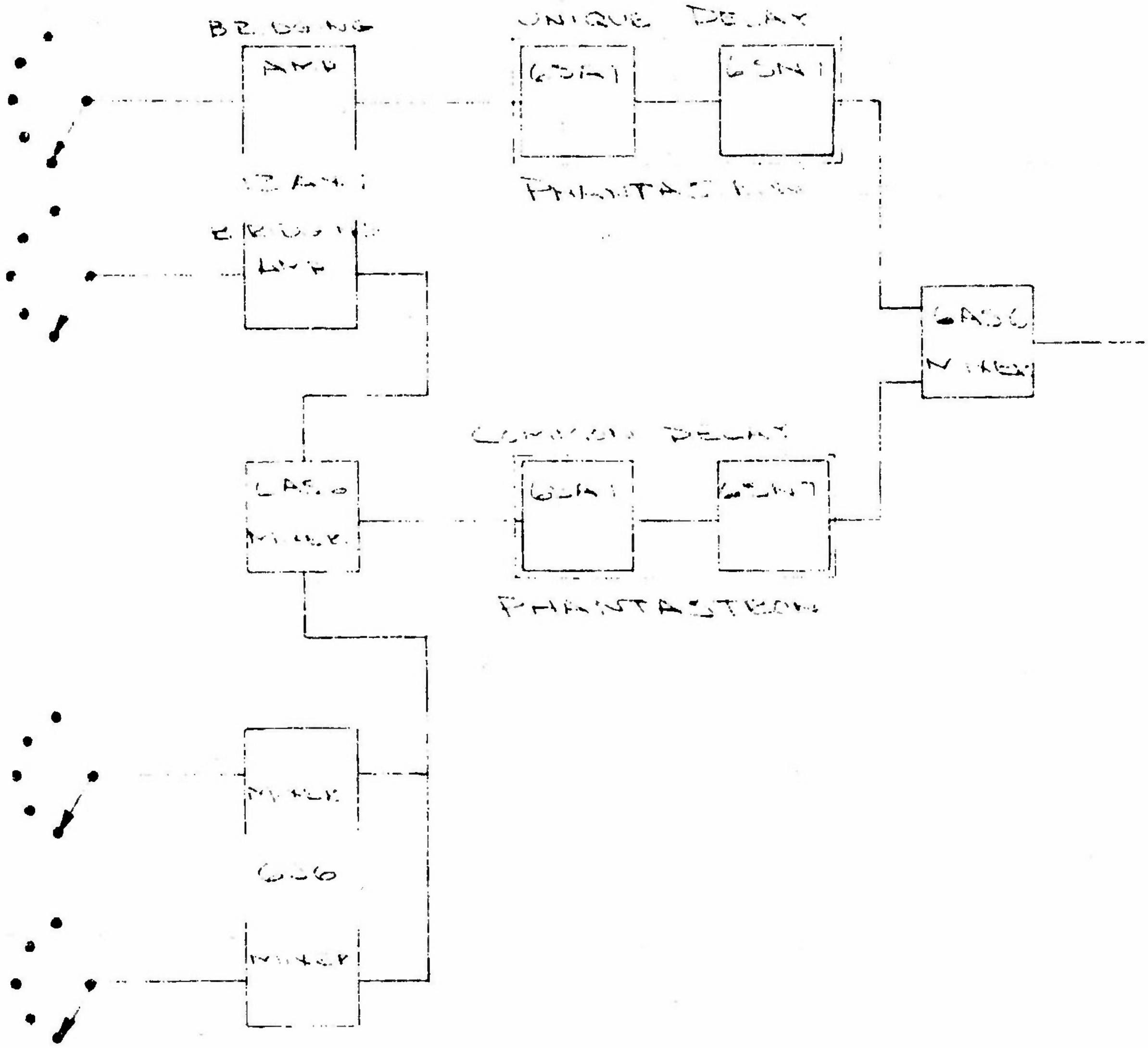

Figure 62. Valve Marker Generator, Block Diagram

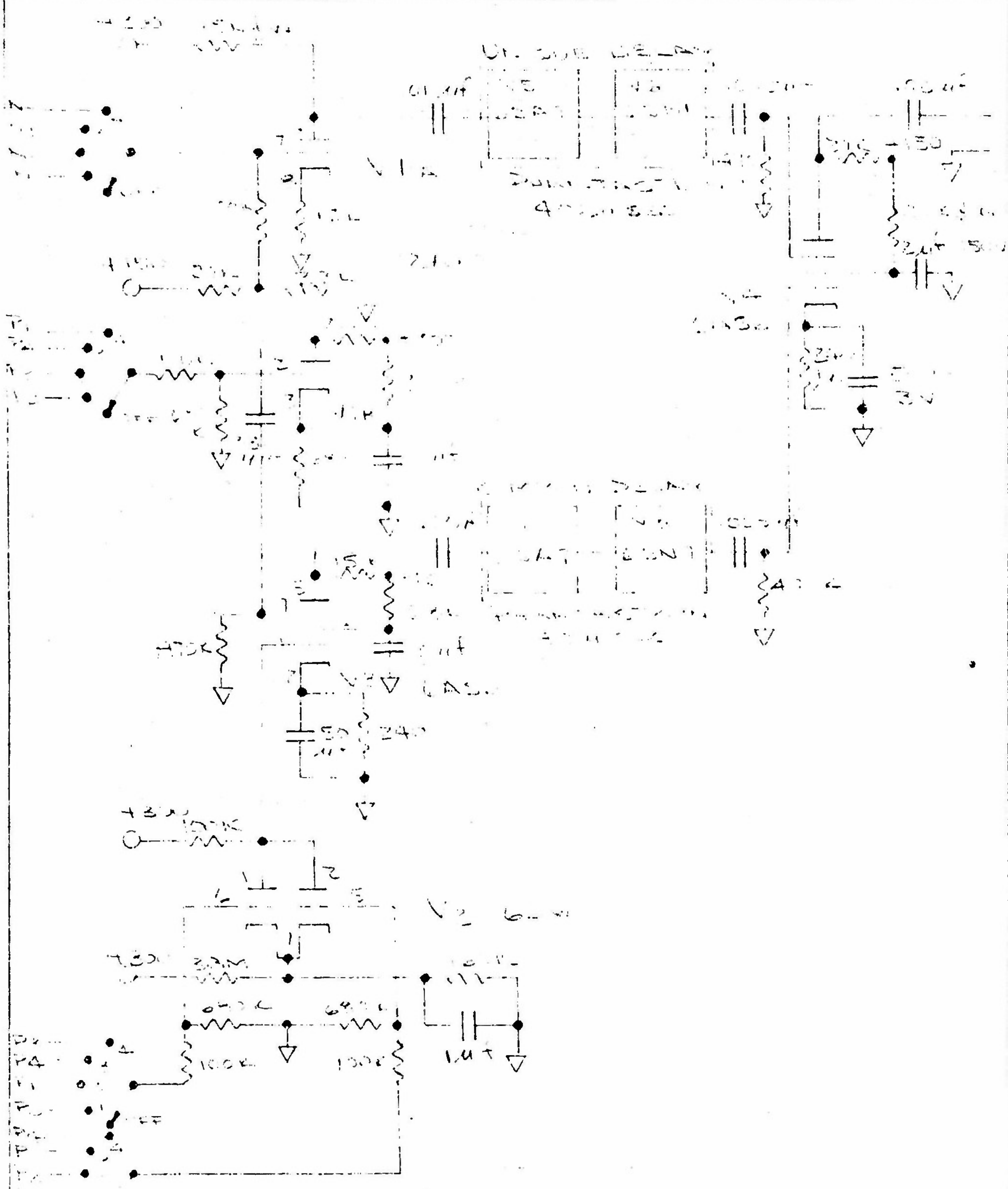

Figure 63. Valve Marker Generator, Schematic

strons are similar to the one described heretofore in subsection A.2.3. and in Reference 9. In actual construction of the phantastrons the principal difference between these phantastrons and those previously described is simply that the 20,000 ohm potentiometers which control the delay time are screw-driver-adjusted with locking collars instead of multiturn pots. V4 mixes the outputs of the two phantastrons. Its output contains, for each engine cycle, one pulse which is unique in duration and three pulses which have a common duration, and may be represented as three short duration pulses followed by a long duration pulse. A photograph of the oscilloscope trace showing the beam modulated by the above mentioned pulses is shown in Figure 23 (Section III).

A.3 Recording, Storing, and Reviewing Pressure-Time Histories.

Because of the advantages of demonstrating below-ambient pressures during a part of the engine cycle, it was considered necessary that a recording means which would preserve the steady state as well as the cyclic pressures be selected. This can be accomplished by a frequency-modulated recording system. Furthermore, a means for accurately recording valve timing signals simultaneously with the pressure-time histories was needed. It appeared that the Ampex 309 dual channel (frequency modulated and pulse width modulated) magnetic tape recorder would best fulfill the above requirements.

A.3.1 Recording Pressure-Time Histories and Valve Timing Marks.

Since the output of the dynagage is a voltage waveform which is a linear function of the pressure acting against the pickup diaphragm, the search for a frequency modulator indicated that a voltage-controlled oscillator would serve adequately for recording the pressure-time histories. It was decided that a commercially available voltage controlled oscillator should be obtained. The Bendix TOE-17 was chosen since it preserves the highest required modulation frequencies. This unit requires 6 volts at 750 milliamperes for filaments and 108 volts at 8.4 milliamperes for plate supply. Since the filaments are the cathodes, the use of raw ac introduces 60- and 120-cycle components into the output, and its use should be avoided for critical applications. An attempt first was made to use a lead-acid storage battery for filament supply, but because of the problems attendant in this installation, it became necessary to construct instead a dc filament supply. The schematic diagrams for filament and plate power supplies are shown in Figure 64. Unfortunately, the available oscillators did not have input voltage ranges corresponding to the output of the dynagage indicator. Therefore, in order to match these ranges and provide a means for putting step modulation functions of voltage on the tape at will, a voltage-controlled oscillator input adapter was constructed. It was decided to obtain a voltage-controlled oscillator having a 0- to +5-volt range and to incorporate a steady bucking voltage of 5.000 volts, thereby using the 0- to -5-volt portion of the Dynagage to drive the voltage-controlled oscillator over the corresponding range of +5 to 0 volts. This, in effect, would shift the zero of the 0- to -5-volts range of the Dynagage so that the resulting signal would have a new value +5 to 0 volts. This can readily be accomplished, as is shown by the circuit illustrated in Figure 65.

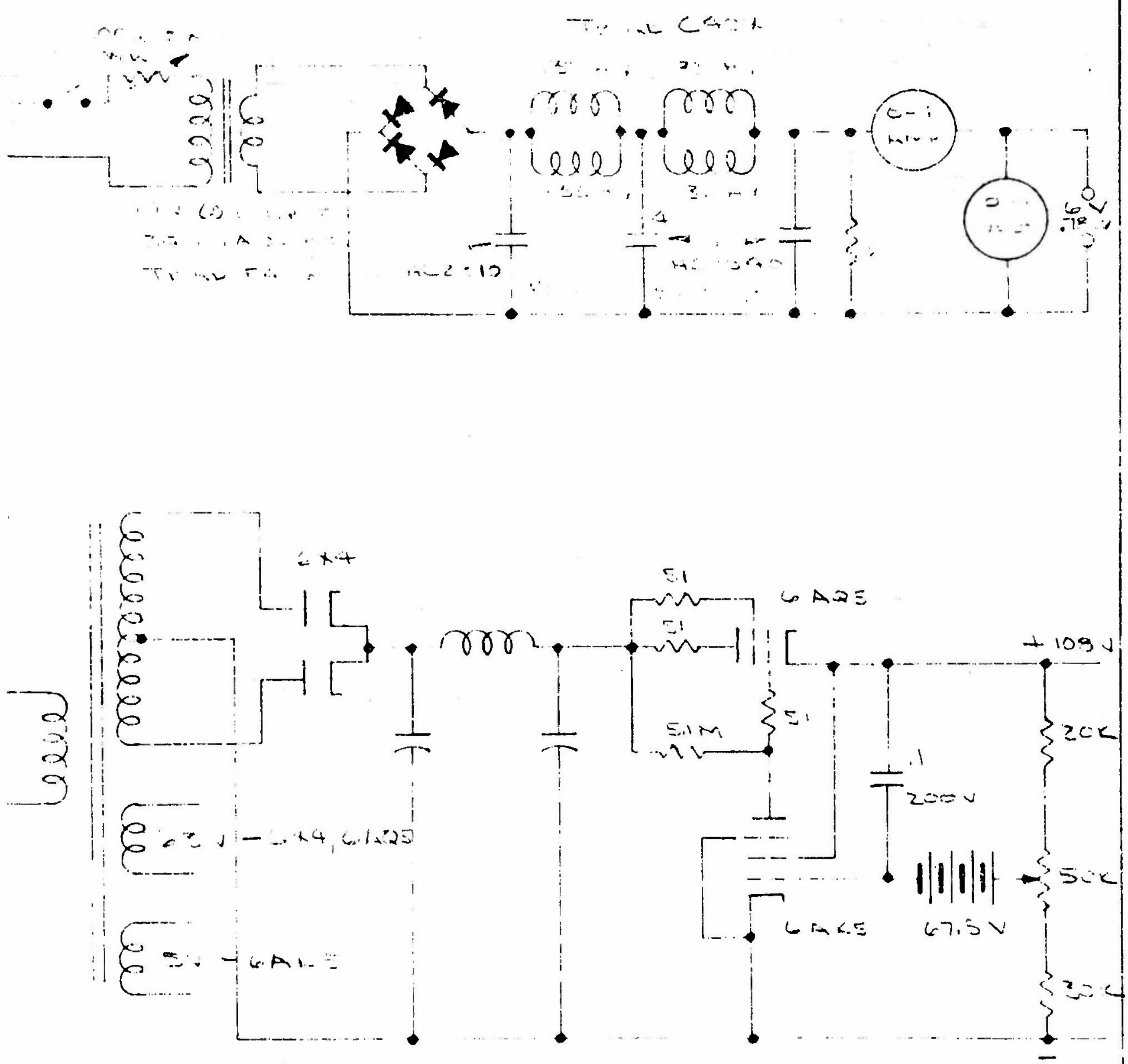

Figure 64. Filament & Plate Power Supplies for TOE-17

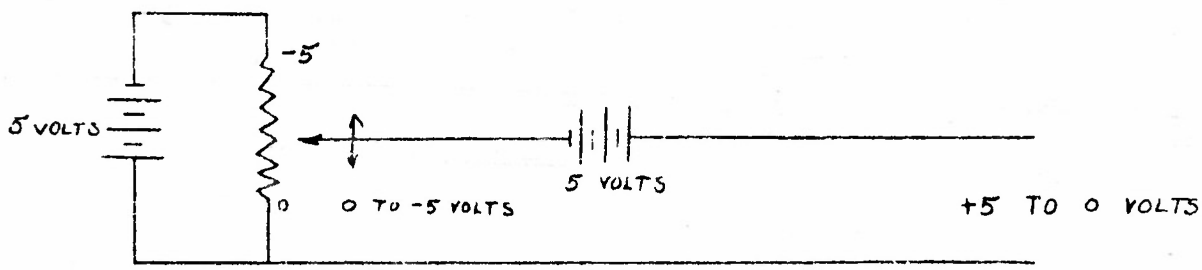

Figure 65. Zero Shift for Input to the Bendix Oscillator.

Since it is necessary, if the circuit is to yield reproducible results, that a steady 5.000 volts be available, a standardizing means is provided. The bucking voltage is provided by 0.00100 ampere current flowing through a series-chain of precision (0.1 percent) resistors totaling 5000 ohms. One of the units in this series is a 25.00 ± 0.05 percent ohm resistor. The IR drop across this one resistor is periodically measured and recorded. When the recorded voltage deviates from 25.0 millivolts, a potentiometer in series with the 5000-ohm string of precision resistors is adjusted to restore the proper current level so that a current of 5.000 ± 0.005 volts is always produced for the bucking circuit. For dc, this 5-volt source has an impedance of 5,000 ohms, but it is shunted by a fairly large capacitor so that its impedance to AC would be negligible in relation to the input impedance of the Bendix oscillator.

The pressure pickup calibration was determined by plotting calibration points of static pressure in <u>inches of Hg</u> units <u>vs</u> the <u>output voltage</u> of the dynagage. In order to simplify the reduction of data from the magnetic pressure information records, it was considered desirable that step-function voltage information be inserted on the magnetic tape. Therefore, as shown in Figure 66, one 475-ohm and nine 500-ohm precision resistors were included with the previously mentioned 25.00 (±0.05 percent) ohm resistor in order to provide ten equal incremental voltages. An eleven-position rotary stepping switch was used to sample first zero then the ten 0.500-volt steps and connect them to the input of the voltage controlled oscillator. In this manner, step voltage calibrations can be recorded on the magnetic tape simply by dialing the desired step on a telephone-type dial. A photograph of the oscilloscope beam showing the step-function voltage calibration is shown in Figure 67.

For convenience in identifying the records of the several engine test runs, a dynamic microphone, a three-stage speech amplifier, and a changeover relay are used to record a voice identification on the tape. The schematic for the speech amplifier is included in Figure 66, since this amplifier is mounted on the same chassis as the VC oscillator input adaptor and calibrator and the Bendix oscillator.

Valve timing markers are recorded concurrently on the PWM channel of the Ampex 309 recorder. The valve timing signals are the three short signals and one long signal generated by the equipment described in subsection A.2.5 (diagramed in Figures 62 and 63 and shown in Figure 23, Section III).

A.3.2 Playback of Recorded Information. The playback system selected was that used and reported in Reference 11. There is a moderate degree of frequency-vs-amplitude distortion inherent in this system. However, because of the step calibration system described in

PREPARED BY: AT	AEROPHYSICS DEVELOPMENT CORPORATION	REPORT NO. 2003-1-R6
CHECKED BY: CPH	PACIFIC PALISADES, CALIFORNIA	DATE Oct. 1, 1954

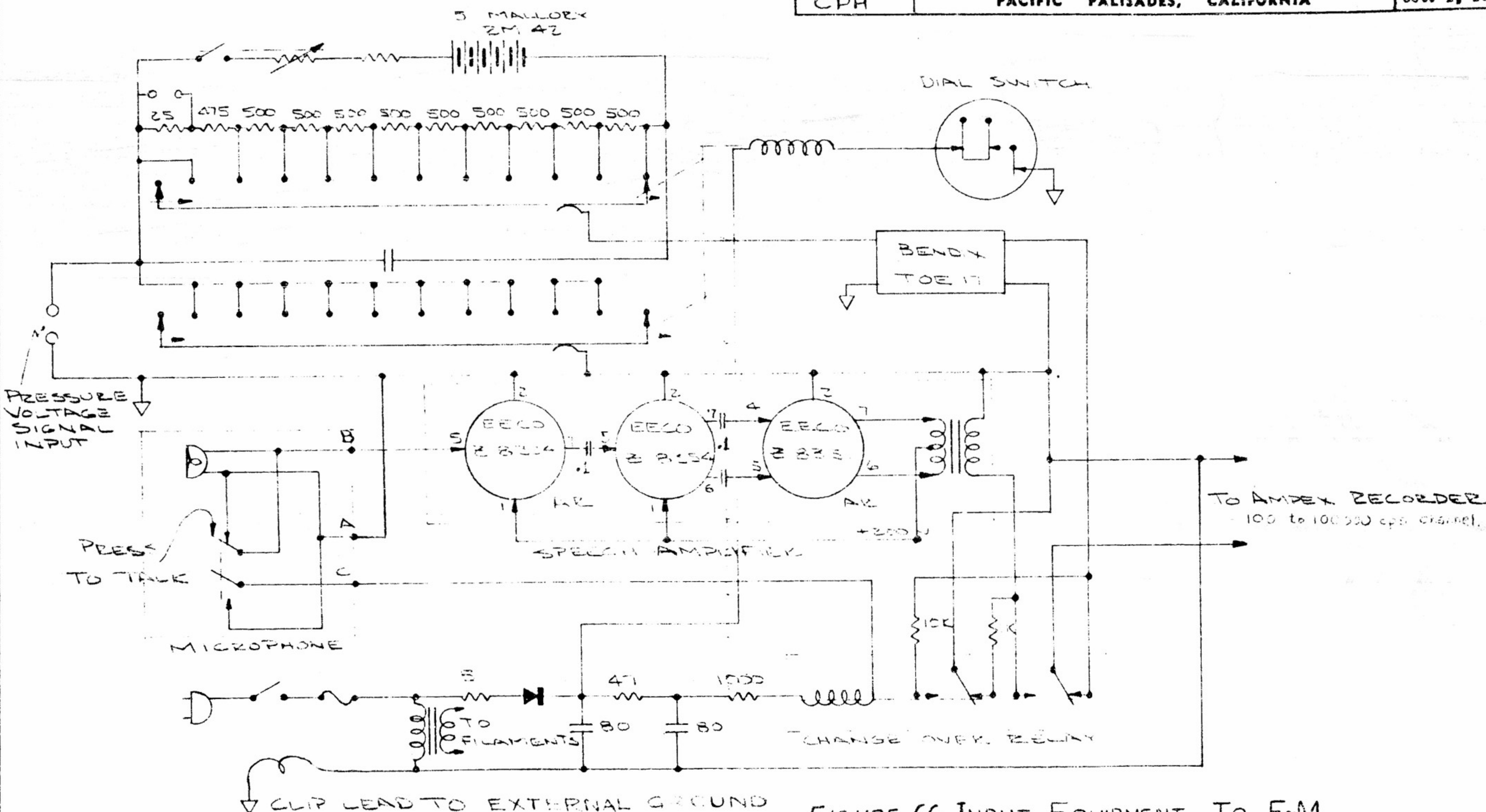

FIGURE 66 INPUT EQUIPMENT TO F-M RECORDER CHANNEL

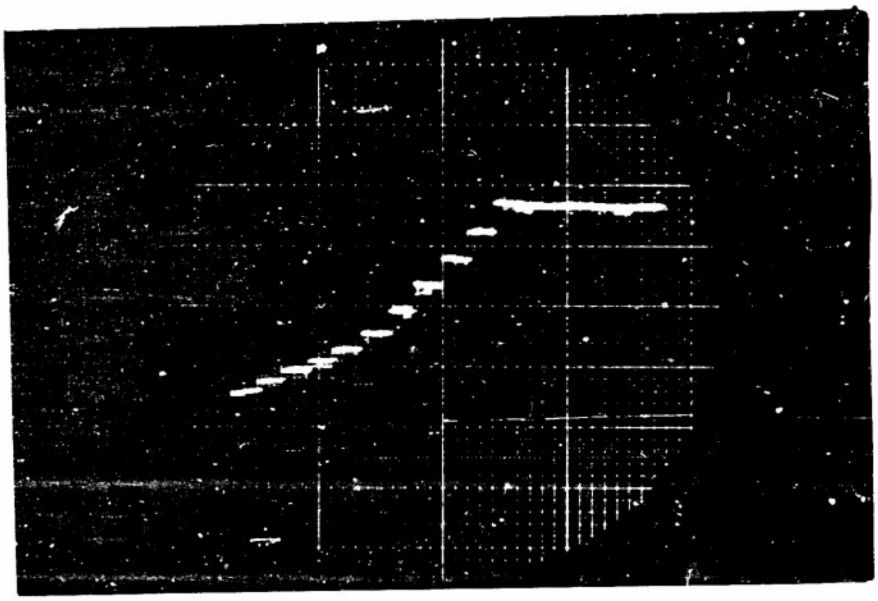

Figure 67. Calibrating Voltage Steps on Oscilloscope Trace (Each Step = 1/2 volt Deflection).

Subsection A.3.1, this non-linearity was considered acceptable.

The discriminator system can be most simply described as a triggered variable-duration pulse generator having a high degree of pulse duration stability and having an output which is limited, integrated, and low-pass filtered to remove carrier ripple. Variations in the level of the integrated output conveys the information.

The pulse generator used is a plug-in unit[1]. It is described as a Quick Recovery One-Shot. In order to use this system, it is necessary that a one-shot be made to deliver a pulse having a period which is half that of the highest frequency -- 7.44×10^4 cps, or about 1/2 of 13.45 musec = 6.73 musec. This pulse should be held constant at 6.73 musec duration. As the carrier is modulated (shifted to lower frequencies by the modulating input), the pulse must hold a constant duration and the interval between pulse leading edges must vary as the reciprocal of the carrier. Thus, in effect, the pulse output would be a rectangular wave varying from a square wave (i.e., 50%-50%) to a rectangular wave with 44.25%-55.75% as a limit of unbalance.

The output available from the frequency-modulated electronic chassis of the Ampex 309 recorder is adjusted for 1.23 rms volts into 500 ohms. It can, however, be turned up as high as 4 rms volts or 11.2 volts peak to peak.

The input stage is a high-speed cathode-coupled bistable multivibrator known as the Schmitt Trigger circuit (see References 12 and 13 and Figures 68 and 69). It will trigger satisfactorily from an input of 5 volts peak to peak. The input impedance of 1 megohm does not

[1] Type 28889, manufactured by Electronic Engineering Company, 180 S. Alvarado Street, Los Angeles, California.

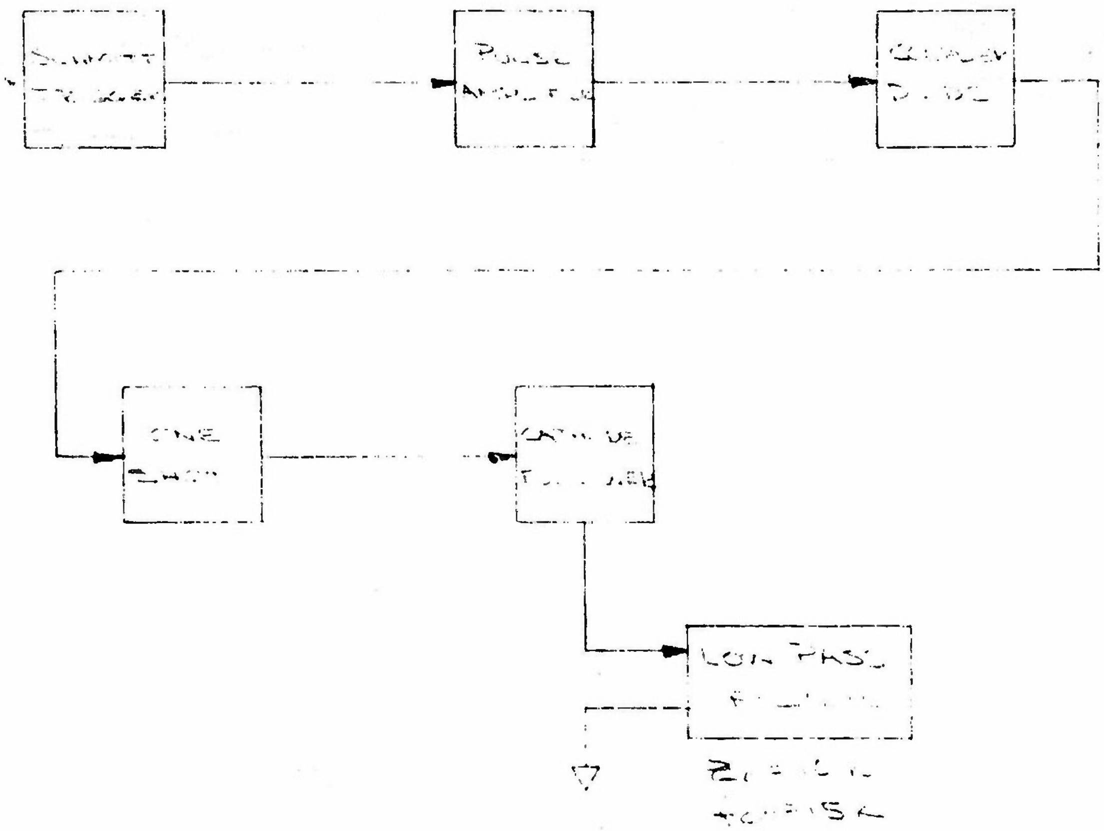

Figure 68. Pressure-Time Playback Equipment, Block Diagram

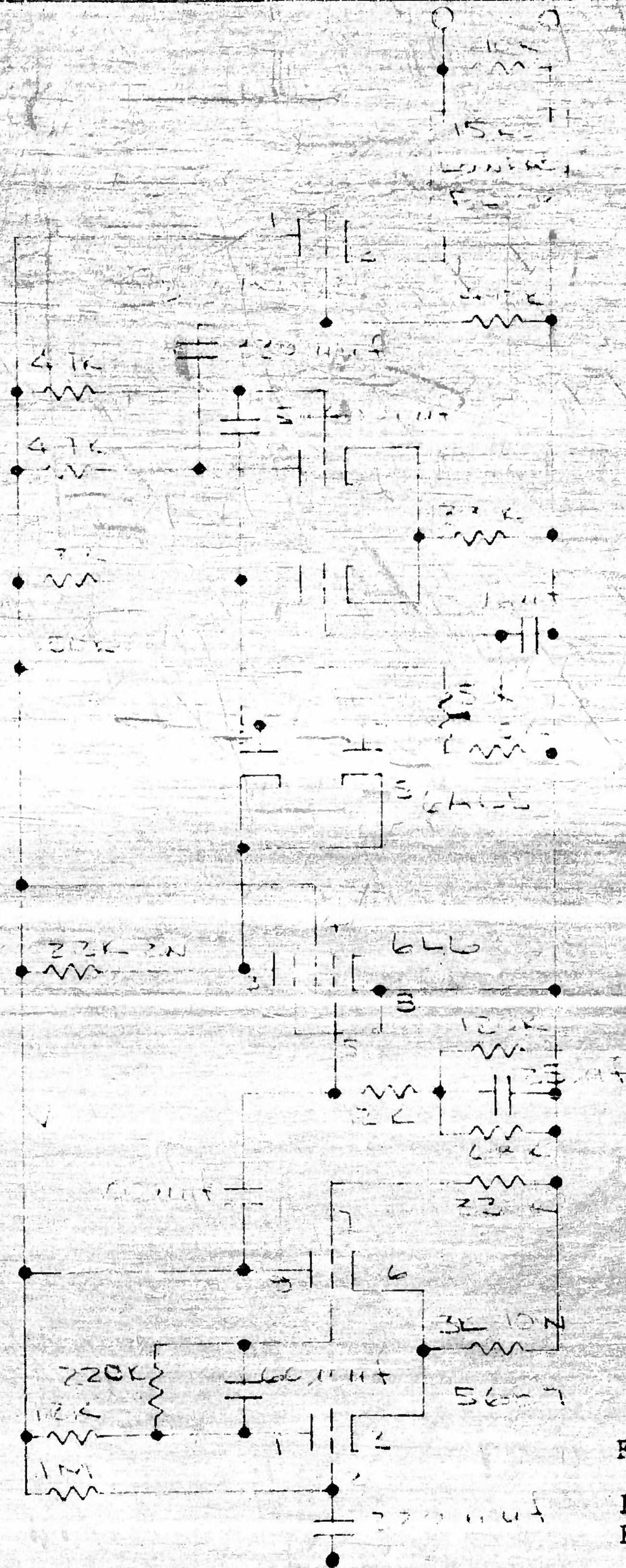

Figure 69.

Pressure-Time Playback Equipment, Schematic load down the source. The output of this stage is a 20 volt peak to peak rectangular wave having a time rise well under 1 microsecond. It is capable of operation from 20 cps to 200 kcps and is thus adequate for our 65-75 kcps operation.

RC interstage coupling is employed to a 6L6 grid normally biased beyond cutoff. The 6L6 plate is diode-coupled (6AL6, both sections) to pin 7 of the Quick Recovery One Shot. The coupling is such that, as 6L6 conducts and its plate drops from B+ to its conducting value, the 6AL5 cathode voltages are carried down, and these in turn pull down the plate voltages, starting the Quick Recovery One Shot cycle.

The Z8889 is rc coupled to the grid of a 12AU7 which is returned to ground through a 470,000 ohm resistor. The 60-volt driving amplitude effectively clamps the grid voltage to the dc above-ground level, which just begins to draw grid current. The 12AU7 section is thus on for a constant time determined by the Z8889 and off again for a period of time determined by the reciprocal of the frequency of the input signal. The plate is returned to B+, and the cathode circuit has a properly terminated 10,000 ohm low pass (f_o = 15 kcps) filter. For viewing the recorded information, the signal appearing across the 10,000 ohm-terminating load resistor is applied to the Y input of the oscilloscope.

The valve position markers are obtained from the pulse-width modulated track of the tape recorder. The output of the PWM playback amplifier is guaranteed to produce at least 110 volts across 600 ohms unbalanced. This is enough to produce easily visible intensity modulation of a normally brilliant trace, so that no further processing is required. The output of the PWM playback amplifier is applied directly to the Z input of the oscilloscope.

Because of the frequent engine shaft speed changes during the recording, it was not convenient to use the multiple (three short, one long) pulses as a sync source for the driven oscilloscope sweep during playback. Therefore, a simple counting circuit (see Reference 14) was built (see Figure 70) and set to count 4:1 in order to provide one sync pulse for each engine cycle. Its output is used to trigger the drive sweep during playback.

A.4 Measurement and Recording of Forces, Temperatures and Reference Voltages.

Two Brown Electronik Multipoint recording potentiometers were required for permanently recording low-frequency data such as temperatures, forces, standardizing potentials, and engine rpm. The uses to which these recorders were put include:

1. The recording of thrust or impulse -- three force-ring thrust pickups incorporating strain gage bridges were used.
2. The recording of temperatures -- generally of three types:
   a. operational-check temperatures, such as combustion tube walls (Pt - Pt_{87} + Rh_{13} thermocouple);
   b. engine- and equipment-safety temperatures -- bearings, valve housings, coolant water for pressure pickup, base flange of pressure pickup, etc. (chromel-alumel and copper-constantan);
   c. performance-measuring temperatures such as the temperature of gaseous fuel at the flowmeter and the temperature

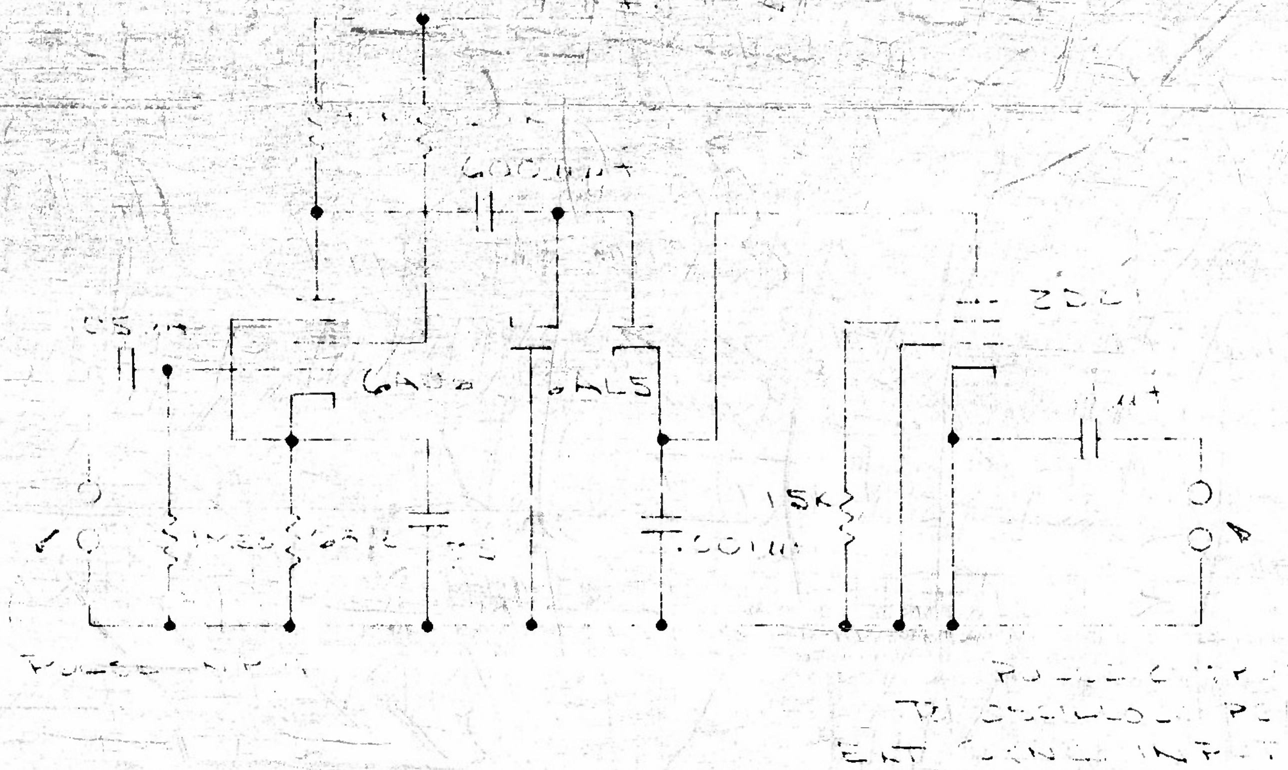

Figure 70. Sync Divider

of air at the orifice plate (copper-constantan).

3. Engine RPM -- for recording the speed at which the engine was driven, the IR drop across a resistor in series with the tachometer meter described in Subsection A.2.2 was used.

4. Standard Voltages -- precision voltage dividers, appropriately tapped, were used to provide a means for checking any drift in the voltage of the inputs to the strain gage force rings and in the dc bucking voltage for pressure-time history recording.

Means were provided for zero-shifting or suppressing up to 100 millivolts (see Figure 71(a)) any ten of the twenty-four input channels. This flexibility was achieved by wiring the twenty-four recorder input pairs so that one side of each was normalled through a standard jack panel strip (see Figure 71(b)). By means of patch cords, the desired potential could be applied in series aiding or opposing the signal voltages on any of the 24 channels.

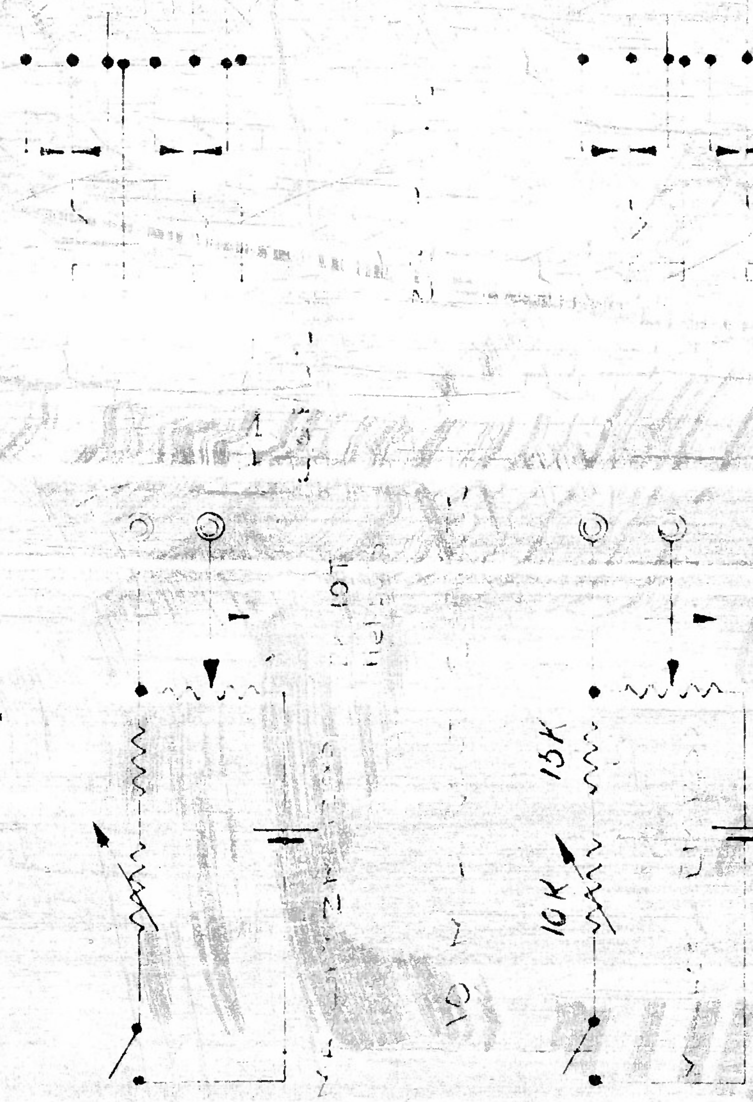

Figure 71.
a) Zero Shift Millivolt Source
b) Brown Recorder Input Patch Panel

APPENDIX B

SUMMARY OF TESTS MADE WITH TEST ENGINE NO. 2

(NOTE: Tube dimensions and relative phase lengths are summarized in Tables 1 and 2 Section 4.3.)

TEST NO.	PURPOSE	OBSERVATIONS	MAXIMUM AIR FLOW (lbs/sec)	MIN. HEATING PERIOD TO MAX. TUBE TEMP. (mins)	PEAK CYCLE PRESS. RATIO	MAX. TUBE TEMP. (^{o}F)	CONCLUSIONS	REMARKS
1, 2, 3, 4	Check ignition system, fuel system and engine operation	Firing erratic				500	Discovered intake valve led exhaust valve by 17^{o}	Valves shifted so 17^{o} pulse compression is obtained
5	Check 17^{o} pulse-compression valve setting	Firing better, tube wall temperature still low		$\approx$ 60		740	Pulse compression seemed too long	Valves shifted so 5^{o} pulse compression is obtained
6, 7, 8, 9	Check 5^{o} pulse-compression valve setting	Warm-up period too long		$\approx$ 60		1200		Various air-flow rates, fuel-flow rates, and cycle frequencies tested. None gave short tube-heating period
10, 11	Find best pre-heat conditions for fast warmup			$\approx$ 60		1400		
12, 13	Find best pre-heat conditions for fast warmup	Firing still erratic	.013	45-60		1800	Front valve housing held flame	
14, 15	Check effects of (a) injecting fuel directly into combustion tube and (b) decreased volume in inlet-valve housing		.013	10-15		1950		Open volume in front valve housing decreased. Fuel injected directly into tube
16, 17	Check (a) effect of cooling rear valve plate and (b) heating rate	Tube ends cooler than center portion	.009	10-15		1950		Binding of valves and overheating of drive motors abbreviate runs
18, 19	Check effect of increasing resistance of heat path from combustion tube to valve-plate housings	Tube ends hotter than in previous test	.019	5-10		2000	Increasing heat paths successful	
20	Find conditions for smooth operation on surface combustion		.021	5-10		2200	High RPM ($\approx$ 3500) is required for fast heating rate	
21, 22	Check original exhaust impulse target	No exhaust thrust measured	.020	5-10		2200	Original exhaust target not satisfactory	Installed flat plate with wire screen for exhaust target
23, 24, 25	Check inlet target and new exhaust target	No net thrust obtained						Flat-plate exhaust target calibrated successfully with cold steady flow
26	Test 9" tube 5/8" diameter	No net thrust obtained	.013	5-10		1950		Valve edges bevelled

APPENDIX B
(Continued)

TEST NO.	PURPOSE	OBSERVATIONS					CONCLUSIONS	REMARKS
			MAXIMUM AIR FLOW (lbs/sec)	MIN. HEATING PERIOD TO MAX. TUBE TEMP. (mins)	PEAK CYCLE PRESS. RATIO	MAX. TUBE TEMP. (^{o}F)		
27, 28, 29	Check effect of bevelled valves	No noticeable difference in engine operation					Bevelled edges not detrimental to operation of engine	
30, 31	Check operation of pressure pickup mounted on 1/2-in. square tube		.015	10-15		1400	Operation of pickup satisfactory. Cooling of pickup sufficient	Heating period long again. Tube temperature low
32, 33, 34	Check operation of pressure pickup mounted on 1-in. round tube	Smooth running on surface combustion	.030	5-10	≈1.5	2200		
35	Test 1-in.- ID tube 6 in. long	Poor run, valve clearances suspected to be too large						Valve clearances reduced
36	Check effect of 0.005-in. clearance at rear valve	Alternate firing with high pressures. Steady firing with lower pressures	.064	2-4	≈4 alt. ≈2 steady	2000		Increased pressures, no net thrust. Mechanical shock broke Metamic tube
37, 38, 39	Measure heating rates and pressures for 9/16-in. square tube 5 in. long	Long heating period, low tube temperatures	.020 .030	25		1500	Smaller ID tube seemed to be detrimental to operation of engine	Metamic tube broke again due to mechanical shock
40	Test type-304 stainless steel tube with 1-in. ID and 6-in. length	Alternate firing	.066	10	3.2 alt.	2200	Coil in body of pressure pickup overheated	Pickup returned to Photocon. Cooling chamber added to pickup
41	Test (a) tube with 12-in. length and (b) valve setting with 17° exhaust		.060	10		2300	New cooling system for pressure pickup satisfactory	
42, 43	Check (a) 17° exhaust phase (b) tube with 9-in. length	Firing alternate or steady depending on test conditions	.065	4-5	2-2.5	2300		Tube melted
44, 45	Check tube made of type-321 stainless steel		.065	4-5	2-3.5	2300	Type-321 stainless steel satisfactory for tubes in test engine	
46	Check fuel injection ahead of inlet valve	Very high fuel/air ratios required. Firing erratic. Front valve housing became too hot					Injecting fuel upstream of inlet valve not satisfactory	

APPENDIX B
(Continued)

TEST NO.	PURPOSE	OBSERVATIONS	MAXIMUM AIR FLOW (lbs/sec)	MIN. HEATING PERIOD TO MAX. TUBE TEMP. (mins)	PEAK CYCLE PRESS. RATIO	MAX. TUBE TEMP. (°F)	CONCLUSIONS	REMARKS
47	Check new valve setting (22° exhaust)	Smooth operation on surface combustion	.074	4-10	3.0-4.0	2300	Exhaust gases deflected in direction opposed to direction of valve-blade motion	No not thrust. Exhaust-target screen melted
48, 49	Photograph exhaust with high-speed camera		.074			2300	Conclusion for Test 47 confirmed	Provision for water cooling exhaust target made
50	Check fuel injection ahead of inlet valve	Front valve housing became too hot again. Poor operation of engine						Fuel injection directly into tube used for remaining tests
51, 52	Check 24°, 20° and 18° exhaust phases	Smooth operation on surface combustion	.074	5-15	3.0-3.5	2000	Tests with these several different valve settings give approximately same results	
53, 54, 55	Check (a) new valve-plate configuration (b) 20.5° exhaust phase and (c) water cooled thrust target	Smooth operation on surface combustion	.074	8	3.0-4.0	2000	Cooled thrust target operated satisfactorily	
56, 57	(a) Check diaphragm joint on inlet target (b) measure net thrust	Plastic diaphragm material ruptured. No net thrust measured	.074	8		2000	Plastic diaphragm material will not withstand the heat at the inlet	Rubber-impregnated cloth diaphragm installed
58	Measure net thrust	No net thrust measured						
59, 60	Check valve configuration giving 0° pulse compression phase and 14.4° exhaust phase	Drive motors burned out					Best configuration used to date	Drive motors were heating up during almost every test. DC drive system replaced finally by a Varidrive unit
61	Same as for 59, 60	Firing regular and loud. SFC 8-10 lb/hr per lb thrust. Net thrust 1.30 lbs/in^2	.086	4-5	6.5-8	2050		
62, 63, 64	Same as for 59, 60	Tube ruptured before thrust could be measured			5-6.5			
65	Same as for 59, 60 except try a Metamic tube in place of the stainless steel tube	Mechanical shock fractured tube						

APPENDIX B
(Continued)

TEST NO.	PURPOSE	OBSERVATIONS					CONCLUSIONS	REMARKS
			MAXIMUM AIR FLOW (lbs/sec)	MIN. HEATING PERIOD TO MAX. TUBE TEMP. (mins)	PEAK CYCLE PRESS. RATIO	MAX. TUBE TEMP. (°F)		
66, 67, 68	Same as for 59, 60 except use stainless steel tube again	SFC 8-10 lb/hr per lb thrust. Net thrust 1.30 lbs/in^2	.066	10	5-6.5	1800	Results of best performance were repeated	
69, 70, 71, 72, 73	Use same valve plates. Try 3° pulse compression 17.4° exhaust	Cycling steady. Low combustion-chamber pressure. No net thrust	.060-.070	10	≈ 4	1800	Burning and scavenge phases too long	Inlet total pressures higher than when same flow conditions existed in tests 66-68
74	Check effects of valve configuration providing shorter burning and scavenging phases	Cycling steady only at very low cycle frequencies	.073	3-5			Further study of this configuration needed	Combustion-chamber pressures appeared to be high

REFERENCES

1. Bitondo, D., et al. Preliminary Performance Studies of the Multi-Jet, Aerophysics Development Corporation Report No. 2000-1-R1, January, 1953.

2. "Strahlschubmessungen mit Prallplatten" (Employment of Baffle Plates for Thrust Measurements), Jahrbuch des Deutschen Luftfahrtforschung, 1940, Band Triebwerk, s. 304.

3. Grinstead, C. E.; Frawley, R. N.; Chapman, F. W.; Schultz, H. F., An Improved Indicator for Measuring Static and Dynamic Pressures, SAE Journal (trans.), vol. 52, No. 11, November, 1944.

4. de Haller, P., The Application of a Graphic Method to Some Dynamic Problems in Gases, Sulzer Technical Review, 1945, No. 1, pp 6-24.

5. Jenny, E., Unidimensional Transient Flow with Consideration of Friction, Heat Transfer, and Change of Section, Brown Boveri Review, 1950, No. 11, pp 447-461.

6. Campbell, A. S., The Time Required for Constant-Volume Combustion, Paper No. 51-A15. ASME, November 25, 1950.

7. Dugger, C. L., and Simon, D. M., Prediction of Flame Velocities of Hydrocarbon Flames, Research Memorandum No. E52J13. Cleveland: National Advisory Committee for Aeronautics, January 2, 1953.

8. Pressman, Ralph, "How to Design Bistable Multivibrators", Electronics, April, 1953, p 164ff.

9. Terman, F. E., and Pettit, J. M., Electronic Measurements, Second Edition, Section 13-15, pp 593ff, McGraw Hill Book Co., Inc., 1952.

10. Close, R. N., and Lebenbaum, M. T., Design of Phantastron Time Delay Circuits, Electronics, Vol. 21, p 100, April 1948.

11. Petes, Joseph, "FM Magnetic Tape Recording and Playback Instrumentation System", Navord Report 2713.

12. Bernstein, Sergio, and Spaven, William J., "Single Tube Square Wave Generator", Electronics, Vol. 27, No. 6, p 206, June, 1954.

13. Schmitt, O. H., "A Thermonic Trigger", Journal of Scientific Instruments, p. 24, 1938.

14. Terman, F. E., Radio Engineering, Third Edition, Ch. 12, Sec. 8, p. 606.